

METHODS AND APPLICATIONS OF ACOUSTIC EMISSION. COMPARATIVE ANALYSIS

I. MALECKI and J. RANACHOWSKI

Institute of Fundamental Technological Research
Polish Academy of Sciences
(00-049 Warszawa, Świętokrzyska 21)

1. Some historical data

Acoustic signals which accompany internal changes of the structure of a continuous medium have been observed for centuries, and were often utilized as warning signals of oncoming catastrophes. These signals provoked also an interest as indicators of homogeneity and strength of material. First scientific concern for this kind of acoustic phenomena dates from the third decade of the twentieth century [1], and refers to "micro-seismic" signals. Further investigations [2] proved that the micro-seismic signals precede the mining catastrophes. Still the level of electronics of that time precluded an effective separation of the signals from the background noise, and measurement of the parameters of these signals. The research on acoustic phenomena in metals was undertaken at the beginning of the fifties, and resulted in discovering of (among other things) the so called Kaiser effect [3]. It was not, however, before the end of the fifties that the investigations of acoustic signals in different media developed on greater scale; they were first of all concentrated on the ones that appear in metals, as a result of mechanical loads.

Since 1962 (symposium at San Antonio) [4] the investigation of materials on the ground of acoustic signals has been presented at the scientific conferences on non-destructive testing of materials. In those days the term "acoustic emission" (abbreviation "AE") began being commonly used, displacing such terms as "stress wave emission", or "materials sounds". This term is not entirely exact, in as much as it comprises a wide band of frequencies: from infrasound to ultrasound. The acoustic emission is generally defined as a phenomenon based on the appearance of the elastic waves inside, or on the surface of a continuous medium. This term is often reduced to the phenomenon of the appearance of elastic waves as the result of a local, dynamic variation of the structure of the medium. It is not entirely well-grounded however, because also the acoustic signals in physical-chemical processes, for example during chemical reactions in liquids, should be regarded as the acoustic emission.

The essential development of applications of AE dates from the second half of the sixties. It could take place, first of all, due to the extension of the range of AE measurements to high frequencies, up to 30 MHz [5]. The application of computer technology in the last decade opened new possibilities of selection of AE signals, and determination of their parameters. At the same time the theoretical and experimental work has been conducted, aimed at interpreting the mechanism of creation of the AE signals. For instance, models of stimulation of the vibration of crystal lattice by a group of dislocations [6], and also a model based on the classical fracture theory, have been elaborated. Many research works from that period concerned the interrelation between the velocity of micro-cracks development, and the acoustic emission in brittle and semi-brittle materials [8]. As before, great attention was paid to the acoustic signals generated during rock mass motions, finding analogies between AE signals and the sounds that precede earthquake [9].

After specimen testings, evaluations of complete technical objects by means the AE method have appeared. The control of shielding of atomic reactors [10], degree of fatigue of aircraft parts [11], large-scale constructions (such as water dams [12]) may be mentioned here. Another direction of application is the control of technological processes, especially welding [13].

Further historical data will be quoted later on, when different applications of the AE methods will be discussed.

In Poland, the first works to master the AE measurements techniques date from the beginning of the seventies; at that time the first attempts of technical applications were made. The references to these works will be specified further, in connection with the analysis of separate topics.

The real development of scientific and technical activities in the field of AE in Poland dates from the beginning of the eighties. They were carried out first within the so-called key projects, and since 1985 within the Central Project of Fundamental Research (CPBP No. 02.03) [14], that enabled better financing and coordination in the whole country. The national reporting Symposia, which were held by the end of each year, offered a good occasion to exchange of the experiences, and to assess the research progress. As the consequence of the economic transition, which recently took place in Poland, the system of central projects has been terminated. Nevertheless, numerous research projects concerning acoustic emission have been still centrally financed by a system of grants. The work initiated in the eighties has been continued and developed. The exchange of experience is now facilitated by organizing occasional symposia.

It is difficult to list all scientific institutions which deal with the AE phenomenon and its application; here only the ones are mentioned which have participated in the previous Central Project and are still continuing their work on AE; they are arranged according to the order of their consideration in this work (the range of applications being enclosed in brackets). They are as follows:

— Institute of Fundamental Technological Research of the Polish Academy of Sciences — Warszawa (metals, ceramics, rocks, instrumentation),

- Institute of Fundamental Metallurgy of the Polish Academy of Sciences — Kraków (metals),
- Institute of Inorganic Technology of the Warsaw Technical University — Warszawa (ceramics, technology),
- Institute of Physics of the Silesian Technical University — Gliwice (mining, superconductors),
- Institute of Fundamentals of Electronic and Electrotechnic of the Wrocław Technical University (superconductors),
- Institute of Building Engineering of the Wrocław Technical University — Wrocław (concretes, constructions),
- Department of High Pressures of the Polish Academy of Sciences — Warszawa (powdered materials, reference sources),
- Institute of Wood Technology of the Agricultural Academy — Poznań (wood technology),
- Institute of Mechanics of the Technical University — Lublin (soils),
- Institute of Building Engineering of the Technical University of Świętokrzyskie Mountains — Kielce (rods),
- Institute of Applied Mechanics of the Technical University of Świętokrzyskie Mountains — Kielce (composites),
- Institute of Applied Mechanics of the Technical University — Poznań (machinery parts),
- Institute of Vibroacoustics of the Academy of Mining and Metallurgy — Kraków (machinery parts),
- Institute of Electrotechnics of Engineering College — Opole (welding, electrical power devices),
- Institute of Chemical Analysis of the Warsaw University (chemical processes),
- Institute of Electrotechnics — Warszawa (partial discharges),
- Otolaryngological Clinic of the Medical Academy — Warszawa (oto-emission).

2. Classification of AE sources and applications

The appearance of AE in materials and objects is of very miscellaneous origins, and often a few different factors play simultaneously their roles in the process of the AE generation; nevertheless, certain classification would be useful for further considerations. The following classification, in accordance with the physical processes being the source of AE, will be assumed:

- (1) Motions of the lattice imperfections in metals. These are mainly motions of dislocations and groups of vacancies, as well as transitions of atoms between different energy levels.
- (2) Formation and propagation of micro-cracks, which may appear both in metals and ceramics.
- (3) Creation and shape transformations of local material flaws, having for example the form of micro-cracks or pores.

- (4) Mutual displacements of the layers of a medium, which take place, for instance, in rock masses.
- (5) Reconstruction of the microstructure of a medium, relevant for instance to phase transitions or heat treatment.
- (6) Chemical reactions, accompanied by local variations inside the medium, e.g. gas bubbling.
- (7) Local motions of a gas medium. These may be caused, for instance, by electric discharges. It is however disputable if this kind of phenomena might be classified as the AE.

Another classification may be introduced by taking as a basis the kind of medium or object in which AE appears; this classification is almost identical with the classification according to the applications, being however not entirely coherent. We shall remain at this classification after all, mainly because of the fact that the activities of research laboratories may be divided in accordance with it. Let us assume the following division of the media, or the objects in which AE appears:

- (1) Materials of plastic properties, metals are included here.
- (2) Brittle materials, mainly ceramics.
- (3) Materials which are macroscopically heterogenous, such as wood, concretes, composites.
- (4) Geological layers; this group comprises rocks and soils.
- (5) Machinery, and civil engineering objects, as well as their components, for example high pressure vessels, dams.
- (6) Physical-chemical processes, mainly such as chemical reactions, incomplete electric discharges.
- (7) Biological processes; it is a new, separate domain of the AE investigations, initiated by the oto-acoustic research of AE signals, taking part in the hearing process.

3. AE signals and source-receiver path

Acoustic emission appears usually inside the tested object. Before AE signal reaches the receiver on the surface of the object, it is subject to the attenuation and multiple reflections. Because of this, the absolute measuring of the intensity of the AE signals may be carried out only exceptionally. Usually AE signals versus time are measured in relative units, based on the receiver readings.

Taking into account the general character of the time changes, the following kinds of AE may be distinguished:

- (a) Continuous emission, in which separate pulses merge, because their growth and collapse times are greater than the pauses between them;
- (b) Burst emission which is characterized by the occurrence of groups of strong, distinctly discernable pulses.

Together with the development of the AE methods, a range of descriptors to characterize the AE signal have been introduced, they may be divided into three groups.

(1) The descriptors that characterize the time changes of the signal, comprising:

- sum of counts N , being the sum of the AE pulses which exceed an assumed discrimination level during a measuring period,
- count rate, which is the sum of pulses exceeding the discrimination level in time unit dN/dt ,
- event, being an envelope of a sequence of pulses which exceed an assumed discrimination level.

The sum of events and event rate are suitably characterized.

On the basis of a closer analysis of the time changes, the following terms may also be defined:

- region of pulses, which have exceeded a discrimination level in a time unit,
- discrimination level, by which a specified number of crossings with depended curve take place,
- comparison of the count rate during successive observations.

(2) Shape of the pulse. The attempts of classification of the shapes of single pulses was undertaken [11]. Approximately the two basic shapes may be distinguished: relaxative and accelerative.

(3) Descriptors which describe the energy of signal:

- Root mean square RMS. This value relates to the voltage of an electric signal within the time T :

$$V_{\text{RMS}} = \sqrt{\frac{1}{T} \int_0^T u^2(t) dt}. \quad (1)$$

— Distribution of the energy in the spectrum, defined as the share of the signal energy that belongs to the given frequency band.

— The mean energy of a single pulse, measured directly by a suitable electronic gauge, or defined as:

$$\frac{V_{\text{RMS}} T}{N}. \quad (2)$$

For the purpose of measuring the AE signals it is essential to determine a general relationship between the electric parameters at the output of a measuring transducer: voltage $v(t)$, and current $i(t)$, and the mechanical factors on the surface of the tested object, which is in an undisturbed state. These are the displacements $\| u_0(x, t) \|$, and the force acting upon the unit of surface $\| f_0(x, t) \|$. Both the values are tensors. In an ideal example the following relationship might be written

$$\left\{ \begin{array}{l} \| u_0(x, t) \| \\ \| f_0(x, t) \| \end{array} \right\} \rightarrow \left\{ \begin{array}{l} i(t) \\ v(t) \end{array} \right\}. \quad (3)$$

When measurements are considered, however, it is necessary to take certain simplifying assumptions.

(1) Loading of the object by the transducer can be neglected; therefore $u_0(x,t) = u(x,t)$, $f_0(x,t) = f(x,t)$, where u and f are displacement and force on the transducer.

(2) Values $\|u\|$, $\|f\|$ are the tensors, with components of different vibration modes. It is not possible to realize a measurement of the whole tensor by scalar values, therefore it has been assumed that the separate modes are not mutually associated at the place of measurement, and that the transducer measures the values u and f of only one mode. Then the values may be regarded as scalars.

(3) In majority of cases fields u and f changes smoothly together with the change of x , and it may be assumed that they remain equal on the whole surface of the transducer, what enables elimination of the coordinate x . It means that the following relationship can be admitted:

$$\begin{Bmatrix} u(f) \\ f(T) \end{Bmatrix} \rightarrow \begin{Bmatrix} v(f) \\ i(t) \end{Bmatrix}.$$

(4) It has been assumed that the proportionally exists between the mechanical and electrical values; that is to say, the system is linear. In a general case the response of the system has a form of a square matrix T_{ij} . To perform the measurement properly, stability of parameters of the mechanical configuration (impedance of the transition object-transducer), and the electrical parameters (input impedance of the preamplifier) is necessary. When assuming it, it is sufficient to determine of the relation between two values, for instance v and f , and the matrix T_{ij} reduces to one coefficient T . Then

$$(i) \text{ Physical-chemical processes } (a) \quad v = T u.$$

For the purpose of AE measurements, determination of the distribution of the amplitudes of the signals received is essential. For continuous AE a Gauss distribution of amplitudes, stationary in time, may be accepted, the counts rate n being

$$n(x_0) = \int_{x_0}^{\infty} dx \int_{-\infty}^0 -\ddot{x} p(x, \dot{x}, \ddot{x})_{x=0} dx, \quad (3)$$

i.e. the function of joint probability of displacement x , velocity \dot{x} , and acceleration \ddot{x} .

In case of a narrow transfer band the Rayleigh distribution is appropriate. The detailed calculations of the intermediate distributions may be found in paper [15]. In case of the burst emission, a single impulse produces an attenuated sine curve at the output. When the discrimination level equals x_0 , the number of pulses received at the initial pulse (event) of amplitude x_i equals:

$$n = \frac{\omega_0}{2\pi\alpha} \ln \frac{x_i}{x_0}, \quad (4)$$

where: α — attenuation coefficient for a sequence of pulses.

If it is assumed that the amplitudes of events form the Rayleigh distribution, it will be possible to state that the events rate equals

$$n_e(x_i) = \left(\frac{n'_e x_i}{\xi^2} \right) \exp \left(- \frac{x_i^2}{2 \xi^2} \right), \quad (5)$$

where: n'_e — total events rate of different amplitudes, ξ — the value of x_i for maximum of n_e .

The shape of the spectrum of AE signal depends on several factors. In the general case, when the signal appears as the result of vibration of a group of elements of a medium which are of different relaxation times τ and function $F(\tau)$, the spectrum is given by the relationship:

$$G(\omega) = 4 \int_0^{\infty} \frac{\tau^{-1}}{\tau^{-2} + \omega^2} F(\tau) d\tau, \quad (6)$$

where: $F(\tau) = \frac{kT}{\tau} F(E)$, E — activation energy, k — Boltzmann constant.

For example, if $F(E) = \text{const}$

$$G(\omega) = 1/\omega, \quad (7)$$

if $F(E)$ has a narrow maximum, the shape of the spectrum is of Lorentz type,

$$G(\omega) = \frac{\tau^{-1}}{\tau^{-1} + \omega^2}. \quad (8)$$

4. AE in metals

The starting point for applications of AE that appear in metals was investigation of the cracking processes occurring in macro-scale, when metal is regarded as a homogeneous body. It appeared before long, however, that in order to understand the essence of these processes it is necessary to investigate the relationship between the changes of metal microstructure and the signals generated by the changes [17].

The main source of AE in metals are motions of dislocations. These motions take place as the result of external or internal stresses during fatigue processes, or local temperature variations. The necessary condition for AE to arise is the existence of courses of cumulation and release of the energy contained in a crystal lattice. It occurs as the results of changes of density and velocity of dislocation, what is described by the general relationship

$$n = f \left(N_m, \frac{\partial N_m}{\partial t}, \frac{\partial N_0}{\partial t} \right) \quad (9)$$

where: n — count rate, N_m — density of mobile dislocations, N_0 — the density of all dislocations.

It has been observed long ago that in certain metals an approximate, linear relationship exists between n and N_m , or n and $\frac{\partial N}{\partial t}$ [17].

The authors of [16] estimated that in the process of generation of a single AE impulse $10^5 \div 10^6$ segments of dislocation lines take part. The character of the dislocation motion depends on the ratio between the stress, and glide resistance. If the stress exceeds the glide resistance, dislocations move continuously, and in the opposite case, the step movement occurs. The dislocation is then slowed down by the potential barriers of the crystal lattice but, owing to the thermal activation, this obstacle may be overcome, and the dislocation can move to the next potential barrier. It is the so-called jerky glide.

A dislocation has a certain inertia, adequate to the deceleration time $\tau = 10^{-12} \div 10^{-10}$ s. During slowing down it then returns its energy to the neighbouring atoms, emitting an AE signal. The way of slowing down a dislocation in pure metals, at room temperature approaches $10^{-10} \div 10^{-9}$ m, therefore the entire effect occurs in micro-scale. Near the surface, the dislocation is exposed to an additional acceleration, and the complex processes of their interaction take place. The energy of the dislocations which reach the surface is partially utilized to create the surface roughness, the rest is the source of AE signals.

In a situation of external stresses, the originating macro- and micro-cracks alter the configuration of dislocations, and facilitate their passage to the surface.

A number of theories exist that connect the micro-processes which occur in metals with the generation of acoustic emission. The frequently applied model [19] assumes that the length of a free path of the dislocation, and its slide path must be longer than certain limiting values, for AE to occur. The length of the dislocation line which is capable of being displaced, is limited by distances to the pinned points, namely to the nodes of the crystal lattice. Taking this assumption, it may be stated that the minimal detectable deformations ε of the surface of the cylindrical sample of the section S are proportional to:

$$\frac{bL^3}{Sd}, \quad (10)$$

where: L — diameter of the slide area, b — Burgers vector, d — spacing of the dislocation source.

Experimental investigations show that AE can not be detected for dislocation source spacing smaller than $0,4 \mu\text{m}$. According to expectations, the influence of the grain diameter is observed. For example, in 99.99% aluminium AE counts rate maximum occurred for the grain diameter of $350 \mu\text{m}$. Together with the increase of the diameter of grains, the slide path of dislocations also increases, therefore the AE rises. However, above a certain diameter of grains the possibility of the dislocation generation on the boundaries of grains decreases, and the activity of AE drops (Fig. 1).

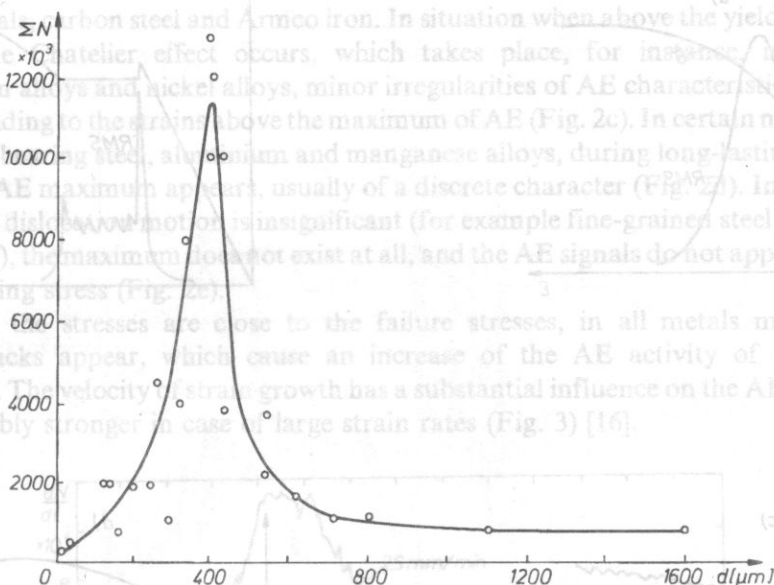
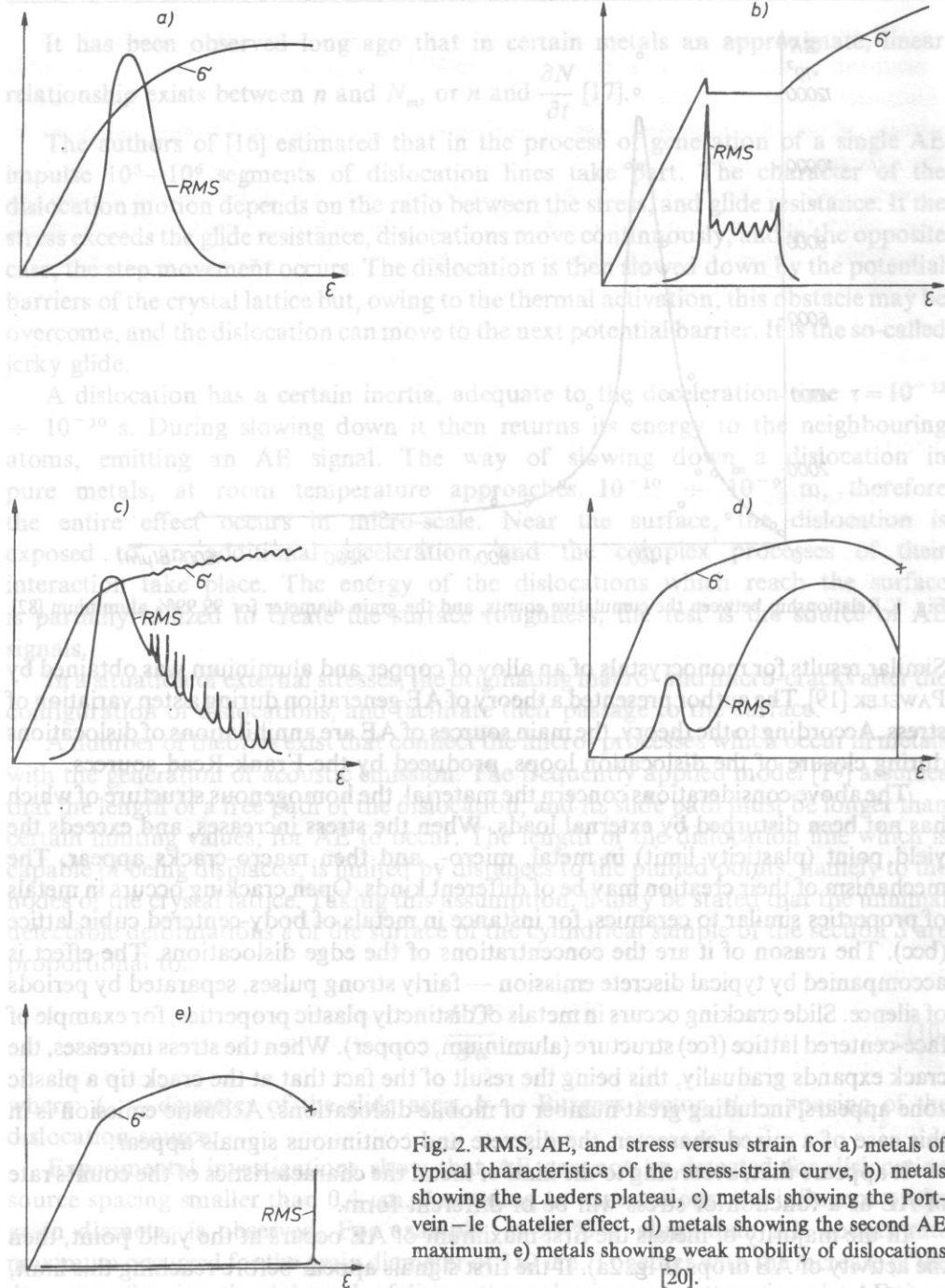


Fig. 1. Relationship between the cumulative counts, and the grain diameter for 99.99% aluminium [82].

Similar results for monocrystals of an alloy of copper and aluminium was obtained by PAWELEK [19]. The author presented a theory of AE generation during a step variation of stress. According to the theory, the main sources of AE are annihilations of dislocations during closure of the dislocation loops, produced by the Frank-Read sources.

The above considerations concern the material, the homogenous structure of which has not been disturbed by external loads. When the stress increases, and exceeds the yield point (plasticity limit) in metal, micro-, and then macro-cracks appear. The mechanism of their creation may be of different kinds. Open cracking occurs in metals of properties similar to ceramics, for instance in metals of body-centered cubic lattice (bcc). The reason of it are the concentrations of the edge dislocations. The effect is accompanied by typical discrete emission — fairly strong pulses, separated by periods of silence. Slide cracking occurs in metals of distinctly plastic properties, for example of face-centered lattice (fcc) structure (aluminium, copper). When the stress increases, the crack expands gradually, this being the result of the fact that at the crack tip a plastic zone appears, including great number of mobile dislocations. Acoustic emission is in this case of a mixed character, the discrete and continuous signals appear. It appears that, according to the kind of metal the characteristics of the counts rate of AE as a function of stress will be of different form.

In the majority of metals the first maximum of AE occurs at the yield point, then the activity of AE drops (Fig. 2a). If the first signals appear before reaching this limit, and if in the stress-strain characteristics the Lueders plateau exists, then, after a single peak, the AE activity remains on a steady level within this plateau, after that it decreases and assumes a steady character (Fig. 2b). Such a characteristics have, among



other metals, carbon steel and Armco iron. In situation when above the yield point the Portvein-le Chatelier effect occurs, which takes place, for instance, in case of aluminium alloys and nickel alloys, minor irregularities of AE characteristics appear, corresponding to the strains above the maximum of AE (Fig. 2c). In certain metals, like titanium, bearing steel, aluminium and manganese alloys, during long-lasting strains, a second AE maximum appears, usually of a discrete character (Fig. 2d). In metals in which the dislocation motion is insignificant (for example fine-grained steel after heat treatment), the maximum does not exist at all, and the AE signals do not appear before the breaking stress (Fig. 2e).

When the stresses are close to the failure stresses, in all metals micro- and macro-cracks appear, which cause an increase of the AE activity of a discrete character. The velocity of strain growth has a substantial influence on the AE, which is considerably stronger in case of large strain rates (Fig. 3) [16].

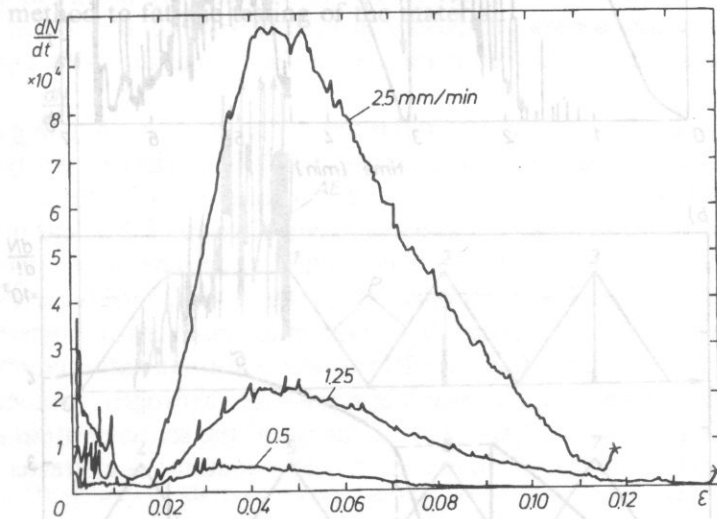


Fig. 3. Count rate during different velocities of the strain increase: (a) 0.5 mm/min, (b) 1.25 mm/min, (c) 2.5 mm/min [16].

For the application of the AE method it is important that AE signals should accompany these changes of material microstructure which have not yet effected the load characteristics. The research of the degree of defectiveness of steel by the AE method was initiated in Poland by Z. PAWŁOWSKI [85]. The investigation of AE generated by microstructural changes has been developed by PILECKI and SIEDLACZEK [20], while PILECKI expanded the investigation of processes of motions of dislocations [21]. The same authors investigated in detail [22] the behaviour of railway rails. It has been demonstrated that the AE method is a valuable tool to monitor the fatigue. In a new material (Fig. 4a), the AE activity is much stronger than in the rails which have been used for a few years (Fig. 4b).

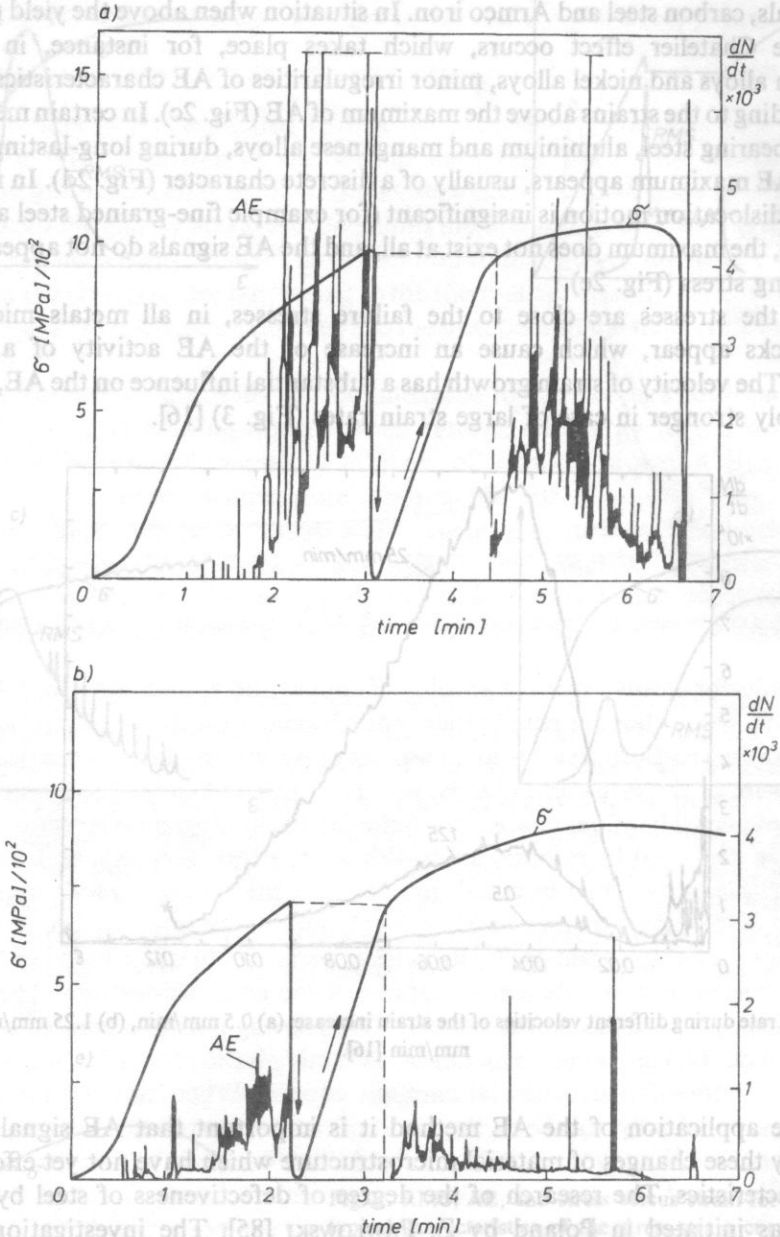


Fig. 4. Kaiser effect in steel St90PA (a) new, (b) exploited [20].

In metals an evident impact of the „history” of applied loads on AE exists. It is the Kaiser effect, based on shifting of the threshold of the AE initiation after relieving and repeated loading of the material (Fig. 4). Assume the material was exposed to the load σ_p , by which the AE activity appeared; after its relieving and the repeated loading, the

AE will appear only when $\sigma_{II} > \sigma_I$. This effect does not always appear, however. It is not observed in metals, in which AE appears also during unloading of the sample. It is relevant to the Bauschinger effect, which is based on the observation that after loading the material in one direction above the yield point, and subsequently in the opposite direction, the yield point of the material of the sample decreases. The occurrence of AE during application of cyclic loads to steel was the object of research of PILECKI and SIEDLACZEK [24], [22]. Three zones have been observed:

In the first zone, which comprises a few initial cycles, the Kaiser effect causes a gradual attenuation of AE signals, till their complete fading in the II zone, what is probably relevant to the fixed dislocation structure of the material. The III zone begins at the half of the number of cycles necessary to destroy the specimen; at this time gradually growing AE signals appear corresponding to the initiation of micro-cracks (Fig. 5). It should be noted that the AE method monitors the initiation of these cracks earlier than the optical methods, which opens considerable possibilities of application of the AE method to fatigue testing of the material.

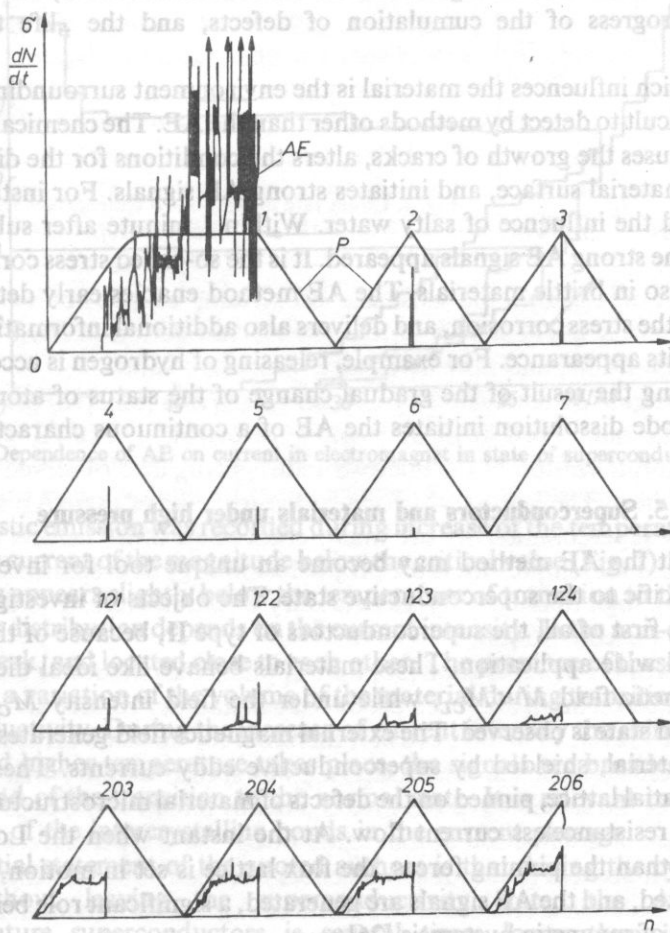


Fig. 5. AE at cyclic load [24].

The processes occurring during the cyclic loads are more complex than those at static loads. The state of dynamic equilibrium exists between production of the new dislocations during subsequent cycles, and the annihilation of the existing ones. The process of production of the new dislocations is proportional to the density of dislocations, while the process of annihilation is proportional to the square of that density, therefore this status of dynamic balance stabilizes only after a sufficiently large quantity of cycles [21]. It should be remembered, however, that the fatigue processes and the appearance of the AE signals, depend strongly on the state of the metal surface [23], and the motion of the dislocations emerging at the material surface increases with its roughness. The nucleation of the fatigue cracks begins therefore on the material surface, initiating the burst AE.

During the cyclic load of the order of 10 cycles per second, the counts rate values are distributed (as a function of time) apparently chaotically. However, as it has been indicated by PAWŁOWSKI [86], it is possible, by means of the cluster analysis, to determine certain regularities of the distribution and, on this basis, to estimate the progress of the cumulation of defects, and the „life time” of the specimen.

A factor which influences the material is the environment surrounding it, and this influence is difficult to detect by methods other than the AE. The chemically aggressive environment causes the growth of cracks, alters the conditions for the dislocations to emerge at the material surface, and initiates strong AE signals. For instance, PILECKI [87] investigated the influence of salty water. Within 1 minute after submerging the metal sample, the strong AE signals appeared. It is the so-called stress corrosion effect, which occurs also in brittle materials. The AE method enables early detection of the initial stages of the stress corrosion, and delivers also additional information about the mechanisms of its appearance. For example, releasing of hydrogen is accompanied by a burst AE, being the result of the gradual change of the status of atom activation, whereas the anode dissolution initiates the AE of a continuous character.

5. Superconductors and materials under high pressure

It seems that the AE method may become an unique tool for investigating the phenomena specific to the superconductive state. The objects of investigation by the AE method are, first of all, the superconductors of type II, because of their practical significance and wide application. These materials behave like ideal dielectrics only under the magnetic field $M < M_{CL}$, while under the field intensity $M_{CL} < M < M_{CZ}$ a so-called mixed state is observed. The external magnetic field generates then certain cores in the material, shielded by superconductive eddy currents. These are fluxes which form a spatial lattice, pinned on the defects of material microstructure. The fixed fluxes enable a resistanceless current flow. At the instant when the Lorentz forces become greater than the pinning forces, the flux lattice is set in motion, the residual stresses are relaxed, and the AE signals are generated, a significant role being played at it by the effects of magnetic hysteresis [26].

Results of the Polish research by WOŻNY and others [27], [28], [82] have indicated that the count rate of AE in an electromagnet NbTi, measured in liquid helium of temperature 4.2 K, in the cycle of increasing and subsequent decreasing of the current ($I > I_c$), attains its maximum near the critical current. In the two next cycles the count rate decreases considerably (Fig. 6). These investigations confirm the dependance of AE activity on the effect of flux pinning. The reduction of the count sum in the successive measuring cycles is caused possibly by "freezing" of the flux lattice. A formal analogy to the Kaiser effect exists here. The same authors investigated a superconductive high temperature ceramics $YBa_2Cu_3O_x$, during variations of the temperature.

6. AE in brittle materials

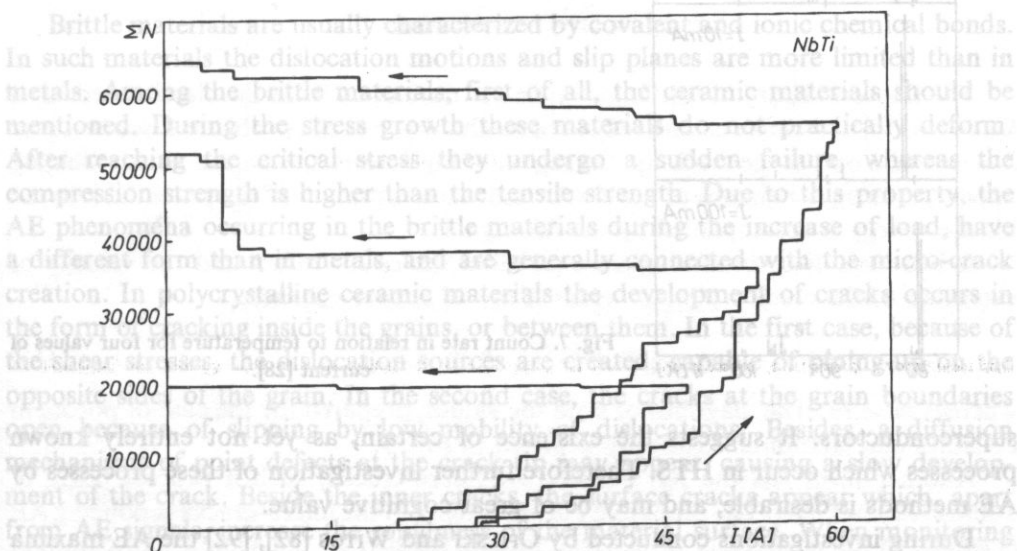


Fig. 6. Dependence of AE on current in electromagnet in state of superconductivity [28].

The acoustic emission was recorded during increase of the temperature, and for the flow of direct current of the magnitude below the critical value (Fig. 7). The main group of AE signals appears slightly below the temperature of transition to the normal state, whereas their distribution depends on the current intensity. In the non-current state the signals are weak, and located close to each other. The presence of these signals may be explained by a variation of the volume of the material during transition from the state of superconductivity. During the increase of current intensity the shift of the group of pulses toward higher temperature takes place, the signals are broadened and appear also at the end of the transition to the normal state. It is relevant to the increase of participation of the intercrystalline bonds in the current passage.

An essential statement of the quoted authors is that during the cyclic changes of current, without leaving the superconductivity state, the AE activity in high-temperature superconductors is several times lower than in the classical

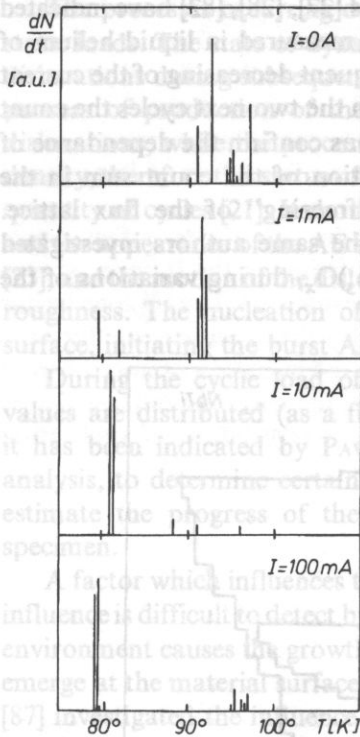


Fig. 7. Count rate in relation to temperature for four values of current [28].

superconductors. It suggests the existence of certain, as yet not entirely known processes which occur in HTS. Therefore further investigation of these processes by AE methods is desirable, and may be of great cognitive value.

During investigations conducted by OPILSKI and WITOS [82], [92] the AE maxima were found in the same HTS at higher temperatures $180 \div 210$ K, which may be relevant to the normalization of the microstructure, being also observed by measurements of specific heat. The factors which cause disturbances of these AE signals which are produced by superconductivity are micro-cracks and other defects of the tested samples. Therefore very important is the proper technology of preparation of the HTS samples, ensuring high homogeneity and stability of parameters. The dimensions of grains should not exceed $10 \mu m$.

Two methods of HTS preparation [58] were applied: the reaction in solid state, and the co-precipitation method, and both produced satisfactory results. In thick samples it was difficult, however, to avoid porosity, therefore for acoustic measurements thin layers of HTS were applied. The $YBa_2Cu_3O_{7-x}$ was spread on the $NbLiO_3$ substrate. The attenuation of ultrasonic wave was investigated by means of the edge transducers. A distinct increase of attenuation at the region of critical temperature was observed. Also strong deformation of the sequence of echoes has been noticed, which is probably relevant to local mechanical stresses or structural changes of the medium. In the critical point minor variations of the velocity followed, of the order of $\Delta c/c = 10^{-3}$.

As it results from these observations, the distinct interdependence exists between the AE activity and the changes of acoustic properties of the medium for HTS. It seems that a qualitative research of this interdependence might contribute to a better understanding of the phenomena which occur in the region of the critical temperature.

In addition to superconductivity, the case which has been investigated by the AE methods is exposition of the material to high pressure. Heterogeneous materials, such as metal powders, and multiphase materials are of concern in the case. The research in this area has been initiated by WITCZAK [29].

6. AE in brittle materials

Brittle materials are usually characterized by covalent and ionic chemical bonds. In such materials the dislocation motions and slip planes are more limited than in metals. Among the brittle materials, first of all, the ceramic materials should be mentioned. During the stress growth these materials do not practically deform. After reaching the critical stress they undergo a sudden failure, whereas the compression strength is higher than the tensile strength. Due to this property, the AE phenomena occurring in the brittle materials during the increase of load, have a different form than in metals, and are generally connected with the micro-crack creation. In polycrystalline ceramic materials the development of cracks occurs in the form of cracking inside the grains, or between them. In the first case, because of the shear stresses, the dislocation sources are created, capable of pining-up on the opposite sides of the grain. In the second case, the cracks at the grain boundaries open because of slipping by low mobility of dislocations. Besides, a diffusion mechanisms of point defects at the crack tip may appear, causing a slow development of the crack. Beside the inner cracks, the surface cracks appear which, apart from AE signals, increase the roughness of the material surface. When monitoring the AE in samples, the two processes should be distinguished: increasing of the notch, usually intentionally prepared in the specimen and generation of micro-cracks in the entire volume of the specimen. The first process is accompanied by a burst emission, while the second produces mainly the continuous emission. Generally the specimens subject to double torsion or to the three-point bending are used; depending on the specimen geometry and load application, the stress intensity coefficient K is determined, and the AE activity is determined as a function of this factor. In Poland the specimens subject to double torsion were applied, of the shape shown on the Fig. 8.

In majority of ceramic materials the elongation of the notch versus the coefficient K has four ranges. During the loading below K_0 the standard notch does not change. In the range II, $K_0 < K < K_I$, the velocity of the notch expansion depends on the increase of K ; in the range III, when $K_I < K < K_{II}$ in spite of growing load, the velocity of the notch elongation remains constant, in the range IV, when $K_{II} < K < K_c$, the notch increases quickly enough, and after reaching the critical value it grows violently till the failure of the sample.

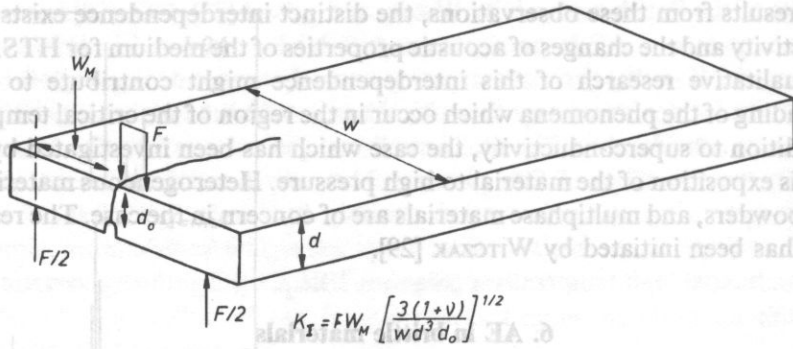


Fig. 8. Sample for double torsion [32].

The fracture theory of brittle materials has developed from the classical works of GRIFFITH [30] to form an extensive field of mechanics. For the problems discussed here it is essential that at the crack tip, the region of high stress and partial plastic yielding appear, causing the growth of the crack, and transformation of the potential into the kinetic energy is accompanied by the AE signals.

It has been discovered long since [31] that the count rate n and the velocity of extension of the crack v plotted versus K are of similar character

$$n = B K^{m'}, \quad v = A K^m, \quad (11)$$

whereas $m \approx m'$. The diagrams of both the values, prepared for the case of porcelain ceramics and aluminium oxide are depicted in Fig. 9.

Another form has the AE initiated by micro-cracks, such a process being of a statistical character. The probability of occurrence of the micro-cracks producing AE is equals to the probability of material failure, defined by the Weibul's distribution

$$\Pi = 1 - \exp \left[- \left(\frac{\sigma}{\sigma_r} \right)^r \right]. \quad (12)$$

where: σ_r and r are characteristic constants of the distribution for the material in question.

The complex research performed in Poland on ceramics, by the team directed by RANACHOWSKI [32], [81], [82], [83], enabled us to collect the experimental data concerning the AE activity as a function of load, and the relationship between AE and the material strength.

Testing of the sample consists of the three stages: (1) linearly increasing load, $\dot{\sigma} = \text{const}$, (2) constant load, $\sigma = \text{const}$, and (3) — unloading, $\dot{\sigma} = \text{const}$. The analytical formulae have been derived for count rate at each stage. The combined effect of the micro-crack creation, and elongation of the cracks for constant loads σ_2 and $\sigma_1 = 2\sigma_2$ is shown in Fig. 10. As it can be seen, after a certain period of time the sudden increase of AE starts, preceding the failure of the sample.

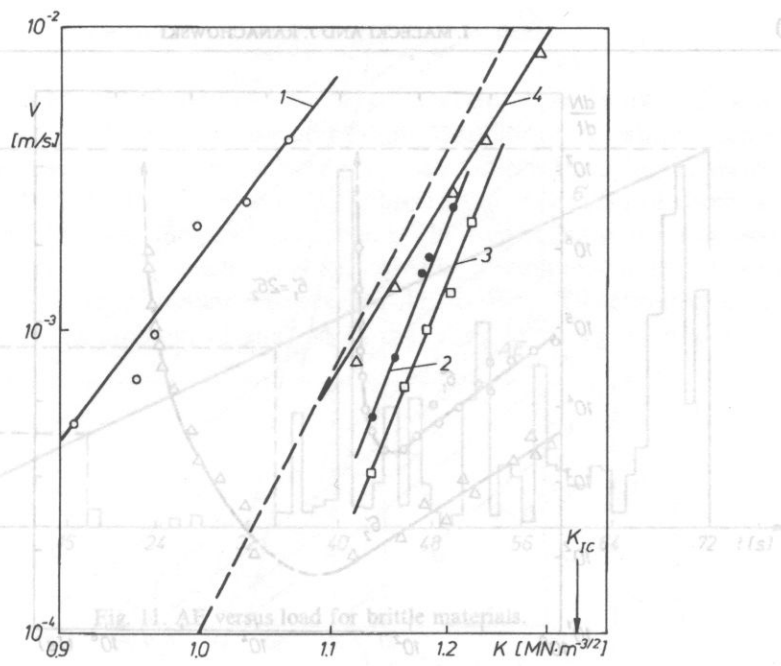


Fig. 10. AE count rate at stresses $\sigma_1 = \sigma_2 = \sigma_3$ [31].

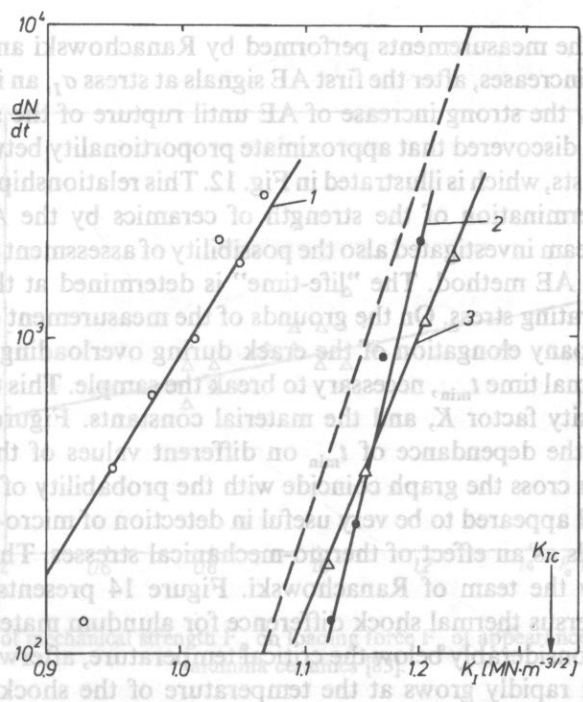


Fig. 9. AE count rate and velocity of notch elongation [83].

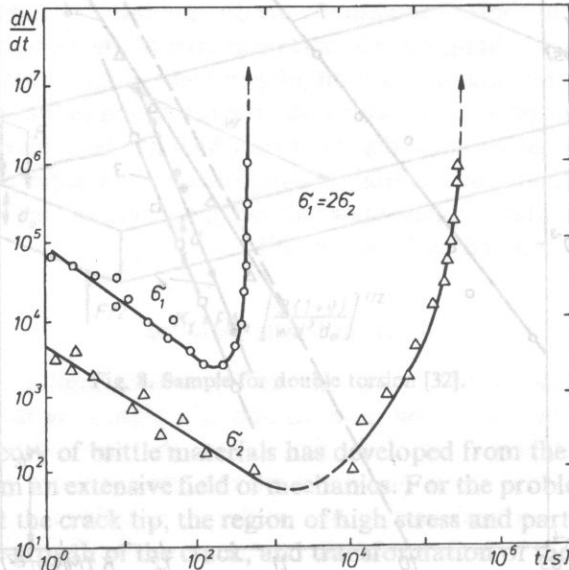


Fig. 10. AE count at stresses σ_2 , $\sigma_1 = 2 \sigma_2$ [31].

The results of the measurements performed by Ranachowski and his team show that when the load increases, after the first AE signals at stress σ_I , an interval of silence comes, followed by the strong increase of AE until rupture of the sample (Fig. 11). Besides, it has been discovered that approximate proportionality between σ_I or F_I and the failure stress exists, which is illustrated in Fig. 12. This relationship may be regarded as a basis for determination of the strength of ceramics by the AE method. The above-mentioned team investigated also the possibility of assessment of the "life-time" of ceramics by the AE method. The "life-time" is determined at the overload R in relation to the operating stress. On the grounds of the measurement of the AE counts rate, which accompany elongation of the crack during overloading, it is possible to determine the minimal time t_{\min} , necessary to break the sample. This time is a function of the stress intensity factor K , and the material constants. Figure 13 presents (in logarithmic scale) the dependance of t_{\min} on different values of the overload. The straight lines which cross the graph coincide with the probability of material failure.

The AE method appeared to be very useful in detection of micro-cracks produced in ceramic materials as an effect of thermo-mechanical stresses. The work on it has been developed by the team of Ranachowski. Figure 14 presents the mechanical strength and AE versus thermal shock difference for alundum material. As it can be seen, AE appears considerably below the critical temperature, afterwards it maintains a steady level, and rapidly grows at the temperature of the shock ΔT 800°C. The analysis of the AE parameters may then be useful in investigating the various phases of the thermal cracking process, whereas it appears that the descriptors which yield especially valuable information are: duration of the event, and its amplitude. The low

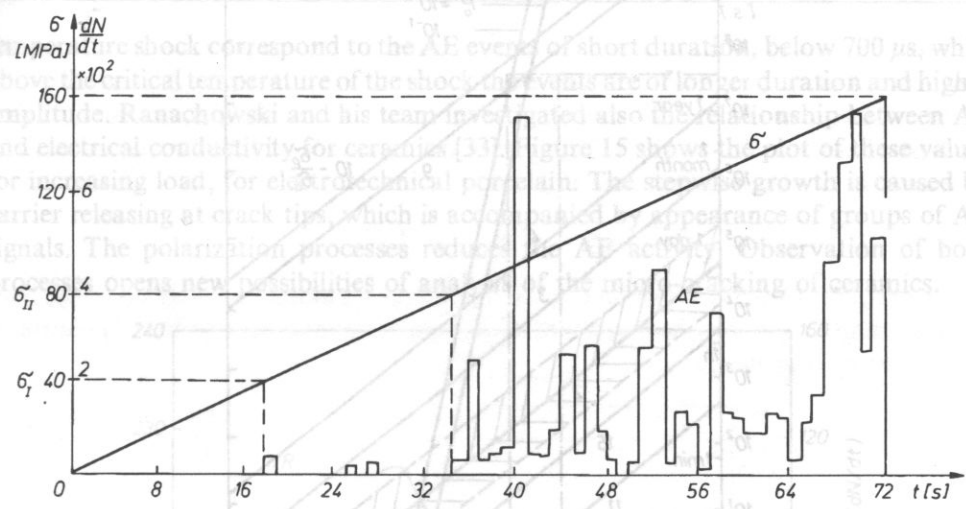


Fig. 11. AE versus load for brittle materials.

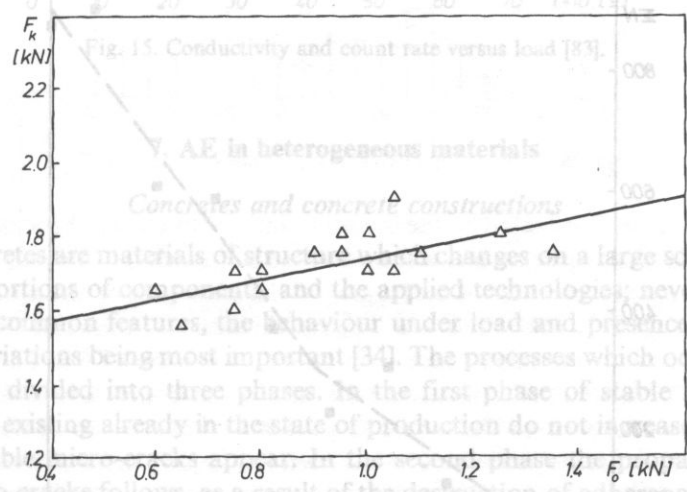


Fig. 12. Dependence of mechanical strength F_k on loading force F_0 of appearance of first AE signals for alumina ceramics [83].

7. AE in heterogeneous materials
Concretes and concrete constructions

The concretes are materials of structural changes on a large scale, subject to various proportions of concrete and the applied technology; nevertheless, they hold certain common features, the behaviour under load and presence of long-term structural variations being most important [34]. The processes which occur under the load may be divided into three phases. In the first phase of stable initiation, the micro-cracks existing already in the state of production do not increase, whereas the new, also stable, micro-cracks appear. In the second phase of progressive development of the existing micro-cracks follows, as a result of the destruction of adifference between the grains of the aggregate and the matrix. In the third phase of final development of the micro-cracks begins, ending with the appearance of macro-cracks. The stresses σ_1 and σ_2 , which are accordingly named the initiating stress and critical stress, are characteristic for the transitions from one phase to another. The identification of both the stresses is of primary importance for the evaluation of the operating parameters of concrete, and for the elaboration of the optimal technology of manufacturing.

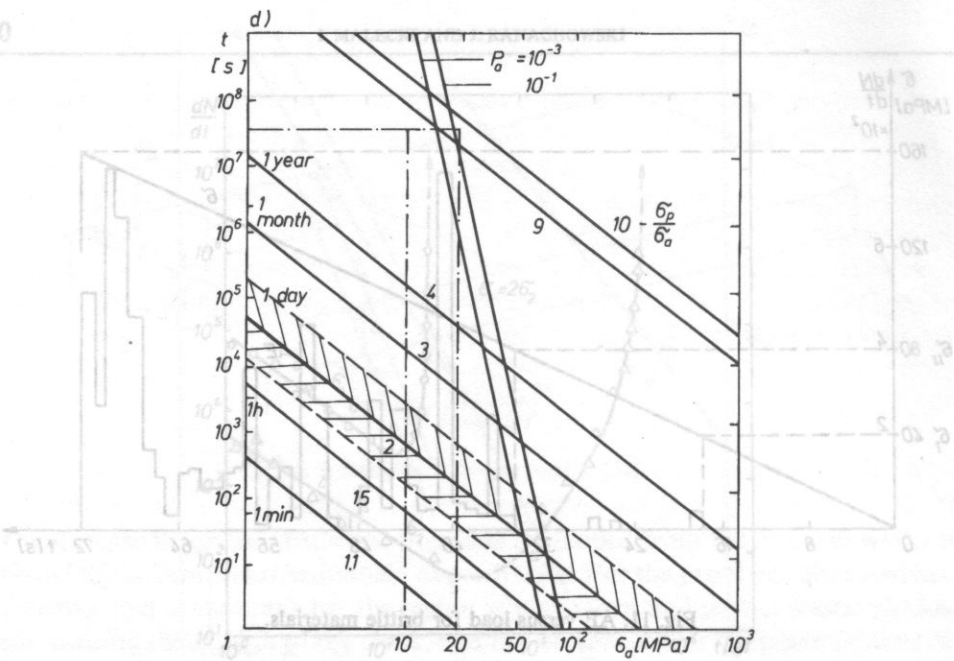


Fig. 13. Dependence of life time duration on load [83].

The results of measurements performed by Kanachowski and his team show that when the load increases, after the first AE signals at stress σ_1 , an interval of silence comes, followed by the strong increase of AE until rupture of the sample (Fig. 11). Besides, it has been discovered that approximate proportionality exists between σ_1 or P_1 and the failure stress σ_{cr} , which is illustrated in Fig. 12. This relationship may be regarded as a basis for determination of the strength of ceramics by the AE method. The above-mentioned team investigated also the possibility of an assessment of the "life-time" of ceramics by the AE method. The "life-time" is determined at the overload R in relation to the operating stress. On the grounds of the measurement of the AE counts rate, which accompany elongation of the crack during overloading, it is possible to determine the minimal time t_{min} necessary to break the sample. This time is a function of the stress intensity factor K , and the material constants. Figure 13 presents (in logarithmic scale) the dependance of t_{min} on different values of the overload. The straight lines which cross the graph coincide with the probability of material failure.

The AE method appeared to be very useful in detection of microcracks produced in ceramic materials as an effect of thermo-mechanical stresses. This work on it has been developed by the team of Kanachowski. Figure 14 presents the mechanical strength and AE versus shock difference for the studied material. As it can be seen, AE appears considerably earlier than the crack. Towards it maintains a steady level and rapidly grows at the temperature of the shock $\Delta T = 800^\circ\text{C}$. The analysis of the AE parameters may also be useful in investigating the various phases of the thermal cracking process, whereas it appears that the descriptors which yield especially valuable information are: duration of the event, and its amplitude. The low

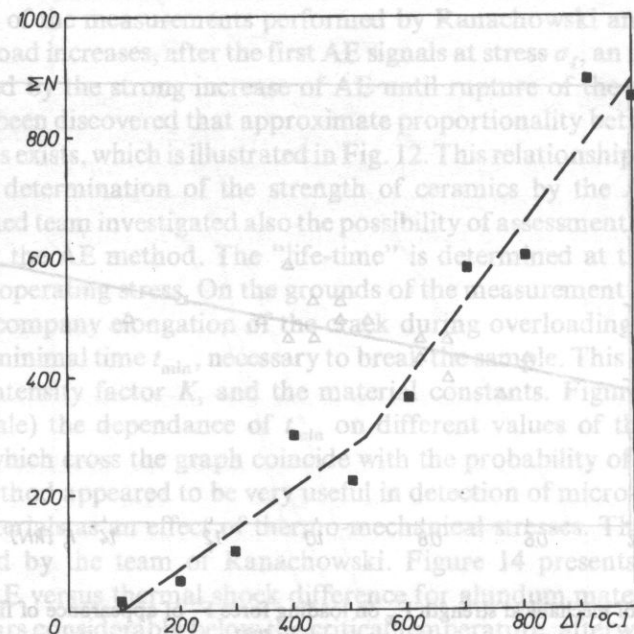


Fig. 14. Strength and AE activity versus temperature difference of thermal shock [83].

temperature shock correspond to the AE events of short duration, below $700 \mu\text{s}$, while above the critical temperature of the shock the events are of longer duration and higher amplitude. Ranachowski and his team investigated also the relationship between AE and electrical conductivity for ceramics [33]. Figure 15 shows the plot of these values for increasing load, for electrotechnical porcelain. The stepwise growth is caused by carrier releasing at crack tips, which is accompanied by appearance of groups of AE signals. The polarization processes reduces the AE activity. Observation of both processes opens new possibilities of analysis of the micro-cracking of ceramics.

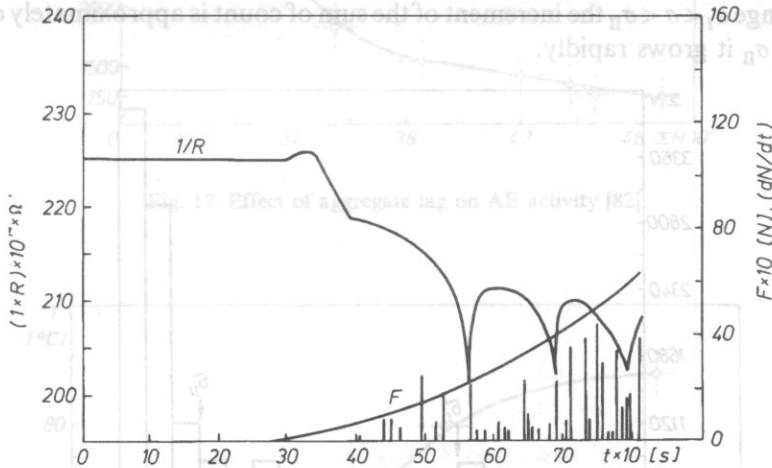


Fig. 15. Conductivity and count rate versus load [83].

7. AE in heterogeneous materials

Concretes and concrete constructions

The concretes are materials of structure which changes on a large scale, subject to various proportions of components, and the applied technologies; nevertheless, they hold certain common features, the behaviour under load and presence of long-term structural variations being most important [34]. The processes which occur under the load may be divided into three phases. In the first phase of stable initiation, the micro-cracks existing already in the state of production do not increase, whereas the new, also stable micro-cracks appear. In the second phase the propagation of the existing micro-cracks follows, as a result of the destruction of adherence between the grains of the aggregate and the mortar. In the third phase unstable development of the micro-cracks begins, ending with failure of the material. Stresses σ_I and σ_{II} , which are accordingly named the initiating stress and critical stress, are characteristic for the transitions from one phase to another. The identification of both the stresses is of primary importance for the evaluation of the operating parameters of concrete, and for the elaboration of the optimal technology of manufacturing.

The fact that both the stresses are accompanied by the characteristic AE signals, constitutes a basis for a practical application of the AE method to the evaluation of the quality of concrete (HOŁA – MOCZKO [35] with Z. RANACHOWSKI [77]). It appeared that the best characteristics of the effects yields the gain ΔN of the sum of count ΣN , between the two stress levels of n and $n+1$

$$\Delta N = \Sigma N_{n+1} - \Sigma N_n$$

The plot of $\Delta N(\sigma)$ is shown in Fig. 16. ΔN increases almost linearly up to the load σ_I , in the range $\sigma_I < \sigma < \sigma_{II}$ the increment of the sum of count is approximately constant, and above σ_{II} it grows rapidly.

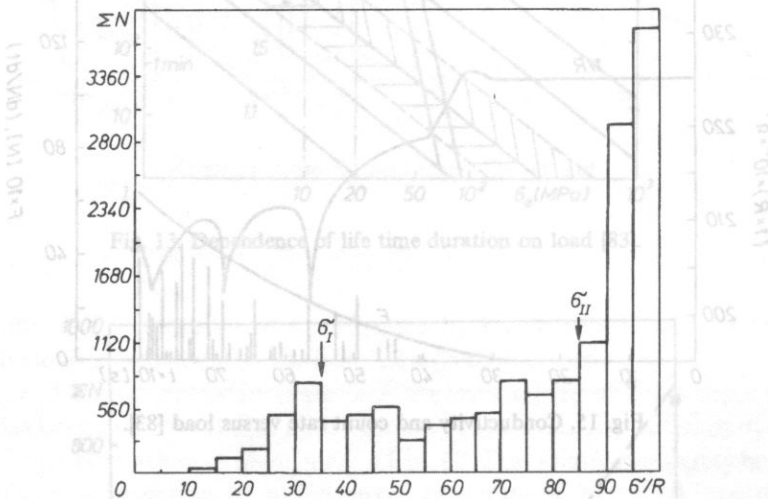


Fig. 16. Dependence of count rate on stress increase [77].

As it has been demonstrated by the investigations of PYSZNIAK, MOCZKO, HOŁA [35], [36], graining of the aggregate has a considerable influence on the sum of count, for instance the apparent thickness of the lagging of the aggregate by the mortar (Fig. 17). When the aggregate is finer, and the lagging thicker, the material becomes more homogeneous, having less micro-cracks, which are the sources of AE. The same author investigated [37] the effect of moisture on the strength of concrete, and found that the counts difference depends on the moisture contents. Presently an artificial curing of concrete is applied on a large scale. As it has been found [38], thermal treatment causes the increase of the sum of count when the concrete is loaded up to failure (Fig. 18). It is probably due to the increased number of micro-cracks, because the products of concrete hydration, which appear at elevated temperature, have more coarse structure. ΣN depends on the temperature of heat treatment and on its duration. As one can see, the AE method yields comprehensive information about parameters of the complex processes which occur during production and operation of concretes.

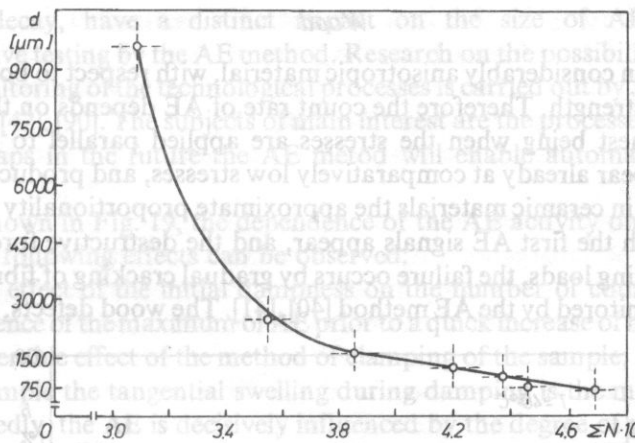


Fig. 17. Effect of aggregate lag on AE activity [82].

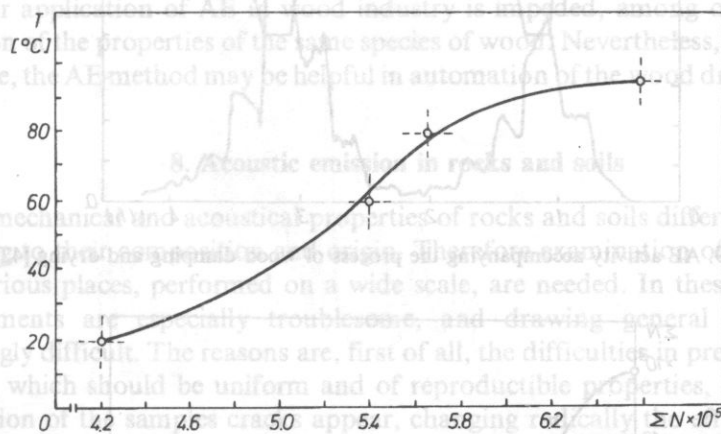


Fig. 18. Effect of thermal treatment of concrete on sum of count [82].

In spite of these obstacles, the investigation of acoustic effects occurring in rocks. Holo and his team have also undertaken a work on comparing the efficiency of the AE method, and the method of measurements of the velocity variations of the ultrasonic wave; however, they have not obtained explicit results. The correlation of results of both methods is a more general problem, it involves also other materials. The difficulty in interpretation of the results is caused, among other factors, by great scatter of the experimental data, and also by a quite different form of the plots of ultrasonic pulse and AE counts rate versus the stress. Some authors claim the AE method monitors micro-cracks later than the ultrasonic pulse velocity method does, however no consensus on the subject has been reached among specialists as yet [39]. In any case, further comparative studies seem to be very desirable.

Wood

The wood is an considerably anisotropic material, with respect to both its structure and mechanical strength. Therefore the count rate of AE depends on the direction of stresses, the highest being when the stresses are applied parallel to its fibres. The micro-cracks appear already at comparatively low stresses, and produce first acoustic signals. Likewise in ceramic materials the approximate proportionality exists between the force at which the first AE signals appear, and the destructive force. During the long-lasting bending loads, the failure occurs by gradual cracking of fibres, which may be effectively monitored by the AE method [40], [41]. The wood defects, as for instance

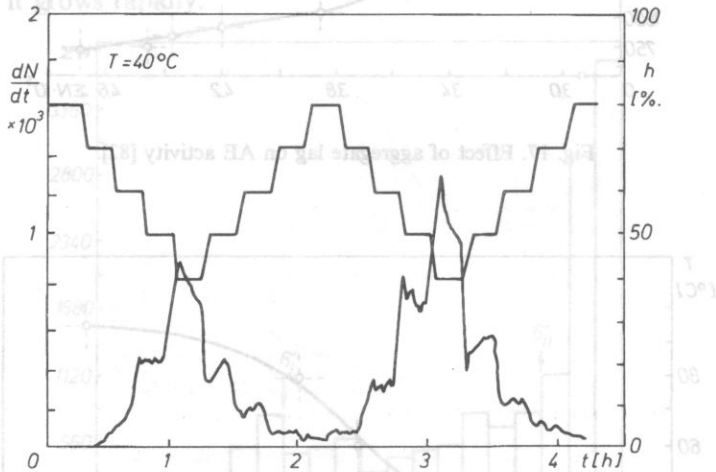


Fig. 19. AE activity accompanying the process of wood damping and drying [42].

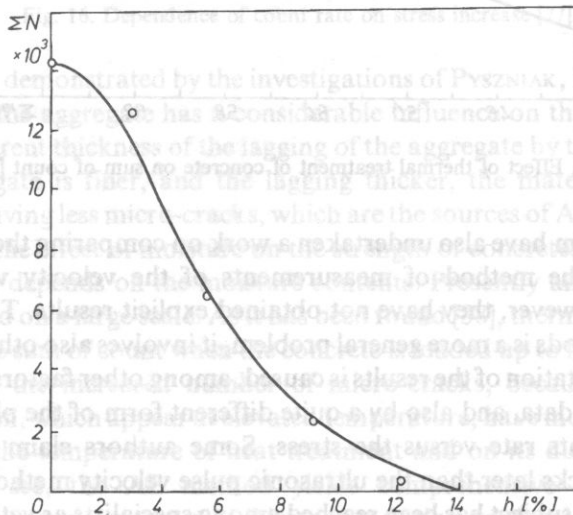


Fig. 20. Effect of initial wood dampness on count rate [82].

knots and decay, have a distinct impact on the size of AE, which enables non-destructive testing by the AE method. Research on the possibilities of application of AE to monitoring of the technological processes is carried out by J. RACZKOWSKI and W. MOLIŃSKI [42], [90]. The subjects of main interest are the processes of damping, and drying. Perhaps in the future the AE method will enable automatic control of the processes.

As it is shown in Fig. 19, the dependence of the AE activity on dampness is very distinct. The following effects can be observed:

- strong effect of the initial dampness on the number of counts (Fig. 20),
 - occurrence of the maximum of AE prior to a quick increase of material shrinkage,
 - considerable effect of the method of clamping of the sample; in case of a simply supported sample the tangential swelling during damping is the main source of AE.
- Undoubtedly, the AE is decisively influenced by the degree of plasticity of wood, which increases together with the increase of its dampness.

The same authors investigated also the impact of the mechanical treatment on the character of AE. They have found, for example, that the inclination angle of the cutting tool, and its orientation with respect to the fibres, considerably alters the AE count rate.

Wider application of AE in wood industry is impeded, among other things, by dispersion of the properties of the same species of wood. Nevertheless, it seems that in the future, the AE method may be helpful in automation of the wood drying processes.

8. Acoustic emission in rocks and soils

The mechanical and acoustical properties of rocks and soils differ fundamentally according to their composition and origin. Therefore examination of samples taken from various places, performed on a wide scale, are needed. In these cases the AE measurements are especially troublesome, and drawing general conclusions is accordingly difficult. The reasons are, first of all, the difficulties in preparation of the samples, which should be uniform and of reproducible properties, because during preparation of the samples cracks appear, changing radically the effect of AE. The second reason is the strong attenuation of acoustic waves in most of the materials being tested, which decreases the intensity of the signals received.

In spite of these obstacles, the investigation of acoustic effects occurring in rocks has been drawing the attention of engineers and scientists for a long time [43]. It was expected that the observation of the AE signals would enable an early warning of a mining catastrophe (a crump) [44], or a catastrophic failure of a technical object, like a water dam. The results were only partially successful, and limited they were to the strictly determined local conditions. Nevertheless, further attempts in this direction seem to be promising, a thorough recognition of the AE characteristics of rock materials being necessary, what requires an extensive laboratory research. Such research is carried out in Poland by three centres, and concerns the coal and accompanying beds in Upper Silesia, the copper ore beds in the Legnica basin, and the soils typical for foundations of engineering structures.

OPILSKI and WITOS [45], [80] have conducted a comprehensive study on the geological beds of Upper Silesia from the point of view of application of the AE method, and they came to certain general conclusions. During loading of the rock four phases of AE activity may be distinguished [46], [47].

- (1) closing of the initial micro-cracks, usually accompanied by a continuous AE, of constant counts rate,
- (2) the elastic strain, when the count rate begins to grow,
- (3) the process of stable propagation of micro-cracks, during which the counts rate increases, subsequently followed by its reduction within a certain range of loads,
- (4) the unstable propagation of cracks, leading to failure, accompanied by a rapid rise of AE.

A typical diagram of count rate for dull coal is shown in Fig. 21, however considerable differences in the characteristics may be observed, depending on the material. Together with the progress of the destruction process, the changes of the

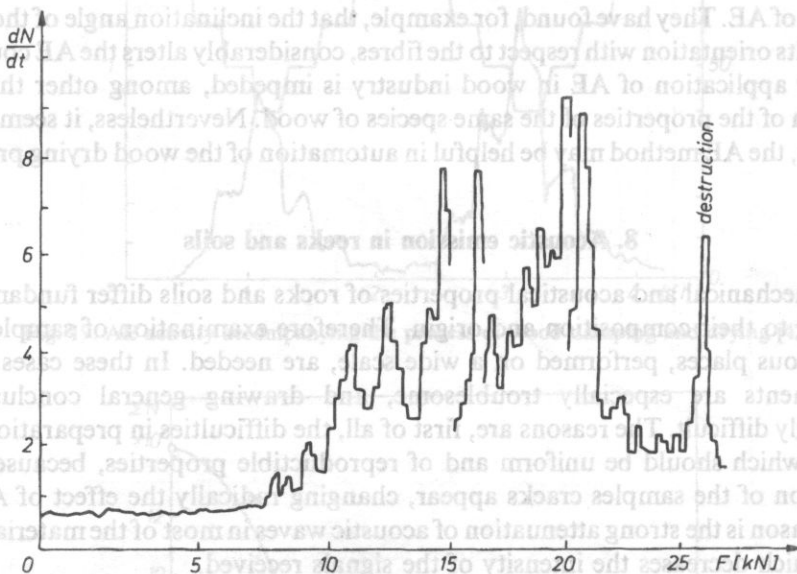


Fig. 21. Dependence of count rate on load for dull coal [81].

frequency distribution may be observed, namely the occurrence — in addition to the 60 ÷ 80 kHz frequency band of the second maximum in the band of 80 ÷ 160 kHz. The quoted authors concluded that the crucial factor was the capability of accumulation of the elastic energy by the rock materials, and introduced the division of materials into the three groups:

- (1) the materials that practically do not accumulate the energy, e.g. bright coal,
- (2) the materials that accumulate the energy partially, e.g. dull coal,
- (3) the materials that strongly accumulate the energy, e.g. sandstone.

A diagrammatic characteristics of the AE activity for the three types of materials is shown in Fig. 22. The Kaiser effect at a variable load is observed, however, depending on the materials damage, it is subject to considerable deviations.

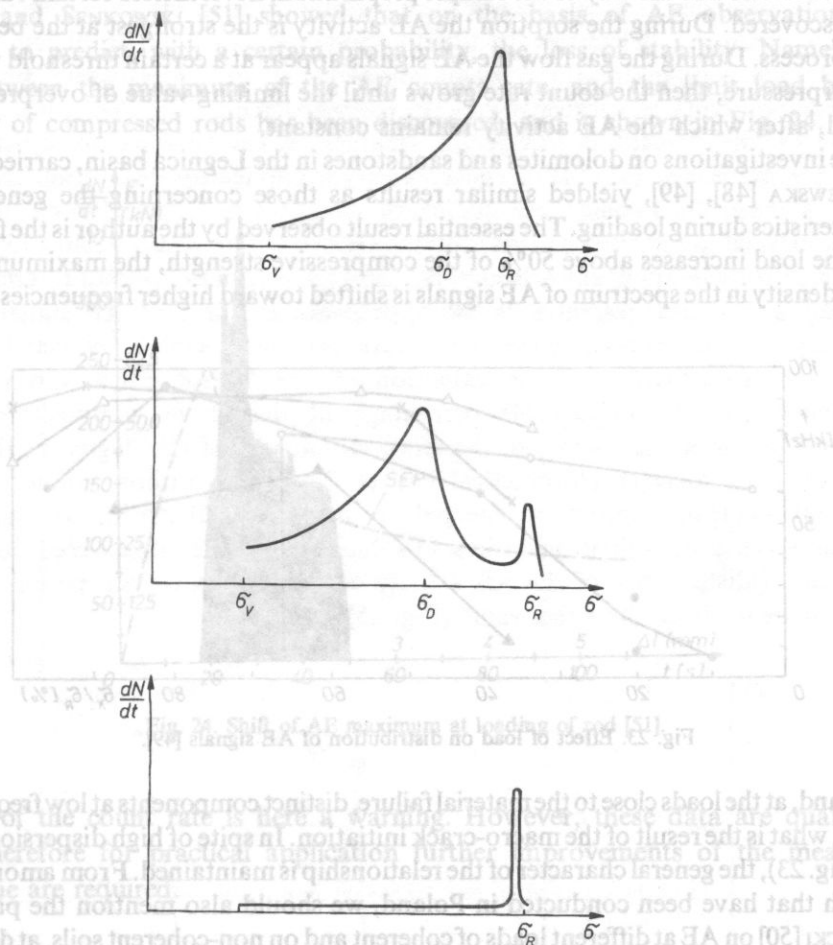


Fig. 22. Characteristics of AE activity for different rock types [82].

It is important for practical applications that, in the majority of cases, the intensified AE activity appears still in the phase of stable micro-cracks, thus warning against the approaching failure of the material. The observations that have been performed hitherto *in situ* do not entitle us to draw any quantitative conclusions as to the relationship between the growing AE activity and a approaching mining catastrophe; nevertheless there are some reasons to expect that such a relationship exists, and its evaluation will be the subject of further research.

The reasons of mining catastrophes might also be the gas explosions. Therefore the investigations initiated in Poland by the team directed by Z. PAWŁOWSKI [84] on the AE signals which accompany the sorption, desorption, and the flow of gas (CO_2) in coal samples, might be of a practical significance. Though the results depend strongly on the kind of material and the way of the sample preparation, nevertheless certain rules have been discovered. During the sorption the AE activity is the strongest at the beginning of the process. During the gas flow the AE signals appear at a certain threshold value of the overpressure, then the count rate grows until the limiting value of overpressure is reached, after which the AE activity remains constant.

The investigations on dolomites and sandstones in the Legnica basin, carried out by JAROSZEWSKA [48], [49], yielded similar results as those concerning the general AE characteristics during loading. The essential result observed by the author is the fact that while the load increases above 50% of the compressive strength, the maximum of the energy density in the spectrum of AE signals is shifted toward higher frequencies. On the

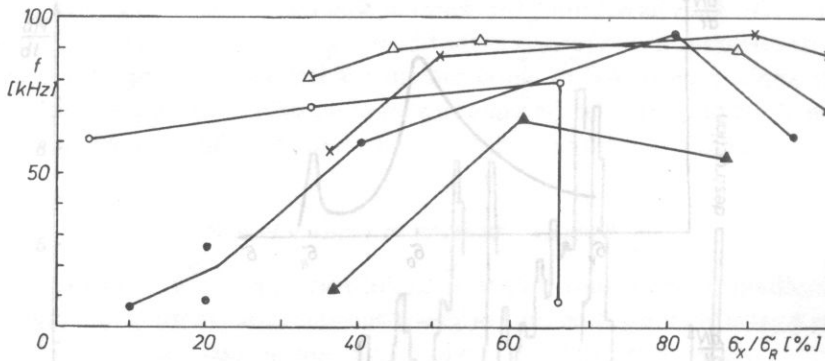


Fig. 23. Effect of load on distribution of AE signals [49].

other hand, at the loads close to the material failure, distinct components at low frequencies appear, what is the result of the macro-crack initiation. In spite of high dispersion of the data (Fig. 23), the general character of the relationship is maintained. From amongst the research that have been conducted in Poland, we should also mention the paper by SKRYNICKI [50] on AE at different loads of coherent and on non-coherent soils, at different temperature and humidity. It may be supposed on the basis of these results that in future the AE methods will be applied on a large scale to monitor the stability of soils.

9. AE in machinery elements and technological processes

Unlike the samples of materials, which are submitted to standard, laboratory tests, the components of machines and engineering constructions are the objects in which complex states of stresses exist, and the AE signals depend not only on materials and sample parameters, but also on the shape of the object. As an example, certain investigations carried out in Poland will be discussed.

Rods

Typical construction components are rods. The classical measuring methods not always enable an accurate determination of the instant of its stability loss. It is especially important in statically indeterminate structures. The investigations of KOWAL and SENKOWSKI [51] showed that on the basis of AE observation it is possible to predict, with a certain probability, the loss of stability. Namely, the shift between the maximum of the AE counts rate, and the limit load bearing capacity of compressed rods has been discovered, and is shown in Fig. 24. A fast

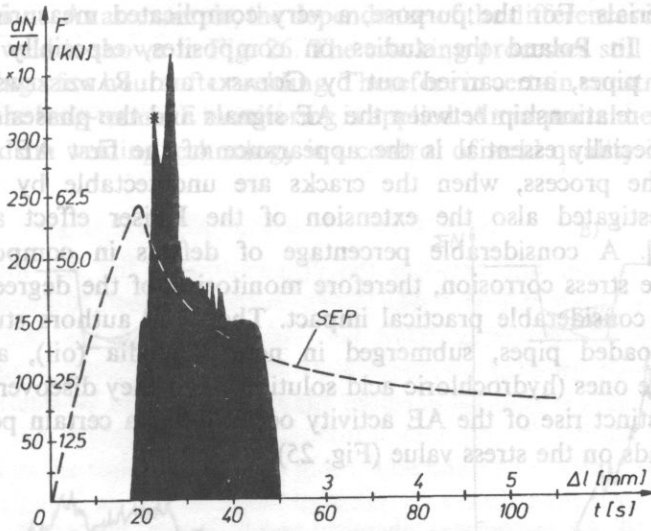


Fig. 24. Shift of AE maximum at loading of rod [51].

growth of the count rate is here a warning. However, these data are qualitative ones, therefore for practical application further improvements of the measuring technique are required.

Conveyor belts

An example of application of AE for the selection of machine components is a method of testing of horizontal conveyor belts in mining industry, developed by A. OPILSKI with his team [52]. The authors found that measurements of events rate and sum of count enable arranging the samples of belts according to their tensile strength. The main difficulty is that the results of measurements vary considerably, according to the dimensions of the sample; it is not possible, therefore, to establish explicitly the standard AE activity, leading to rejection of the belt.

The reasons of mining catastrophes *Composites* be the gas explosions. Therefore the investigations in Poland, especially on the glass fiber-reinforced pipes, are carried out by GOŁASKI and RADZISZEWSKI [53]. They found a distinct relationship between the AE signals and the phases of cracking of these pipes; especially essential is the appearance of the first AE signals at the beginning of the process, when the cracks are undetectable by classical methods. They investigated also the extension of the Kaiser effect appearing in composites [54]. A considerable percentage of defects in composite pipes is produced by the stress corrosion, therefore monitoring of the degree of the stress corrosion is of considerable practical impact. The same authors studied [54] the behaviour of loaded pipes, submerged in neutral media (oil), as well as in chemically active ones (hydrochloric acid solution), and they discovered that in the latter case a distinct rise of the AE activity occurs after a certain period of time. This time depends on the stress value (Fig. 25).

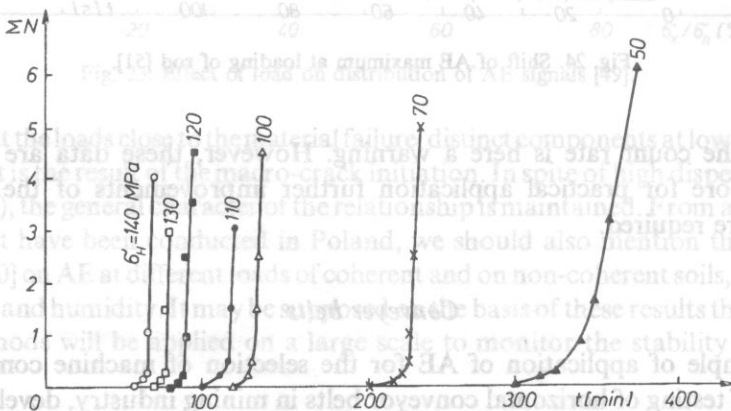


Fig. 25. Effect of environment on stress corrosion of composite pipes [54].

Earlier, Z. PAWŁOWSKI [85] investigated the dependence of the AE counts sum on the load and the time of its action on the glass fibre-reinforced polyester, coming to an empirical formula.

Welding

One of the oldest applications of the AE method was the control of welding [13]. Considerable troubles have been encountered, however, mainly in regard to separation of these AE signals which are generated by welding defects, from the background noise accompanying the welding process. The development of the measuring technique made it possible to overcome these difficulties, mainly by extraction of the characteristic features of the AE signals generated during welding, which appear within a certain period of time after passing of the electrode. In practical application of the method it is possible to detect [55], with a considerable reliability, welding cracks and slag inclusions. As an example, the dependence of the differences in AE signals on the quality of weld is shown in Fig. 26. The cracking processes still proceed, fading gradually, during a few hours after welding. Therefore in certain constructions, such as hulls of ships, the long-term AE monitoring is applied. An important example of using the AE methods in welding technology is a control of weld quality in high-pressure

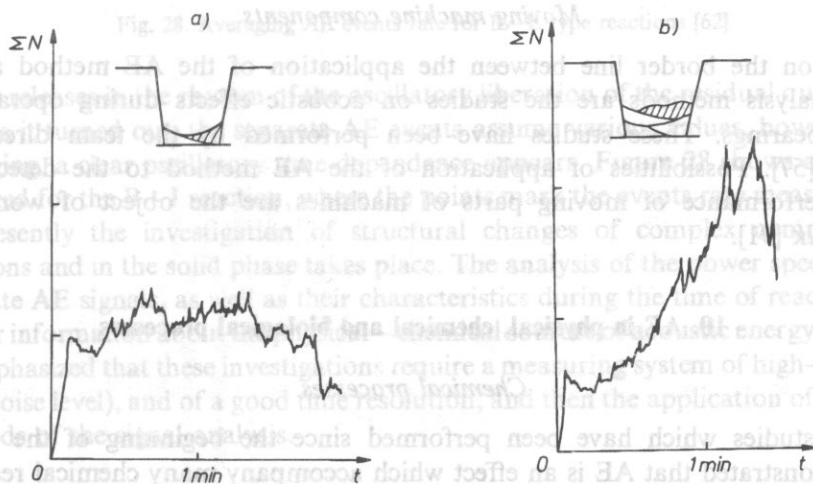


Fig. 26. AE signals from (a) correct, and (b) incorrect weld [56].

pipelines for power plants. The adaptation of the method has been undertaken by SKUBIS and co-workers [56]. A number of samples with welds, cut out of pipelines, were investigated. A general increase of the AE activity was reported, even before plastic deformation, which conforms to the generally known observations in metals. Interesting results were reported concerning the acoustic emission during thermal treatment of a welded pipeline. A typical plot of the sum of count during the treatment is shown in Fig. 27. As it may be seen, the sudden increase of temperature of heated pipeline is accompanied by a rapid growth of the AE activity, which indicates potential possibilities of application of the AE method to monitoring the fitness-for-purpose of long-distance pipelines.

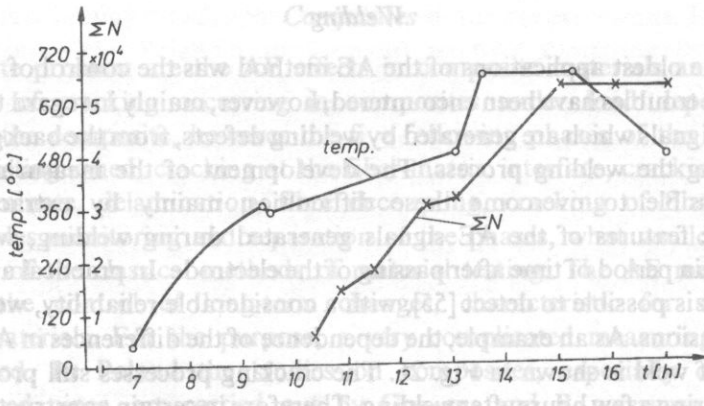


Fig. 27. Sum of count during thermal treatment of nozzle of pipeline [56].

Moving machine components

Just on the border line between the application of the AE method and the noise analysis methods are the studies on acoustic effects during operation of rolling bearings. These studies have been performed by the team directed by CEMPEL [57]. Possibilities of application of the AE method to the detection of faulty performance of moving parts of machines are the object of work of J. ADAMCZYK [91].

10. AE in physical, chemical and biological processes

Chemical processes

The studies which have been performed since the beginning of the eighties [59] demonstrated that AE is an effect which accompany many chemical reactions. The AE method can be therefore utilized, for instance just as the thermal analysis [60], to record the courses of these reactions. The AE measurements and the thermal methods can provide, however, additional information beyond the reach of non-thermal methods in this extent, for instance pertaining to phase transitions. Measurements of the AE which accompany chemical reactions are sometimes very troublesome, because of the low level of the AE signals, strong background noise from the measuring instrumentation, and lateral processes associated with the reaction. The studies performed by RZESZOTARSKA [62] in Poland were focused mainly on the oscillatory reactions. The two oscillatory reactions have been examined using the AE method: the reaction of Biousov—Jabotynski type of oxidation of the malonic acid with bromates, catalyzed by ions of cerium, and the Bray—Liebhavski reaction of decomposition of hydrogen peroxide, in the presence of melanic acid and iodates. The acoustic

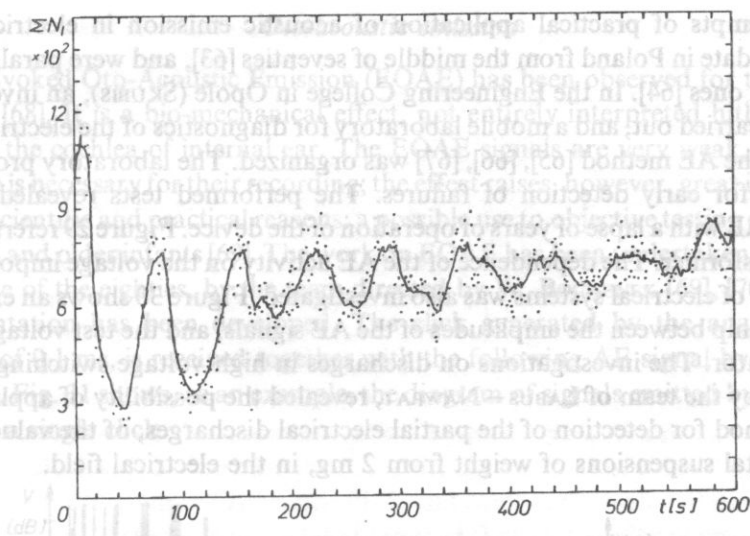


Fig. 28. Averaging AE events rate for B-L type reactions [62].

energy releases in the rhythm of the oscillatory liberation of the residual quantities of gas. As it turned out, the separate AE events assume various values, however, after averaging, a clear oscillatory time-dependence appears. Figure 28 shows a diagram, averaged for the B-J reaction, where the points mark the events rate measurements.

Presently the investigation of structural changes of complex compounds in solutions and in the solid phase takes place. The analysis of the power spectra of the separate AE signals, as well as their characteristics during the time of reaction, may deliver information about the physical-chemical sources of acoustic energy. It should be emphasized that these investigations require a measuring system of high-sensitivity (low noise level), and of a good time resolution, and then the application of statistical methods of the signal analysis.

Electrical discharges

The physical process which can be monitored by the AE method is the partial electrical discharge. These discharges initiate effects which can be audible, because they are confined within the band up to 2 kHz. However the detection of the AE signals of higher frequencies produced by very weak discharges is vital, since they inform about the initial stages of failure. Due to its unique feature, the AE method enables *in-service* monitoring of electrical power devices. However, because of a complex structure of the devices, it is difficult to assess quantitatively the electrical discharges on the ground of the parameters of the AE signals. The second limitation is due to the fact that the signals which are received are coming from discharges occurring in air and oil, whereas the signals approaching from inside of the insulation are strongly attenuated and usually not discernible.

The attempts of practical application of acoustic emission in electrical power engineering date in Poland from the middle of seventies [63], and were parallel in time with foreign ones [64]. In the Engineering College in Opole (SKUBIS), an investigation on AE was carried out, and a mobile laboratory for diagnostics of the electrical power systems by the AE method [65], [66], [67] was organized. The laboratory proved to be very useful for early detection of failures. The performed tests revealed a minor increase of AE with a lapse of years of operation of the device. Figure 29 refers to a high voltage transformer. The dependence of the AE activity on the voltage imposed to the components of electrical systems was also investigated. Figure 30 shows an example of the relationship between the amplitudes of the AE signals, and the test voltage applied to the insulator. The investigations on discharges in high voltage switching stations, carried out by the team of LABUS—NAWRAT, revealed the possibility of application of the AE method for detection of the partial electrical discharges, of the value from 10 pC, and metal suspensions of weight from 2 mg, in the electrical field.

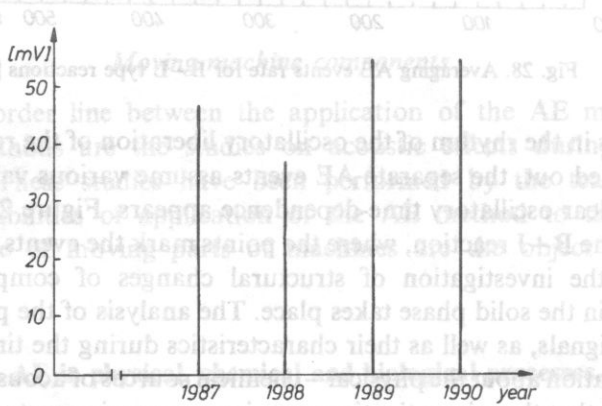


Fig. 29. Increase of amplitudes of acoustic emission produced by discharges in transformer, during four following years [66].

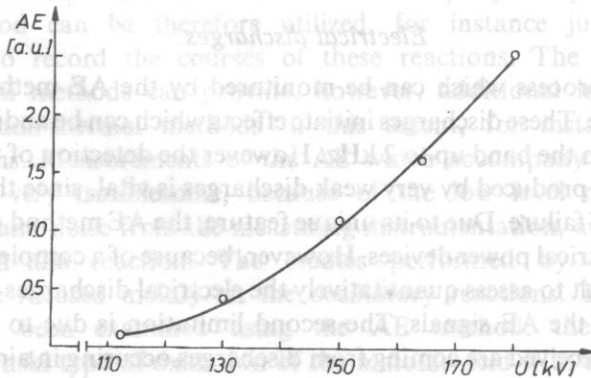


Fig. 30. Dependence of AE amplitude on value of test voltage, from the testing of insulator PKTNK 123/550/630 [67].

Oto-acoustic emission

The Evoked Oto-Acoustic Emission (EOAE) has been observed for the first time by KEMP [68]. It is a bio-mechanical effect, not entirely interpreted hitherto, which occurs in the cochlea of internal ear. The EOAE signals are very weak, so a special technique is necessary for their recording; the effect raises, however, great interest from both the scientific and practical reasons: a possible use to objective testing of hearing of new-born and older infants [69]. The work on EOAE has been undertaken in Poland in the middle of the eighties, by the team directed by W. BOCHENEK [69], [70]. A special instrumentation has been developed. The click generated by the analyzer of the duration of 0.1 ms, is received together with the following AE signal by a miniature earphone. Fig. 31 shows, as an example, the diagram of signals emitted by an ear after imposing a single click.

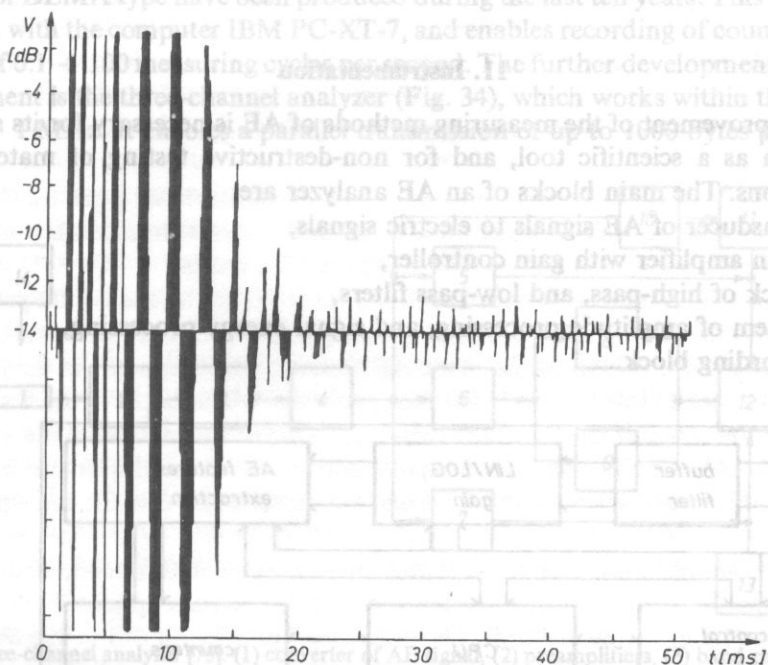


Fig. 31. Evoked oto-emission versus time as effect of single click [70].

The differentiation of the nonlinear component of AE has been performed (Fig. 32). The bars on the graph are proportional to the instantaneous values of these components. The existence of the nonlinear component seems to be an interesting information about the occurring processes. The results obtained are not unequivocal, they enable, however, to draw the conclusion that in the majority (approx. 80%) of young and healthy persons the EOAE clearly occurs.

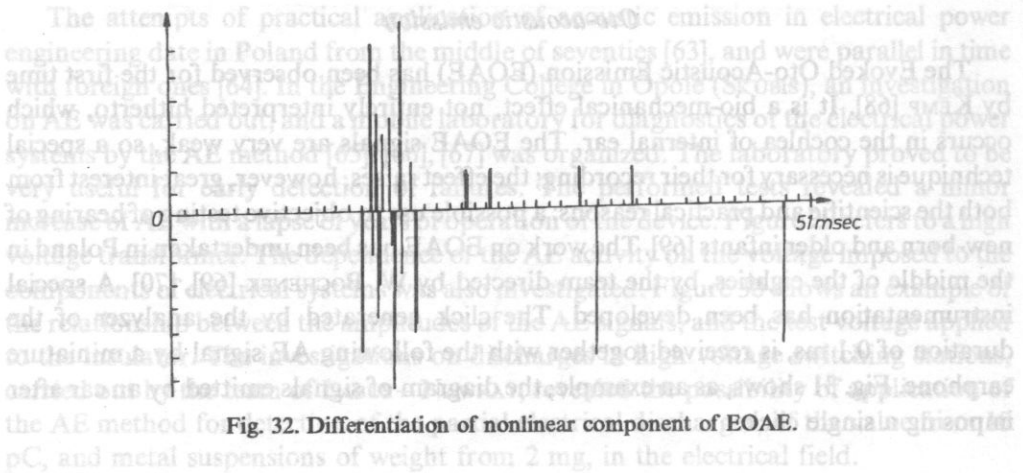


Fig. 32. Differentiation of nonlinear component of EAOE.

11. Instrumentation

The improvement of the measuring methods of AE is necessary for its successful application as a scientific tool, and for non-destructive testing of materials and constructions. The main blocks of an AE analyzer are:

- transducer of AE signals to electric signals,
- main amplifier with gain controller,
- block of high-pass, and low-pass filters,
- system of amplitude processing, and signal energy processing,
- recording block.

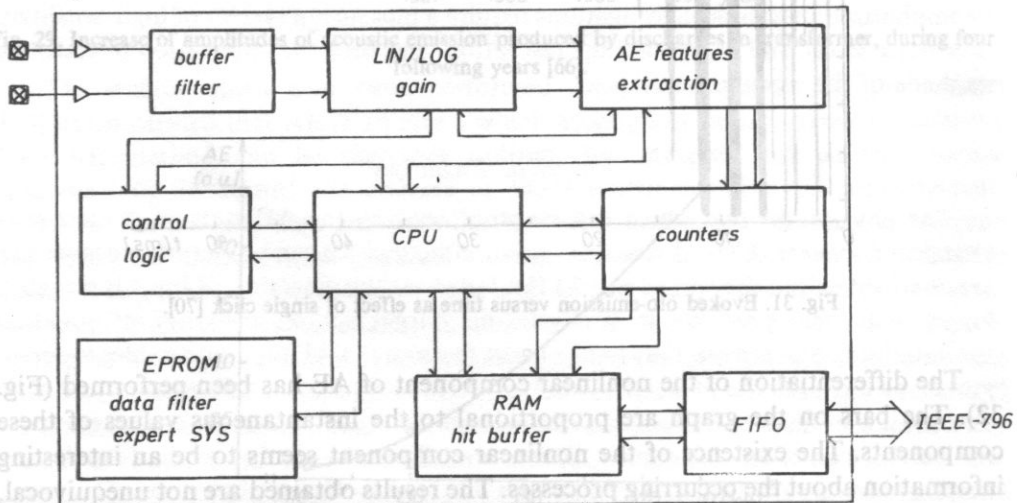


Fig. 33. Transient recorder board (TRA 2.5M) can acquire signals from an ICC output or sensor. The signal is digitized and stored in a 2.5 MB RAM and can be accessed from FFT/Transient recorder [83].

The broad-band and resonant transducers are applied. The analysis of the AE signal parameters is usually preceded by conversion to the binary form, and is performed as a digital process, an essential parameter being the „dead” time. The block diagram of the transient recorder is shown in Fig. 33. For laboratory tests a single measuring channel is usually sufficient, while for the *in situ* measurements of technical objects multi-channel instruments are applied to simultaneous recording of AE signals. It is necessary for the location of the AE sources, for instance. Presently, numerous firms offer the instruments for the AE measurements, of different degrees of complexity: universal or adapted to special tasks.

In Poland, first designs of the analyzers of the AE signals appeared in the middle of seventies (Z. PAWŁOWSKI) [74]. Most widespread are the AE analyzers produced by the Institute of Fundamental Technological Research of the Polish Academy of Sciences; their chief designer is Z. RANACHOWSKI [75], [76], [82]. The different variations of the analyzer of DEMA type have been produced during the last ten years. This analyzer is combined with the computer IBM PC-XT-7, and enables recording of counts with the velocity of $0.1 \div 100$ measuring cycles per second. The further development of this lot of equipment is the three-channel analyzer (Fig. 34), which works within the band of $50 \text{ kHz} \div 1 \text{ MHz}$. It enables a parallel transmission of up to 1000 bytes per second.

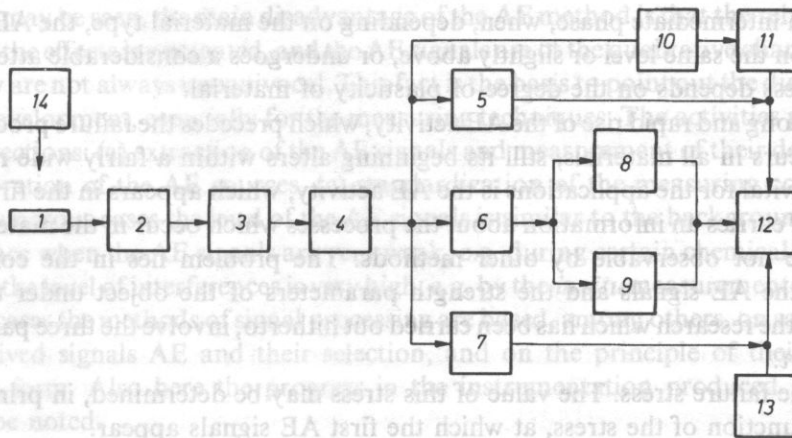


Fig. 34. Three-channel analyzer [75]. (1) converter of AE signal, (2) preamplifiers, (3) band-pass filters, (4) tunable amplifiers, (5) rms value detectors, (6) noise discriminators, (7) pulse counters, (8) delay counter, (9) sample load measuring system, (10) computer interface.

The analyzer can count pulses in two modes. In the first mode, the scalar counts pulses in the intervals 0.1, 1, and 10s, and after the end of the cycle the signals are transferred to the computer. In the second mode the instrument waits for the first signal, and afterwards the suitable channel is blocked; the instrument measures the time delay of the signals coming from the remaining two channels.

The new analyzer, which is now being designed, operates on the principle of the pattern recognition. The analyzer enables simultaneous measurements of

the following AE descriptors: count sum and rate, sum and rate of events, RMS, and signal peak value, parameter of the mechanical load. The operating memory extended to 4 MB enables 500 transmissions per second. The sampling is performed at the frequency of 1 MHz.

12. Scientific and technical problems of AE method

The domains of AE application discussed above have many features in common, therefore the AE methods should be analyzed on a broad basis, taking as a reference point the common measuring techniques and fundamental research [79]. By means of the AE method, the different objects and physical processes are investigated. The most important application consists in monitoring of the AE signals during increase of the mechanical stress. As it has been discussed above, the plot of the count rate, or the count sum versus the stress has a different shape, depending on the material type. Generally however, the following three phases may be distinguished:

(1) Appearance of the first AE signals, which, depending on the material type, grow slower or faster together with the increase of the stress. It takes place after the appearance of stable micro-cracks, still in the range near the limit of elastic deformations.

(2) An intermediate phase, when, depending on the material type, the AE activity remains on the same level or slightly above, or undergoes a considerable attenuation. The process depends on the degree of plasticity of material.

(3) Strong and rapid rise of the AE activity, which precedes the failure process. This phase occurs in all materials, still its beginning alters within a fairly wide range.

Most vital for the applications is the AE activity, which appears in the first phase, because it carries an information about the processes which occur in the material, and which are not observable by other methods. The problem lies in the correlation between the AE signals and the strength parameters of the object under test. The results of the research which has been carried out hitherto, involve the three parameters of the sort.

(a) The failure stress. The value of this stress may be determined, in principle, as a linear function of the stress, at which the first AE signals appear.

(b) „Life-time” of the material. The „life-time” prediction can be drawn from the analysis of the AE signals, first of all for brittle materials.

(c) The degree of material fatigue, or the „history” of the material. Because of the structural changes, and the Kaiser effect, the differences of the AE activities can be found by comparing the new material with that used in machinery or construction elements.

The second group of the AE methods concerns the objects under normal operation conditions. The scale of such objects is very wide, and comprises for instance: high pressure vessels, shields of nuclear reactors, dams, mining tunnels and shafts. In this case the laboratory tests on samples may provide only preliminary information, while the *in situ* inspection of entire objects is necessary. It increases the range of difficulties

in determination of the time correlation between the abnormalities which exist in the controlled object and the AE signals.

The experience that has been collected till now shows that the AE method enables the detection of:

- (a) local increase of mechanical stress,
- (b) initial displacements of the medium,
- (c) leakage of gas or liquid from untight objects,
- (d) local thermal disturbances.

An alarming signal may be considered to be the appearance of the first AE signals or increase of the events rate, exceeding a certain threshold value. An advantage of the AE method consists in the fact that it monitors dangerous effects earlier than other methods can do. Unfortunately, this monitoring is not entirely reliable and quantitatively determinable.

The third group of methods is connected with monitoring of the technological processes. It concerns the chemical reactions occurring due to the thermal treatment, during which the phase structure changes. The AE method enables us to indicate the beginning of the process, and to assess approximately its intensity. The main troubles lie in the extraction of the AE signals from the background noise, and in relating the AE signals to the parameters of the running process.

As it may be seen, the main disadvantage of the AE method is that the relationships between the effects investigated, and the AE signals are of the qualitative character, and that they are not always unequivocal. This fact is the basis to point out the directions of future development, especially for the measuring techniques. The activities proceed in three directions: (a) extraction of the AE signals and measurement of their descriptors, (b) calibration of the AE sources, (c) standardization of the measuring conditions.

In numerous cases the level of the AE signals is similar to the background noise, it takes place when the AE signals are very weak, e.g. during certain chemical reactions, or when the level of interferences is very high, e.g. by the *in situ* measurements in mines. In both cases the methods of signal processing are based, among others, on sampling of the received signals AE and their selection, and on the principle of their specific, iterative form. Also here the progress in the instrumentation produced in Poland should be noted.

Another direction of development consists in limitation of the sources of disturbances, for instance in the testing machines.

The records of the AE signals, plotted against the time axis, especially these coming from the continuous emission, look seemingly chaotic, therefore it is essential to apply a proper technique of the signal processing to obtain the parameters which are correlated with the physical quantities of interest. In the literature [61] the proposals of several descriptors of AE signals can be found. Also interesting are the proposals of the Polish authors concerning, for example, determination of the energy related to a single event [48] and the analysis of usefulness of the AE descriptors [88]. Nevertheless, on the grounds of the work done as yet, it is difficult to decide which of the descriptors might be the most commonly used; the question is still open.

The acoustic—electronic channel for the AE signal transfer contains so many elements, transmission coefficients of which are difficult to determine, that assigning the absolute values to the AE signals appears to be a very difficult task. Determination of such a value is, on the other hand, without practical significance, because a comparison of the measured signals with the simulated AE sources was an object of research long since [71], [72]. The most frequently applied simulated sources are:

- stream of gas,
- breaking of capillary or pencil lead,
- falling ball,
- standard electromagnetic or electrostatic transducer,
- laser pulse.

The comparative analysis of the first three types of the simulated sources was also performed in Poland [89]. These sources are in common use, each of them having its own advantages and defects. The trouble is that the standards used in different laboratories do not always correspond to each other, while in reports and papers the references concerning the standards used are usually not included. So the wide international exchange of experiences, as well as spreading of the best standards among the laboratories throughout the world, would be highly desirable.

To obtain comparable results of testing, standardization of the reference simulated sources together with the intermediate blocks will not be fully satisfactory. The standardization of the measuring conditions is also desirable. During laboratory strength measurements the dimensions of the samples are usually in accordance with the obligatory standards, and it does not create any problem. Instead, the acoustic-electronic channel is developed in a very individual manner, and certain standardization would be useful. It might encompass:

- coupling media,
- transmission characteristics of the transducer,
- characteristics of filters and gates,
- determination of discrimination levels of AE signals.

Standardization of the references simulated sources and terminology has been initiated by the European Working Group on Acoustic Emission [78], the work is continued.

When selecting particular descriptors, their parameters should be determined.

The above mentioned necessity of switching from the qualitative observations to the comparable, quantitative measurements relates to the need of undertaking certain research. It should be focused, among other things, on:

- (a) Collecting more data concerning the relationship between AE and stress in various materials. The statistic analysis of the data will enable a better determination of the connection of AE with the mechanical strength of material [73].
- (b) The relationship between the original AE signal and the value obtained during the measurement. In spite of numerous attempts, the through knowledge of the mechanism of AE signals generation remains open. It is of great cognitive importance to have a AE method capable of providing unique information about the physical micro-processes that take place in various materials and media.

The investigations might concern:

- (a) Generation of AE by groups of dislocations;
- (b) Relationship between appearing of the plastic zones at micro-cracks and the AE signals;
- (c) The effect of the changes of material microstructure, together with the phase transitions, on the AE;
- (d) Generation of the AE signals during chemical reactions.

The AE signals distinguish themselves by a great variety of time-dependence. The general division into continuous and burst emissions is not satisfactory. A more detailed classification of the AE signals coming from different sources, based on the selected descriptors, would be desirable.

Acknowledgment

The present work has been sponsored by the State Committee for the Scientific Research (KBN), grants No. 33148-92-03 and 70761-91-01.

References

- [1] L. OBERT, U.S. Bur. Mines. Rep. Invest. R1-3555 (1941).
- [2] E.A. HODGSON, Bull. Seismol. Soc. Am. **32**, 249 (1942).
- [3] J. KAISER, Arch. f. Eisenhüttenwesen, **25**, 43 (1953).
- [4] G.A. TARTO, R.G. LIPTAI, Proc. Symp. Phys. Non-destructive Testing, San Antonio, Texas (1962).
- [5] H.L. DUNEGAN, D.O. HARRIS, Ultrasonics, **7**, 160 (1969).
- [6] J.R. FREDERICK, Mater. Evolution, **28**, 43 (1970).
- [7] A.G. KONSTANTINOVA, Dokl. Acad. Sc. USSR, ser. Geofiz. **15**, 135-137 (1962).
- [8] W.W. GERBERICH, C.E. HARTBOWER, Intern. J. Fract. Mech., **3**, 1987 (1967).
- [9] K. MOGI, Bull. Earthquake Res. Int., **41**, 615 (1963).
- [10] P.H. HUTTON, D.L. PARRY, Material Res. Stand., **11**, 25 (1971).
- [11] J. NAKAMURA, Materials Eval., **29**, 8 (1971).
- [12] A.E. LORD, Physical Acoustic, ed Mason Acad. Press. N.Y.
- [13] K. NOTVEST, Welding J., N. York, **45**, 173 (1966).
- [14] J. RANACHOWSKI, editor Problems of Acoustics (in Polish), CPBP No 02.03, Institute of Fundamental Technological Research, Warsaw (1990).
- [15] K. ONO, Mat. Evaluation, **34**, 177 (1976).
- [16] H.L. DUNEGAN, A.T. GREEN, Proc. Symposium ASTM, Bul Harbour, 505 (1972).
- [17] D.R. JAMES, S.H. CARPENTER, J. Appl. Phys., **42**, 4685 (1971).
- [18] A.B.L. AGERWAL, J.R. FREDERICK, D.K. FELBECK, Metall Transact., **1**, 1069 (1970).
- [19] A. PAWELEK, H. DYBIEC, W. BOCHNIAK, W. STRYJEWSKI, Arch. of Metallurgy, **33**, 645 (1988).
- [20] S. PILECKI, J. SIEDLACZEK, Arch. Acoust., **14**, 261-281 (1989).
- [21] S. PILECKI, Bull. Pol. Ac. Sc. Ser. Techn. Sc., **17**, 489-496 (1969).
- [22] S. PILECKI, J. SIEDLACZEK, Arch. Acoust., **16**, (1991).
- [23] J.C. GROSSKREUTZ, Phys. Stat. Solidi (B), **47**, 359 (1971).
- [24] J. SIEDLACZEK, S. PILECKI, F. DUSEK, Arch. Acoust., **15**, 465-476 (1990).
- [25] H. NAMURA, K. TOSHICA, K. KOYAMA, T. SEKOI, Cryogenics, **17**, 47 (1977).
- [26] Y. XU, W. GUAN, K. ZEIBIG, C. HEIDEN, Cryogenics, **29**, 281 (1989).

- [27] L. WOŹNY, B. MAZUREK, J. RANACHOWSKI, *Physica B.*, **173**, 309 (1991).
- [28] I. WOŹNY, B. MAZUREK, J. RANACHOWSKI, *Bull. Pol. Ac. Sc. Ser. Techn. Sc.*, **39**, 321 (1991).
- [29] Z. WITCZAK, J. KRÓLIKOWSKI, *Proc. 12 ATRAP and 25 EHPRG Conference Padeborn* (1989).
- [30] A.A. GRIFFITH, *Phil. Trans. Roy. Soc. London A* 221 (1920).
- [31] A.G. EVANS, M. LINZER, *J. Amer. Ceram. Soc.*, **56**, 575 (1973).
- [32] J. RANACHOWSKI, F. REJMUND, *Scientific Instrumentation*, **4**, 17–47 (1989).
- [33] J. RAABE, E. BOBRYK, W. PETROWSKI, Z. RANACHOWSKI, *Electronic materials* **2**, (in Polish). 34–38 (1992).
- [34] T.C. HSU, F.G. SLATE, H.G. STURMAN, *Journ. ACJ*, **60**, 209 (1963).
- [35] J. HOŁA, A. MOCZKO, *Brittle matrix composites 1*. ed. Brand – Marshall Elsevier Appl. Sc. London 527 (1986).
- [36] J. PYSZNAK, J. HOŁA, *Arch. Acoust.*, **16**, 155 (1991).
- [37] J. HOŁA, *Arch. Civ. Eng.*, **39**, 1–2 (1992).
- [38] A. KUŚNIERZ, K. FLAGA, *Conf. Com. Civ. Eng. – WAT, Krynica* **4**, 85 (1987).
- [39] S. MINDESS, *Int. Journ. of Cement composites*, **4**, 173–179 (1982).
- [40] P. NIEMZ, A. HÄNSEL, *Holztechnologie*, **24**, 91–95 (1983).
- [41] K. SATO, T. OKANO, J. ASANO, M. FUSHITANI, *J. Acoust. Emis.*, **4**, 240 (1985).
- [42] W. MOLIŃSKI, J. RACZKOWSKI, S. POLISZKO, J. RANACHOWSKI, *Holzforschung*, **45**, 13 (1991).
- [43] C.H. SCHOLZ, *J. Geoph. Research*, **73**, 1447–1454 (1968).
- [44] M. CHUDEK, T. ZAKRZEWSKI, *Mining Review*, **5**, 83 (1985).
- [45] A. OPILSKI, F. WITOS, Z. RANACHOWSKI, *Acoust. Letters*, **8**, 109–114 (1985).
- [46] R.M. KOERNER, W.M. Mc CABE, A.E. LORD, *Rock Mechanics*, **14**, 27 (1981).
- [47] W.W. KRILOW, *Acoust. Journ.*, **30**, 790–798 (1983).
- [48] M. JAROSZEWSKA, *Arch. Acoust.*, **15**, 3–4 (1990).
- [49] M.C. REYMOIND, M. JAROSZEWSKA, *Journ. d'Acoustique*, **4**, 525–533 (1991).
- [50] J. SKRYNICKI, *Proc. World Congr. NDT Amsterdam* (1989).
- [51] Z. KOWAL, J. SENKOWSKI, *Arch. Acoust.*, **17**, 191 (1992).
- [52] F. WITOS, A. OPILSKI, A. LUTYŃSKI, *Ultrasonics*, **27**, 182–185 (1989).
- [53] L. GOŁASKI, L. RADZISZEWSKI, *Beitrage zum 8 Koll. Schallemission Zitau* (1990).
- [54] L. GOŁASKI, L. RADZISZEWSKI, *Proc. 3th Symp. on Acoust. Emiss. ASNT Paris* 101–108 (1989).
- [55] D.W. PRINE, *Journ. Non-destr. Test.*, **9**, 281–284 (1976).
- [56] J. SKUBIS, G. JEZERSKI, J. RANACHOWSKI, *Reports of IFTR* 11 (1992).
- [57] C. CEMPTEL, M. MAJEWSKI, M. GOLEC, *Proceedings Noise Control 88 Cracow* **1**, 5–7 (1988).
- [58] M. ALEKSIEJUK, J. RAABE, J. RANACHOWSKI, *Arch. Acoust.*, **16**, 387–412 (1991).
- [59] D. BETTERIDGE, M.T. JOSLIN, T. LILLEY, *Anal. Chem.*, **53**, 1064–1072 (1981).
- [60] S. SHIMADA, *Thermochemica Acta*, **196**, 237 (1992).
- [61] A.P. WADE, K.A. SOLSBURY, P.Y.T. CHOW, J.M. BROCK, *Analit. Acta. Chem.*, **246**, 23–42 (1991).
- [62] W. MIKIEL, J. RANACHOWSKI, F. REJMUND, J. RZESZOTARSKA, *Arch. Acoust.*, **15**, 185–192 (1990).
- [63] J. SZUTA, *Energetics* (in Polish). **8**, 336 (1978).
- [64] R.T. HARROLD, *EEE Trans.*, **11**, 8 (1978).
- [65] J. ZALEWSKI, J. SKUBIS, B. GRONOWSKI, *CIGRE Report 15-05/85-27*, Berlin (1985).
- [66] J. SKUBIS, *7th Symp. Technical Diagnostics IMEKO, Helsinki* 286 (1990).
- [67] J. SKUBIS, *7th JSR Dresden Report* 73.05, 109 (1991).
- [68] D.T. KEMP, *J. Acoust. Soc. Am.*, **62**, 1386–1391 (1987).
- [69] W. BOCHENEK, I. MALECKI, Z. RANACHOWSKI, *Proc. 6th FASE Congress Zurich* 31–34 (1992).
- [70] W. BOCHENEK, J. KICIAK, *Congress Franc. Oto-Ringo-Laryngologie Paris 1990 Proc. Libr. Arnette* 137–141 (1991).
- [71] N.N. HSU, F.R. BRECKENRIDGE, *Materials Eval.*, **39**, 60–67 (1979).
- [72] G. ULHMAN, *Zentral Inst. f. Kernforschung Dresden, Blatt* 689 (1989).
- [73] I. MALECKI, J. RANACHOWSKI, *Proc. 14 ICA Congress Beijing, paper* L1–1 (1992).
- [74] P. KARPINIUK, Z. PAWLOWSKI, *Proc. 7th Int. Conf. Non-destructive Testing, Warsaw*, **2**, 211 (1973).

- [75] J. RANACHOWSKI, F. REJMUND, *Scientific Instrumentation*, 5, 167–192 (1990).
- [76] M. BONIECKI, Z. LIBRANT, W. WŁOSIŃSKI, W. MIKIEL, Z. RANACHOWSKI, H. RYLL-NARDZEWSKI, *Glass and ceramics*, 33, 29–43 (1982).
- [77] Z. RANACHOWSKI, *Brittle matrix composites* (book). ed. Brandt Elsevier 234–239 (1991).
- [78] EWGAE Codes, *NDT Intern.* 18, 185–193 (1985).
- [79] R. HILL, Proc. 14 ICA Congress, Beijing, paper L1–5 (1992).
- [80] *Problems and methods of nontemporary acoustics* (book in Polish). ed. J. RANACHOWSKI, vol. 2, PWN Warsaw (1989).
- [81] *Problems and methods of nontemporary acoustics* (book in Polish). ed. J. RANACHOWSKI, vol. 2, PWN Warsaw (1991).
- [82] Acoustic Emission cd., I. MALECKI, J. RANACHOWSKI, (book in Polish). in preparation.
- [83] J. RANACHOWSKI, F. REJMUND, Z. LIBRANT, *Investigation of brittle media by AE method on example of ceramics and concretes*. Reports of IFTR No. 28, Warsaw (1992)..
- [84] Z. PAWŁOWSKI, W. WOJDOWSKI, M. KIERSNOWSKI, *Wiss. Berichte IHZ Zittau*, 11, 6–9 (1986)..
- [85] Z. PAWŁOWSKI, Proc. VII Int. Congress of Non-destr. Testing, Warsaw, paper 7–07 (1973)..
- [86] Z. PAWŁOWSKI, B. PAWŁOWSKA, Proc. XII World Congr. Non-Destr. Testing, Elsevier Science Publ. Amsterdam V 1490–1492 (1989)..
- [87] S. PILECKI, *Archiwum Akust.*, 21, 1, 109–113 (1986)..
- [88] F. WITOS, Reports of IFTR, Warsaw (in print)..
- [89] M. MEISSER, Z. RANACHOWSKI, Reports of IFTR, Warsaw (1992)..
- [90] J. RACZKOWSKI, W. MOLINSKI, Z. RANACHOWSKI, Reports of IFTR No. 27, Warsaw (1992)..
- [91] J. ADAMCZYK, *Mechanika*, Cracow 2, 20 (1989)..
- [92] F. WITOS, A. OPILSKI, Proc. 14 ICA Congress, paper L1–4, Beijing (1992).

Received January 2, 1993

The organ is an instrument which changes continually with durable traces left by each passing epoch on both an external structure and internal elements. No other instrument has passed so long a path of development as the organ did since the times of Ktesibos of Alexandria or those of Heron's water organ till the present times.

From the musical point of view mechanically controlled organs built in the period of baroque are still an unattainable model owing to the fact that this type of control enables possibilities for musical articulation. The contact between the organist and the pipe organ being established right at the moment of touching the key. The possibility of modifying the way in which the sound intensity increases depends on the resistance of the key, which is connected mechanically with the valve of the wind-chest and is stronger at the beginning due to the compressed air, which presses the valve against the air inlet part, then is reduced to merely a value necessary for overcoming the resistance of the return spring of the key. In the opinion of many organists this two-phase nature of resistance of the key makes it possible for the organist to modify the process of growth of the sound [1], [9].

In the course of evolution of control systems of the organ, the pneumatic, then electric systems were invented, which made the task of organ playing much easier, but introduced a "foreign force" between the key and the source of sound, thus making the performance much poorer in respect of variety of musical articulation.

INVESTIGATION OF ARTICULATION FEATURES IN ORGAN PIPE SOUND

B. KOSTEK and A. CZYŻEWSKI

Sound Engineering Department of the Technical University of Gdańsk
(80-952 Gdańsk, ul. Narutowicza 11/12).

The aim of the paper is to approach the problem of existing limitations in the articulation of sound in a pipe instrument with electromagnetic action. The importance of attack transients in articulation phenomena is examined. Hence, detailed investigations in the domain of attack transients in pipe sound were carried out. The applied methods and the results of analyses are discussed.

1. Introduction

The organ is an instrument which changes continually with durable traces left by each passing epoch on both an external structure and internal elements. No other instrument has passed so long a path of development as the organ did since the times of Ktesibos of Alexandria or those of Heron's water organ till the present times.

From the musical point of view mechanically controlled organs built in the period of baroque are still an unattainable model owing to the fact that this type of control enables possibilities for musical articulation. The contact between the organist and the pipe organ being established right at the moment of touching the key. The possibility of modifying the way in which the sound intensity increases depends on the resistance of the key, which is connected mechanically with the valve of the wind-chest and is stronger at the beginning due to the compressed air, which presses the valve against the air inlet part, then is reduced to merely a value necessary for overcoming the resistance of the return spring of the key. In the opinion of many organists this two-phase nature of resistance of the key makes it possible for the organist to modify the process of growth of the sound [1], [9].

In the course of evolution of control systems of the organ, the pneumatic, then electric systems were invented, which made the task of organ playing much easier, but introduced a "foreign force" between the key and the source of sound, thus making the performance much poorer in reflect of variety of musical articulation.

¹ Research sponsored by Komitet Badań Naukowych (KBN) in 1992.

At this point it seems to be indispensable to give a more detailed definition of the notion of articulation, which is used in the domain of music for describing the way in which the musical fragment considered should be performed according to the musical notation. The latter term is secondary and concerns all the conventional marks describing the way of getting a tone or a chord to obtain intended acoustic effect and to emphasize the character of musical work. Principal types of articulation are denoted by conventional signs such as *staccato* (in abrupt, sharply detached manner, *Italian staccare* = to detach, to disconnect), *spiccato* (distinctly, emphatically, *It. spiccare* — to separate, to disconnect, to speech distinctly), *legato* (smoothly, without breaks, *It. legare* — to bind), *portato* (with smooth, not abrupt separation of tones, *It. portare* — to carry), *glissando* (gliding continuously from one pitch to another, *It.*), *portamento* (slight gliding, in singing or violin playing, between two distant tones, *It.*), *tremolo* (trembling, *It. tremolare* — to tremble), *arpeggio* (striking of notes of chord in succession, *It.*, in harp-like manner) and a number of signs, among which there are those of trill, turn of grace note (*appoggiatura*), long and short [7]. As regards various kinds of music or even particular instruments, the evolution of articulation elements was independent. The style of interpretation of organ music is influenced by not only articulation notation but also the type of control system and acoustic properties of the interior in which the organ has been installed.

The aim of the present paper is to discuss results of the research carried out by authors concerning articulation problems of organ sound and analyses which have been made.

2. Analytical description of transient or organ pipe sound

The mechanism of producing vibrations in self-excited aero-acoustic systems such as flue pipes is not yet sufficiently known, the fundamental difficulty being that of efficient separation from the organ pipe system of its component parts that is the system of excitation and vibration. Those systems are connected with each other in a dynamic manner which is a result on the one hand, of contraction inside the air stream flowing out from the pipe slot, defined by the edge of languid and the lower lip of the pipe mouth and, on the other hand, a result of the action of the air column vibrating inside the body of the pipe on the transient values of the velocity vectors of particles of the air jet. Because in the organ pipe system the action of the vibrating air column is essential the mechanism of exciting vibrations in a flue pipe is defined as a process of turbulence type excitation, although the Reynolds number characterizing the flow considered does not exceed, as a rule, a critical value of 2300 which separates the laminar from turbulent flow [2].

The method for analysis of transients in organ sound, based on the nonlinear theory of generation of vibrations in a flue pipe is the subject of Fletcher's studies [2], [3]. He treats an organ pipe as a system constituting two coupled subsystems, namely a linear resonator system with an infinite number of natural vibrations the angular frequency of which is n_i and a nonlinear system of air stream with disturbances of the

vortex layer about the upper lip vibrating with an angular frequency ω_i . Taking into consideration damping due to radiation of internal friction and heat conduction the former system can be described by the following second order differential equation [3]:

$$\ddot{x}_i + k_i \dot{x}_i + n_i^2 x_i = \lambda_i F(t) \quad (1)$$

where: n_i — angular frequency of the i -th mode of linear resonator, $F(t)$ — external force, x_i — displacement of the i -th vortex of the air stream, λ_i — coefficient of coupling between the pipe and the air stream, k_i — coefficient of damping.

If the amplitude of $F(t)$ is constant, and the frequency being the only variable, the amplitude of the resonance frequency is in direct proportion to the ratio λ_i/k_i and its width to k_i .

In the static case, for which it is assumed that acoustic velocity of the air stream v at the outlet of the pipe is constant, the force F can be expressed by the power series expansion:

$$F = c_0 + c_1 \cdot v + c_2 \cdot v^2 + c_3 \cdot v^3 + \dots \quad (2)$$

where: c_n — coefficients of the pressure function of the air system, v — acoustic velocity of the air stream.

In reality the pipe is a nonlinear dynamic system. Oscillations of the air column of acoustic velocity v act on the air stream leaving the inlet aperture, thus producing variations of the force F as a function of the acoustic velocity ($v \sum \dot{x}_i$). The resulting pressure response is established with a certain delay δ , which is equal to the time of displacement of single vortex along the air stream, necessary for the passage across the mouth of the pipe. It should also be borne in mind that the air stream may dissipate its energy in such a manner that δ depends on the frequency. This interaction may result in a phase shift Δ . The frequency ω_i of the i -th natural vibration is related to the resonance frequency n_i , therefore the generalized equation (2) takes the form (3):

$$F(t) = \sum_{m=0}^{\infty} c_m \left[\sum_{i=1}^{\infty} \dot{x}_i (t - \delta_i - \Delta_i/\omega_i) \right]^m \quad (3)$$

where: δ_i — time necessary for a single vortex to be displaced along the air stream leaving the organ pipe mouth, Δ_i — phase shift.

If the feedback in the nonlinear system composed of the organ pipe and the stream is taken into account, the equations (1) and (3) can be expressed in the form:

$$\ddot{x}_i + n_i^2 \cdot x_i = f_i(\dot{x}_j) \quad (4)$$

where:

$$f_i(\dot{x}_j) = -k_i \cdot \dot{x}_i + \lambda_i \cdot F(\dot{x}_1, \dot{x}_2, \dots) \quad (5)$$

Despite the intense development of the theory of nonlinear vibrations, there is no universal method for analysis and solution of a set of nonlinear equations. In the analysis of nonlinear vibrations in the neighbourhood of equilibrium position,

nonlinear systems are linearized usually by the Krylov-Bogolubov method or that of a series of small parameters or the Van-der-Pol method [4]. If the solution of nonlinear equation is an oscillating solution with a time variable amplitude and phase, the variations being very slow, however, the method of slowly varying parameters is used. The condition of slow variation originates from the fact the solution can be obtained only if transient values varying parameters is used. The condition of slow are replaced by their average values found by integrating over a period of the vibrations. An oscillating solution can also be obtained by methods based on the principle of equilibrium of harmonics. In practice high accuracy solution cannot be obtained, however, therefore it is often necessary to use several methods simultaneously. Using the first two methods a periodic solution of the nonlinear equation is sought for in the form of a power series, the convergence of which is ensured for a sufficiently small f_i .

By reducing the original nonlinear second order equation to the form (4) and (5) the nonlinear terms can be separated, so that a periodic solution of the linear equation is obtained as a first approximation.

Assuming that f_i is sufficiently small as compared with the terms on the left-hand side of (4), the possible solution of that equation may assume the form:

$$x_i = a_i \cdot \sin(\omega_i t + \beta_i) \quad (6)$$

where: $\omega_i \simeq n_i$, a_i — amplitude, β_i — phase displacement, a_i, β_i — constants depending on the initial conditions.

For further computation it is assumed that the terms a_i and β_i are functions of time. On differentiating x_i with respect to time one obtain:

$$\dot{x}_i = a_i \cdot \omega_i \cdot \cos(\omega_i t + \beta_i) + \dot{a}_i \cdot \sin(\omega_i t + \beta_i) + a_i \cdot \dot{\beta}_i \cdot \cos(\omega_i t + \beta_i) \quad (7)$$

If the derivate \dot{x}_i is to take form:

$$\dot{x}_i = a_i \cdot \omega_i \cos(\omega_i t + \beta_i) \quad (8)$$

the condition:

$$\dot{a}_i \sin(\omega_i t + \beta_i) + a_i \dot{\beta}_i \cos(\omega_i t + \beta_i) = 0 \quad (9)$$

must be satisfied. Substituting the derivatives of the periodic solution into equation (4) gives, if the condition (9) is satisfied, a set of equations, from which \dot{a}_i and $\dot{\beta}_i$ are found:

$$\dot{a}_i = \frac{1}{\omega_i} f_i(\dot{x}_j) \cos(\omega_i t + \beta_i) - \frac{a_i(n_i^2 - \omega_i^2)}{\omega_i} \cdot \sin(\omega_i t + \beta_i) \cdot \cos(\omega_i t + \beta_i) \quad (10)$$

$$\dot{\beta}_i = \frac{1}{a_i \omega_i} \cdot f_i(\dot{x}_j) \sin(\omega_i t + \beta_i) + \frac{(n_i^2 - \omega_i^2)}{\omega_i} \cdot \sin^2(\omega_i t + \beta_i) \quad (11)$$

If the functions $\dot{a}_i, \dot{\beta}_i$ are replaced by their average values, which will be denoted by $\langle \dot{a}_i \rangle$ and $\langle \dot{\beta}_i \rangle$, respectively, and which are found by integrating the right-hand forms of the above equations over one vibration period, one obtain:

$$\langle \dot{a}_i \rangle = \frac{1}{\omega_i} \cdot \langle f_i(\dot{x}_j) \cos(\omega_i t + \beta_i) \rangle \quad (12)$$

$$\langle \dot{\beta}_i \rangle = -\frac{1}{a_i \omega_i} \cdot \langle f_i(\dot{x}_j) \sin(\omega_i t + \beta_i) \rangle + \frac{(n_i^2 - \omega_i^2)}{2\omega_i} \quad (13)$$

Assuming that the vibrations are stationary these functions may be expanded in Fourier series. In this case the aim of the integration operation is to separate the harmonics ω_i from the functions $f_i(\dot{x}_j)$.

A condition of the nonlinear set of equations of oscillations in an organ pipe being solvable in the harmonic form (6) with the parameters a_i and β_i varying slowly in time, is that all the secular terms in (12) and (13), that is terms of the type $t \sin \omega t$ and $t \cos \omega t$, which are markedly dependent on time are to be neglected. Those terms, the character of which does not vary for a few periods are retained. Moreover, the average values $\langle \dot{a}_i \rangle$ and $\langle \dot{\beta}_i \rangle$ should be sufficiently small as compared with a_i , ω_i .

The averaging operation which has been performed in equations (12) and (13) as a first approximation confirms the variability of ω to the type of $\omega \pm \omega_i$. Then, the slowly varying functions for which the condition $\omega \pm \omega_i \approx 0$ is satisfied being the only retained, the simplification of the form of solution becomes considerable. To illustrate the form of the expressions (12) and (13) which have been obtained, only the first three modes of the pipe are taken into account, for which $n_i \approx i \cdot n_1$, the characteristic of the air stream being expanded up to the third power terms. The d/dt derivative of the phase angle $(\omega_i t + \beta_i)$ may be considered as an instantaneous value of the pulsation which is, for the i -th mode $(\omega_i + \dot{\beta}_i)$. From the condition of the natural vibrations preserving a strictly harmonic relationship and the condition of β being independent of time one obtain, on substituting $n_1 = (\omega_1 + \dot{\beta}_1)$ and, similarly $n_i = i \cdot (\omega_1 + \dot{\beta}_1)$, the condition:

$$\omega_i + \dot{\beta}_i = i \cdot (\omega_1 + \dot{\beta}_1) \quad (14)$$

By analysing consecutive stages of organ sound "non-musical" modes can be observed in a steady state and in the phase of growth of the sound as well. They are connected with the fact that the satisfaction of the condition $\omega_i = n_i$ is only approximate and, therefore, with the existence of interrelations between particular components of the sound.

Assuming, after Fletcher, that the attack transient behaviour of the air stream can be described in the form [3]:

$$p(t) = p_0 + (p_1 - p_0) \exp(-t/\tau) \quad (15)$$

where: $p(t)$ — pressure of the air stream in the growing stage, p_1 — maximum pressure, p_0 — steady state pressure, τ — time necessary for the pressure to obtain the value p_0 .

The initial conditions are:

$$\begin{aligned} v_i &\simeq (0.5p_1/i) \sin(n_i t) \\ a_i^0 &= 0.5p_1/i \cdot n_i, \quad \beta_i^0 = -\pi/2, \\ \Delta &\simeq \pi \\ \omega_i &= n_i \end{aligned} \quad (16)$$

Particular values of the coefficients are denoted by: $l, c_0, c_1, c_2, c_3, n_1, n_2, n_3, k_1, k_2, k_3, \lambda_1, \lambda_2, \lambda_3, \gamma, \delta$, where: γ — scale factor for the interaction between the air column and the air stream, δ — propagation delay.

As a result this makes possible numerical solution of the equations (12) and (13).

The expression (15) can be related to the way of opening the air inlet to the pipe. If $p_1 \gg p_0$ it may be assumed that the valve is opened in an abrupt manner, thus producing a distinct pressure peak. If $p_1 = p_0$, the sound grows rapidly, the steady state being reached immediately. In the third case, $p_1 \ll p_0$, the growth of the transient is slow [3].

Showing the dependence of the growing phase of organ sound on the way of opening the air flow, Fletcher does not relate, however, those phenomena directly to the problem of musical articulation. In view of the lack of appropriate references in the literature this problem requires an original method of investigation to be devised. The related problems will be discussed in what follows.

3. Methods for studying articulation parameters

In view of the lack of verified techniques of recording articulation parameters of organ playing such investigation was conducted, under laboratory conditions, then the same method was used for studying various musical articulation of organ sound with instruments located in real interiors. The method proposed for studying the phenomenon of musical articulation is based on the measurement of the time of displacement of the key from the position at the rest to state of full depression with simultaneous observation of the process of the growing sound.

3.1. The method of extraction of articulation parameters

To extract a parameter of organ sound related to the problem of musical articulation one should first analyze the articulation features transferred by the organ player on the motion of the key. As mentioned in Sec. 1 musical articulation may be referred to all the conventional marks contained in the musical notation (tabulature), therefore indirectly, by translating them into language of physical phenomena, to the force acting on the key, the velocity of its motion and possibly, the use by the player of a means consisting in stopping momentarily the motion of the key in various positions

during the action of key pressing. However, the latter idea cannot be accepted due to the fact that during the stop of the valve in a position of partial opening, the pipe sounds out of tune. This fact has been confirmed by organists, who consider this way of organ playing to be incorrect and, therefore useless from the point of view of investigation of articulation features of organ playing.

Now, the study of the valve system with the electromagnetic control systems shows that the force may be also eliminated from the considerations [1], [8]. The use of a greater force of pressure on the key cannot influence the way in which the pipe blowing process is started except the case in which greater force means greater velocity of motion of the key. Thus, it is the relation between the velocity of motion of the key and the sound generated by the pipe which will be assumed in the present consideration as a basis for studying objective features of articulation. As a consequence the velocity of touch on the key, which should not as a rule remain in a position corresponding to the half-open position of the valve may be replaced with another parameter, easier to measure, that is the time of displacement from the rest position to the bottom position, which is that of the state of full depression [5].

From the above assumptions it follows that the system of recording measurement signals should ensure synchronous record of the displacement time of the key and the sound of the organ. The diagram of the recording system for the purpose of investigation into the objective features of articulation in organ music is shown in Fig. 1.

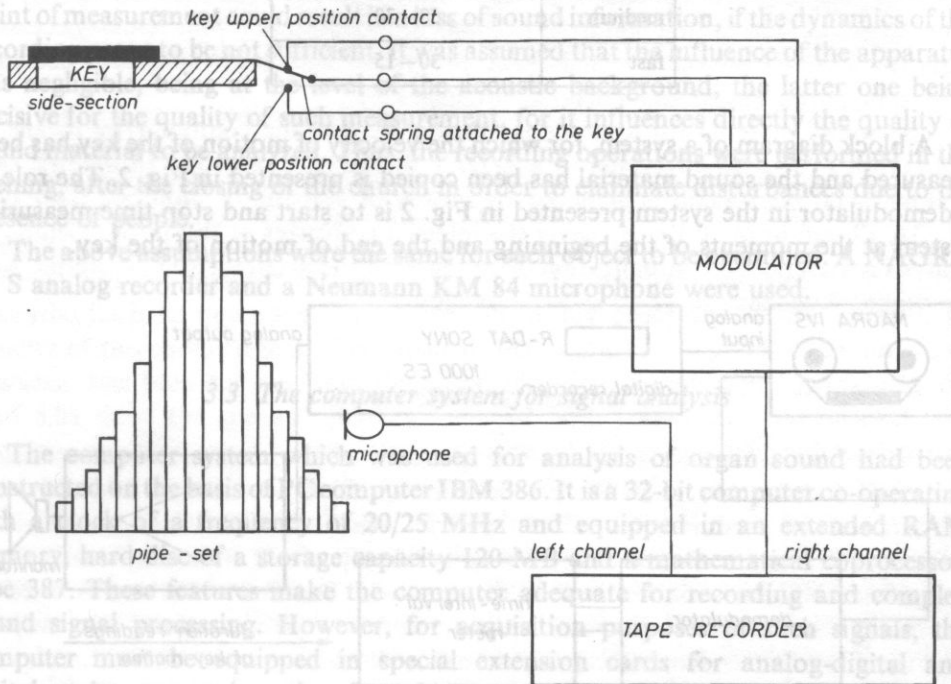


Fig. 1. Diagram of the recording system of the measurement material.

The role of modulator in Fig. 1 is that of generating a rectangular signal at a frequency of about 10 kHz over that period of time during which the middle spring of the change-over switch resting upon a of the key is not in contact with lateral sets of contacts. This corresponds to the case in which the key is between the position of rest and the bottom position that is the state of maximum key depression.

In the first phase of the carried investigation the changing over time of the key was recorded in a synchronous manner with the organ sound in the case slow and fast motion of the key. The sound material was recorded on a tape recorder, then copied on a R-DAT digital recorder thus making it possible to mark the beginnings of particular fragments for the purpose of automatic searching. Some preliminary analyses were also made, the aim of which was to study the relation between the velocity of displacement of the key and the articulation. This enables to fix the values of the time interval corresponding to the velocity of displacement of the key. Table 1 shows values of time intervals for a slow, moderate and fast touch on the key.

Table 1. Speed of key motion as expressed in terms of the time of travel between the initial and final position of the key

Key speed	Duration of travel [ms]
slow	90–50
medium	50–30
fast	30–15

A block diagram of a system, for which the velocity of motion of the key has been measured and the sound material has been copied is presented in Fig. 2. The role of a demodulator in the system presented in Fig. 2 is to start and stop time measuring system at the moments of the beginning and the end of motion of the key.

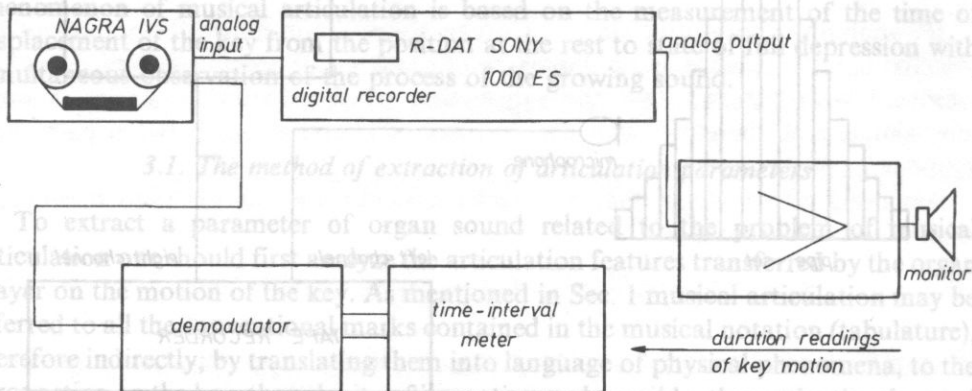


Fig. 2. Block diagram of the copying recording system.

3.2. Investigation of organ sounds

Organs with mechanical tracker action (St. Nicholas Church and St. Mary's Basilica) and, for comparison, organs with electric and electropneumatic control (Oliva Cathedral) were selected for measurements.

The organ stops to be recorded were selected taking into consideration particular properties of the organs and also repeatability of the tests. The fundamental organ stop is Principal, an open cylindrical flue pipe. In addition flute pipes (Bourdon, Gedackt) can be found in every organ, therefore the investigation was confined to recording the sound of pipes of the two types mentioned above. For each voice the tone *a* was recorded on an analog tape recorder for each octave beginning from the lowest. In order to facilitate latter analyses a single tone was recorded.

Another factor decisive for the quality of measurements is the location of the microphone, which depends on the size of the instrument, the arrangement of stops in the organ and the acoustics of the interior. Making use of the information available on the location of an organ pipe, the microphone was installed at the distance not greater than 2 m from the pipe examined in the near field of the organ (the average critical radius being about 3.8 m for St. Nicholas' Church, 4.7 m for the Oliva Cathedral and 5.7 m for the St. Mary's Basilica) having in view recording of the sound heard directly by the organist under normal working conditions, because the choice of a static central point of measurement could result in a loss of sound information, if the dynamics of the recording prove to be not sufficient. It was assumed that the influence of the apparatus was negligible, being at the level of the acoustic background, the latter one being decisive for the quality of such measurement, for it influences directly the quality of sound material to be analyzed. Thus, the recording operations were performed in the evening, after the closing of the church in order to eliminate disturbances due to the presence of people.

The above assumptions were the same for each object to be examined. A NAGRA IV S analog recorder and a Neumann KM 84 microphone were used.

3.3. The computer system for signal analysis

The computer system which was used for analysis of organ sound had been constructed on the basis of PC computer IBM 386. It is a 32-bit computer co-operating with a clock of a frequency of 20/25 MHz and equipped in an extended RAM memory, hard disc of a storage capacity 120 MB and a mathematical coprocessor, type 387. These features make the computer adequate for recording and complex sound signal processing. However, for acquisition purposes of such signals, the computer must be equipped in special extension cards for analog-digital and digital-analog conversion, therefore the computer system was completed with an AES/EBU 16 card [10].

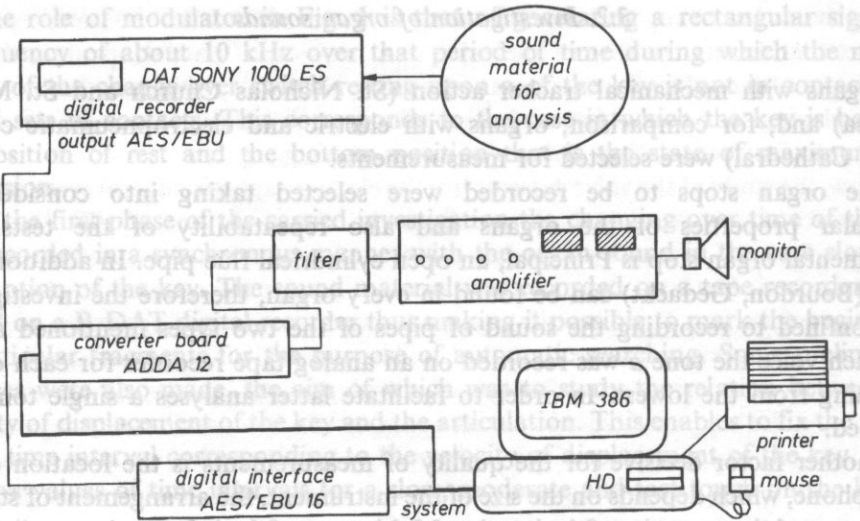


Fig. 3. Block diagram of the computer analyzing system.

A block diagram of the computer system is shown in Fig. 3. This system was designed at the Department of Sound Engineering, Gdańsk Technical University, and constitutes, together with a bundle of fundamental operational programs a necessary basis for analysis of sound signals. The programs mentioned include procedures written in Turbo Pascal and Turbo C languages [6].

The sound material for analysis is introduced into the computer by means of a NAGRA IV S analog recorder or a R-DAT digital tape recorder. In the first case analog-digital conversion is achieved by means of systems of modified card type ADDA 12 and in the other by using the internal converter of the DAT. Computer analysis makes possible visualization of sound with the accuracy to one sample with a sampling frequency of 12 or 24 kHz, as required.

4. Analysis of the results

First of all, one should answer the question as to what are the parameters describing a sound as regards the time and the spectrum which may be decisive for the articulation phenomenon. In the spectral structure of the sound which was defined earlier as a sequence of three stages, namely attack transient, steady state, decay transient, one should above all discern those features which can be used to determine the differences between sounds, therefore also the time and way of growth of particular harmonics, the duration of the transient and the delay of particular components with reference to the moment of initiation of air vibrations in the pipe.

From among all the organ sounds which had been examined only those were selected for analysis, which are representative as examples of behaviour of flue stops under definite articulation conditions.

Figure 4 illustrates the time variation of the tone *a* (110 Hz) of a Principal 8' pipe of the Organ of St. Nicholas Church for slow and rapid touch on the key. Confrontation of the two time characteristics shows clearly the differences during

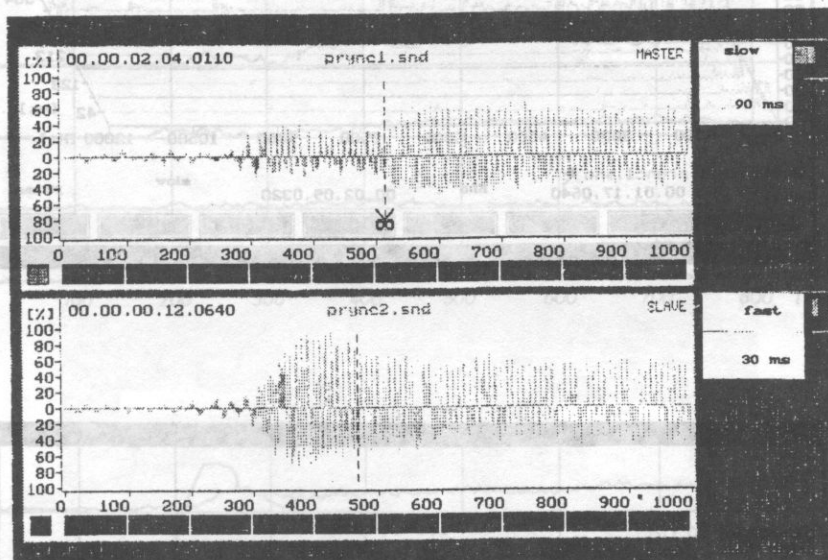


Fig. 4. Time characteristics of the tone *a*, Principal 8', the organ of ST. Nicholas' Church.

the stage of growth of the sound. The fact of the fluctuations in the steady state being small confirms the supposition that the features of the articulation are connected above all with the process of growth of the sound. The computer system used for analysis [6] enables to cut out precisely transients for further analysis. Such an operation does not result in any observable degradation of the quality of the phonic signal. The cursor in Fig. 4 marks the point where the attack transient has been cut out from the signal recorded. Subsequent figures (Fig. 5.a. and 5.b) show the spectral characteristics of both transients. The selected fragments show differences in the way of growth of the sound which has also been confirmed by the analysis of the evolution of the sound of particular components (Fig. 6) and is particularly distinct in the histograms of Fig. 7. From the above observations one can easily indicate those features which are different for the same sound depending on the touch on the key being slow or rapid. The most essential parameter differentiating the sound tested is the way of growth of the first two components. If the touch on the key is slow the fundamental and the second harmonic begin at the same moment and grow slowly and smoothly. The overblown state with two local maxima of the second harmonic which is typical

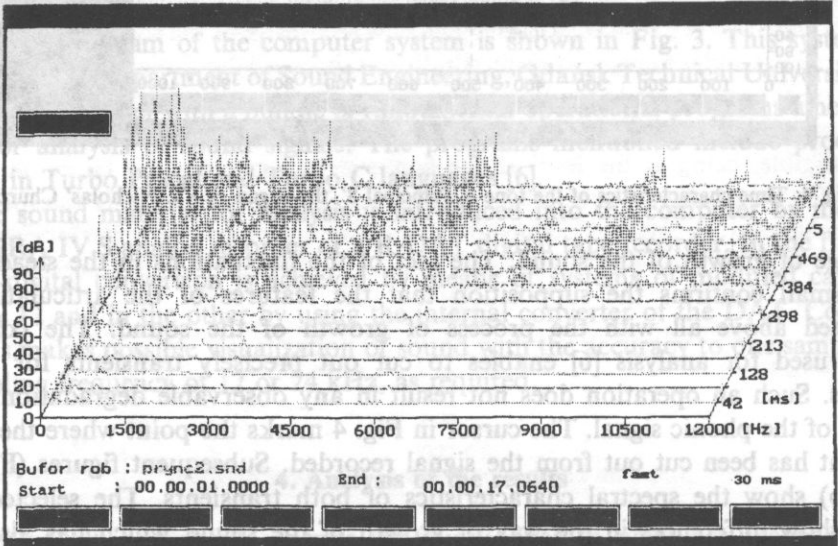
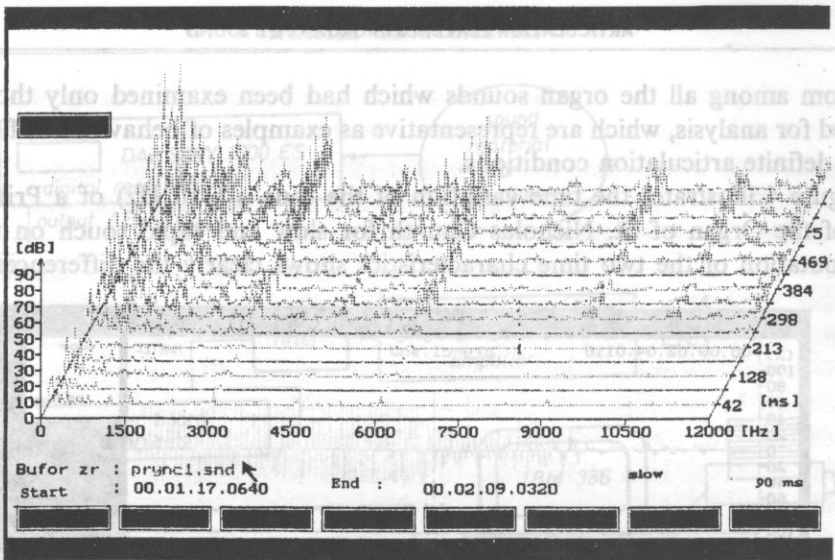


Fig. 5.a. and 5.b. Spectral characteristics of transients of the tone *a*, Principal 8', the organ of St. Nicholas' Church.

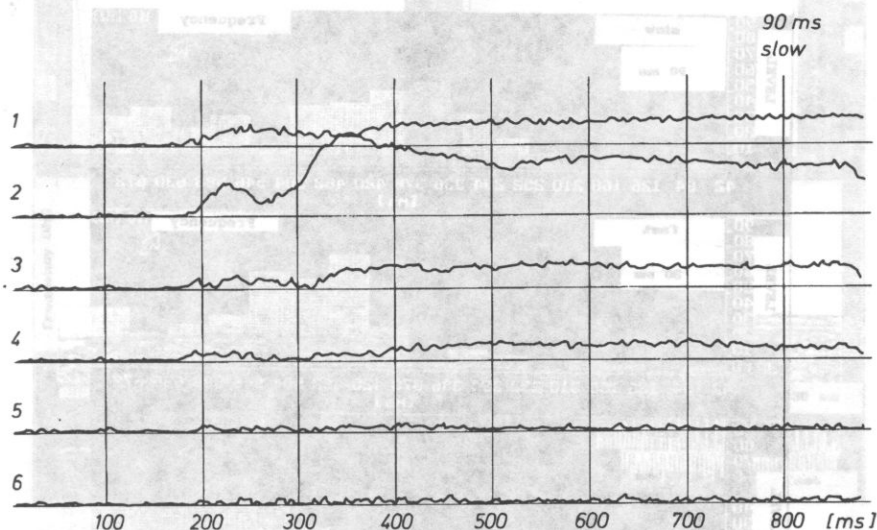


Fig. 8. Cepstral analysis of the tone *a* in the case of slow touch on the key, Principal 8', the organ of ST. Nicholas' Church.

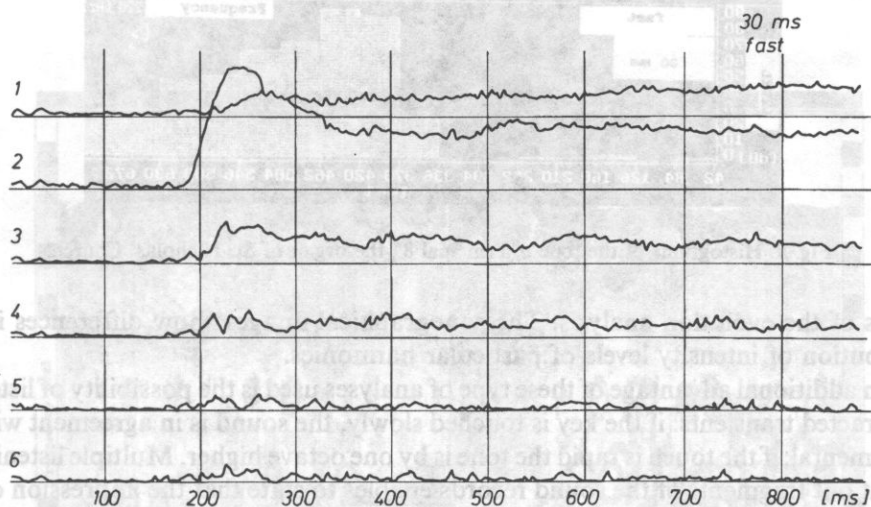


Fig. 6. Evolution analysis of the tone *a* in the case of slow and rapid touch on the key, Principal 8', the organ of ST. Nicholas' Church.

for this class of organ stops is visible, nevertheless its amplitude remains insignificant. In the case of rapid motion of the key the second component is the first of all harmonics to start, while the fundamental is delayed by about 30 ms. The growth of the slope of the second harmonic is immediate and decided and exceeds considerably the amplitude of the fundamental. The capstral and sonographical analysis of the same sounds (Fig. 8) and the LPC (*Linear Predictive Coding*) sonographical analysis (Fig. 9) confirm the

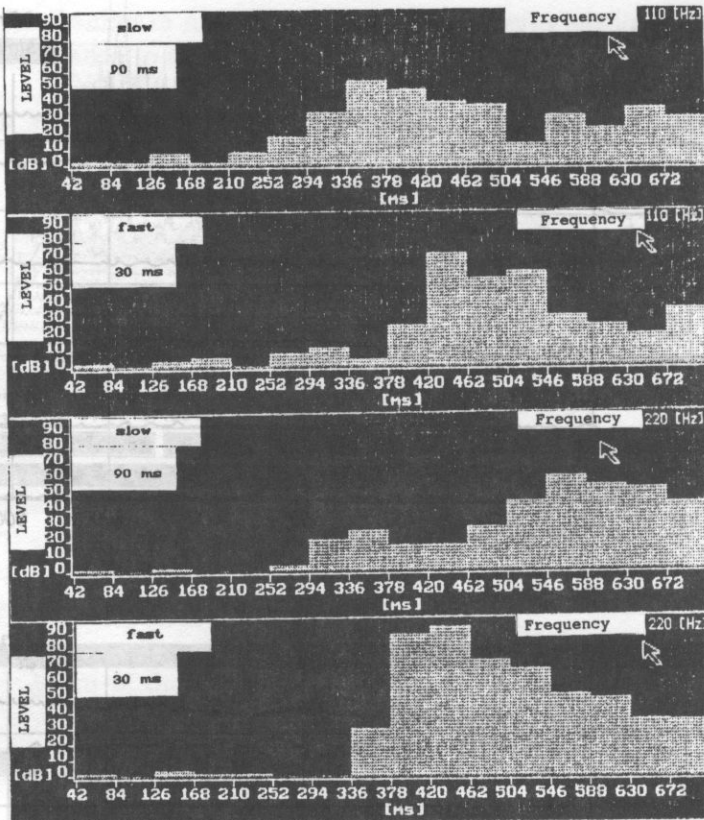


Fig. 7. Histograms of the tone *a*, Principal 8', the organ of St. Nicholas' Church.

results of the evolution analysis. The sonographical images show differences in the distribution of intensity levels of particular harmonics.

An additional advantage of these type of analyses used is the possibility of listening to extracted transients: if the key is touched slowly, the sound is in agreement with its fundamental; if the touch is rapid the tone is by one octave higher. Multiple listening to the cut out fragments of the sound records enables to state that the impression of the pitch being correct of the proper tune having been reached occurs only after some 250 ms. The results observed confirm the hypothesis on the possibility of musical articulation in organs with mechanical tracker action.

By examining the results of evolution analysis and FFT analysis it was observed that the differences between the cases of slow and rapid touch on the key are not significant for higher tones. However, the time variation and the sonographical analysis made enable one to obtain an image of those differences (Fig. 10 to 12).

The studies and analyses of organ sounds in St. Mary's Basilica show agreement with those obtained in St. Nicholas' Church.

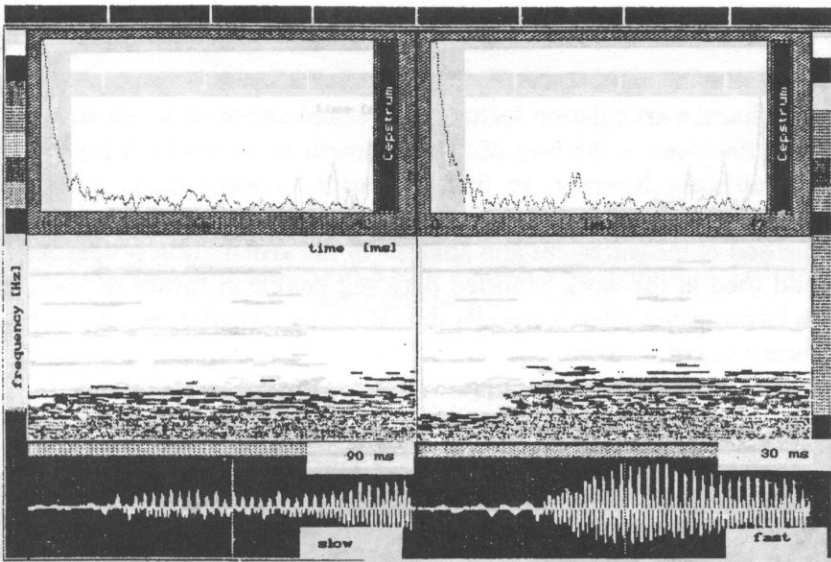


Fig. 8. Cepstral and sonographical FFT analysis of the tone a , Principal 8', the organ of St. Nicholas' Church.

Fig. 12. Sonographical analysis of the tone a^2 , Principal 8', the organ of St. Nicholas' Church.

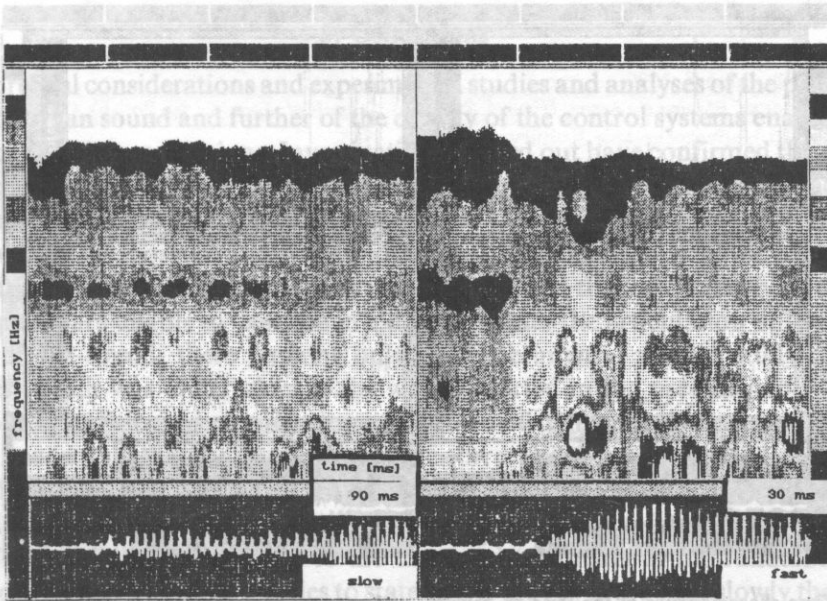


Fig. 9. LPC sonographical analysis of the tone a , Principal 8', the organ of St. Nicholas' Church.

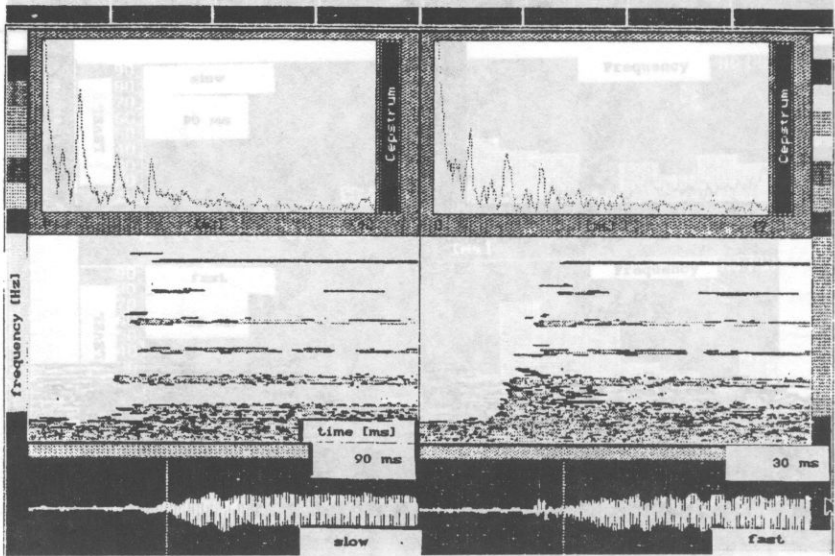


Fig. 10. Sonographical and cepstral analysis of the tone a^1 , Principal 8', the organ of St. Nicholas' Church.

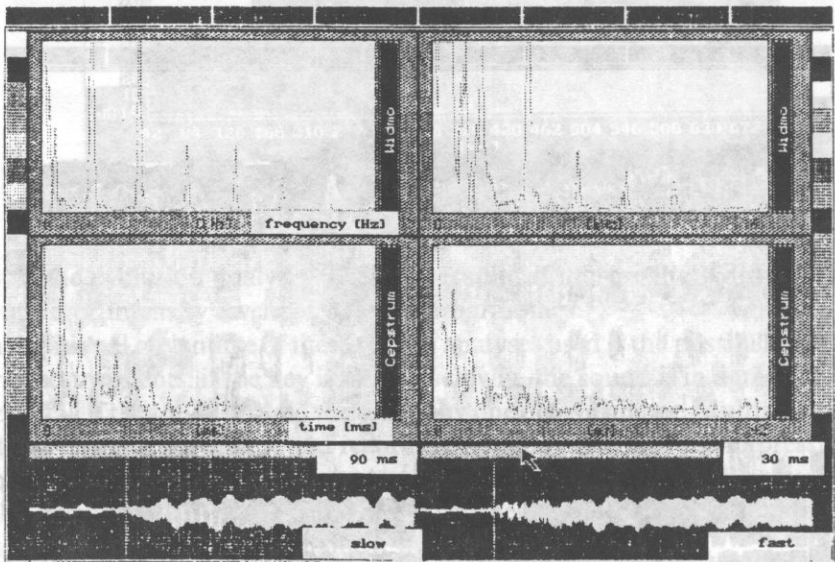


Fig. 11. Time characteristics of the tone a^2 , cepstral and spectral analyses, Principal 8', the organ of St. Nicholas' Church.

By examining the time characteristics of the tone a^2 , it was found that the time characteristics of the tone a^2 are different from those of the tone a^1 . The sonographical analysis made enable one to obtain an image of those differences (Fig. 10 to 12).

The studies and analyses of organ sounds in St. Mary's Basilica show agreement with those obtained in St. Nicholas' Church [432].

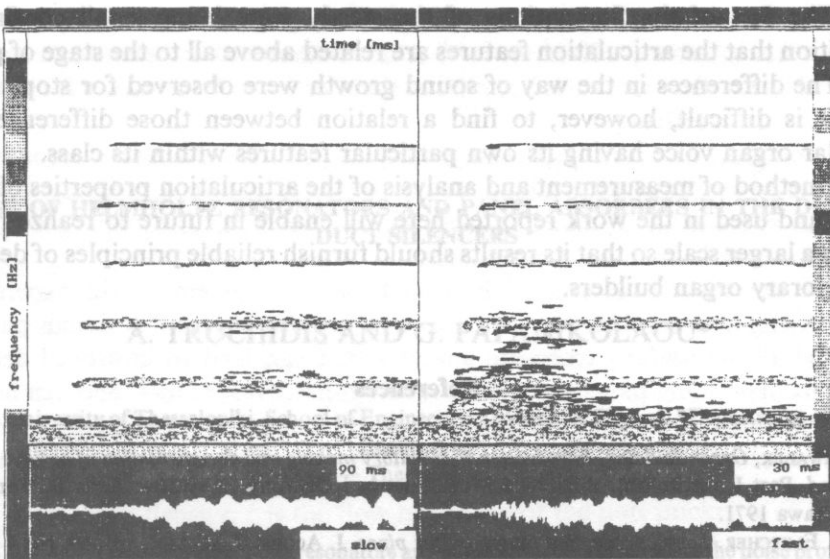


Fig. 12. Sonographical analysis of the tone a^2 , Principal 8', the organ of St. Nicholas' Church.

5. Conclusions

Theoretical considerations and experimental studies and analyses of the problem of quality of organ sound and further of the quality of the control systems enable one to draw the following conclusions. Investigations carried out have confirmed the opinion expressed by musicians that the musical articulation of various kinds can be achieved in organs with mechanical tracker action.

— Because the most advanced methods of analytical description of the phenomena of excitation of vibrations in an organ pipe discussed in the introductory part of the present paper are unable to describe in a direct manner the articulation differences in growth of the sound, there remains only the experimental way of studying those processes, which was undertaken in the work reported in the present paper.

— Multiple listening examinations of cut out fragments of the sound records enabled one to state that the impression of the correct pitch being attained occurs only with a delay of about 250 ms. The results observed confirm the hypothesis on the possibility of musical articulation with organs having mechanical tracker action.

— The possibility of listening to the extracted transients of the fundamental of organ stop, namely Principal enables to state that if the key is touched slowly the sound is in agreement with the fundamental pitch. If the touch is rapid, the transient sounds by one octave higher.

— As a result of the experiments performed some differences have been observed in the way in which the transients grow, depending on whether the key is touched slowly or rapidly.

— The fact of the fluctuations of the steady state being small confirms the supposition that the articulation features are related above all to the stage of growth.

— The differences in the way of sound growth were observed for stops of both kinds, it is difficult, however, to find a relation between those differences, each particular organ voice having its own particular features within its class.

The method of measurement and analysis of the articulation properties of organs devised and used in the work reported here will enable in future to realize research work on a larger scale so that its results should furnish reliable principles of design for contemporary organ builders.

References

- [1] J. CHWALEK, *Organ Building, Introduction to inventory making and documentation of antique organs in Poland*, Part I, (in Polish). Biblioteka Muzealnictwa i Ochrony Zabytków, Seria B, Tom XXXI, Warszawa 1971.
- [2] N.H. FLETCHER, *Sound production by organ flue pipes*, J. Acoust. Soc. Am., vol. 60, No 4 (1976).
- [3] N.H. FLETCHER, *Transients in the speech of organ flue pipes — A Theoretical Study*, Acustica, vol. 34 (1976).
- [4] S. KALISKI, *Applied mechanics* (in Polish), PWN, Warszawa, 1986.
- [5] B. KOSTEK, A. CZYŻEWSKI, *Articulation features in the digitally controlled pipe organ*, 90th AES Convention, Preprint No 3023, Paris (1991).
- [6] P. MRÓZ, A. CZYŻEWSKI, *A system for digital sound editing*, (in Polish), Proc. of XXXVII OSA'90, t. 1, 205–208, Gdańsk, 1990.
- [7] M. RYBNICKI, *Playing the organ, History, Structure, Schools of organists*, (in Polish), Centralny Ośrodek Metodyki Upowszechniania Kultury, Warszawa, 1985.
- [8] *The New Grove Dictionary of Music and Musicians*, Macmillan Publishers Ltd, London, 1980.
- [9] H. WUNDERLICH, *Zur Frage Artikulation in Orgelspiel*, *Organy i Muzyka Organowa* VI, Prace Specjalne 40, Gdańsk, 1986.
- [10] J. ZIAJKA, A. CZYŻEWSKI, *Co-operation of R-DAT digital tape recorder with a PC computer*, Proc. XXXVII OSA'90, t. 2, 361–364, Gdańsk, 1990.

Received January 15, 1991, English version September 15, 1992

THE USE OF HELMHOLTZ RESONATORS AND PANEL ABSORBERS IN THE DESIGN OF DUCT SILENCERS

A. TROCHIDIS AND G. PAPANIKOLAOU*

Aristotle University of Thessaloniki, School of Engineering Division of Physics, *Department of Electrical Engineering
540 06 — Thessaloniki, Greece

The use of Helmholtz resonators and panel absorbers in reducing the noise propagated in ducts is investigated both analytically and experimentally. Using a simple approach, the impedance of the resonators is calculated taking into account the presence of sound absorbing material in the cavity. Equations for the transmission loss are derived in both cases. Parameters such as dimensions, length of the opening and flow resistivity of the lining in case of Helmholtz resonators and panel thickness and dimensions in case of panel absorbers are systematically examined. Comparisons between experimental and predicted values are in good agreement showing that the model developed describes satisfactorily the behaviour of resonators in ducts and can be used for improved design of silencers incorporating resonators.

1. Introduction

There are many practical applications where the conventional types of dissipative mufflers can not be used. Particularly, in cases involving hot gaseous flow the pores of the sound absorbing lining are closed by oil or carbon particles, the fibres are blown out or thermal cracking of the lining occurs. A further disadvantage of dissipative mufflers is their poor attenuation at low frequencies.

In order to overcome the aforementioned disadvantages, silencers incorporating Helmholtz resonators or panel absorbers or a combination of both have been proved very useful [1, 2, 3]. The main advantages of such silencers are their low cost of construction and maintenance, their high resistivity and the good performance at low and mid-frequencies. Furthermore, these silencers can be "tuned" in order to perform in a predetermined frequency range.

Little analytical work has been done [4, 5, 6, 7] concerning the behaviour of resonators in ducts and the development of silencers using resonators has been based on rather empirical procedures.

It is the aim of the present paper to develop a simple model that describes the acoustical behaviour of Helmholtz resonators and panel absorbers in a flow duct. The

model is based on the assumption that only wave propagation is allowed and that the flow velocities are low (<10 m/s), so that the behaviour of the resonators can be considered linear. Our approach is similar to that described by SULLIVAN for modelling perforated tube mufflers [5].

Based on these assumptions, the impedance of both the Helmholtz resonator and panel absorber are calculated taking into account the presence of sound absorbing material in the cavity. By using the calculated impedance, an expression for the transmission loss in both cases is obtained.

Finally, the predicted results are shown to be in good agreement with experimental findings giving thus confidence in the use of the model, at least for design purposes. The model allows useful parametric analyses that can lead to improved design of silencers incorporating panel absorbers and Helmholtz resonators, and can be easily extended to describe the noise reduction in ducts lined with an array of resonators. Further work in that direction is already under way and will be presented in a future publication.

2. Impedances

In the following we calculate the impedance of a Helmholtz resonator and a panel absorber with sound absorptive material in the cavity.

2.1. Impedance of a Helmholtz resonator

We start by analyzing first the resonator element shown in Fig. 1. The length of the resonator element is L , the width is b and its height is h . The length of the opening is l and the cavity is lined with a usual rock wool layer of thickness d . In order to take into account the additional losses due to the lining, we assume a complex propagation constant K_x within the resonator. To calculate K_x one needs to know the wall impedance of the lined side. It is very well known that in case of a plane wave incident

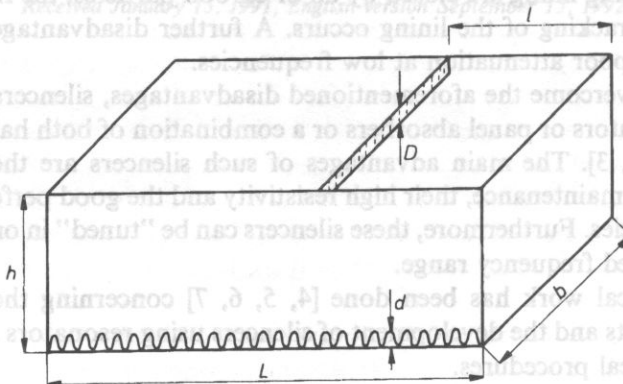


Fig. 1. Geometry of the resonator.

on a locally reacting lining of uniform thickness d backed by a rigid wall, the impedance encountered by the plane wave is given by

$$Z_w = -jY_w \cot(K_w d), \tag{1}$$

where Y_w and K_w are the complex characteristic impedance and propagation constant of the absorptive lining, respectively.

For fiber-based sound absorbing materials often used in mufflers K_w and Y_w are given by [8]

$$\frac{K_w}{K_0} = (\chi)^{1/2} \left\{ 1 - j \frac{\xi}{\rho_0 \omega \chi} \right\}^{1/2} \tag{2}$$

$$\frac{Y_w}{Y_0} = \frac{1}{\sigma} \frac{K_w}{K_0}, \tag{3}$$

where ρ_0 is the air density, ξ is the flow resistance of the unit thickness of the porous bulk material, σ is the porosity, χ is the structural factor and K_0 is the wave number in air. By considering the resonator as an infinite duct of height h lined on one side (Fig. 2), the wavenumber K_x is given as a solution of the well-known transcendental equation [9]

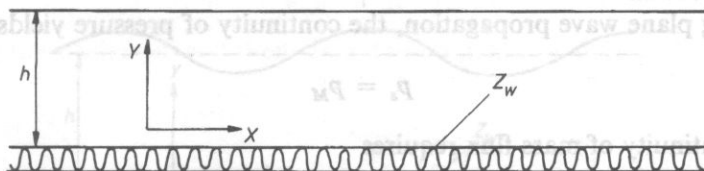


Fig. 2. Resonator element as infinite duct.

$$-j\sqrt{E} \tan \sqrt{E} = \beta,$$

$$\text{with } E = (K_0 h)^2 - (K_x h)^2 \quad \text{and} \quad \beta = K_0 h \rho_0 c_0 1/Z_w. \tag{4}$$

The real and imaginary parts of the first root of Eq. (4) may be obtained by nomograms or numerically. A very reasonable and convenient approximation can be obtained by writing (see ref. [9]).

$$E = \frac{105 + 45j\beta \pm \sqrt{11025 + 5250j\beta - 1605\beta^2}}{20 \pm j\beta}. \tag{5}$$

with

$$\beta = K_0 h \rho_0 c_0 \frac{1}{Z_w} = jh \frac{K_0^2 \sin(K_w d)}{K_w \cos(K_w d)}. \tag{6}$$

Equations (5) and (6) give two complex values for K_x ; the one that gives lower attenuation is of particular importance. The impedance of the resonator consists of the neck inertance and cavity compliance with damping in series. The compliance can be expressed in terms of K_x as

$$Z_s = \frac{P_s}{u_s} = -j\rho_0 c_0 \left(\frac{K_x}{K_0} \right) \frac{\cos K_x(L-l)}{\sin K_x(L-l)} \quad (7)$$

where p_s and u_s are the acoustic pressure and velocity in the resonator.

The inertance of the neck, i.e. the opening can be expressed as

$$Z_M = \frac{F_M}{u_M} = \frac{P_M S_0}{u_M} = j\omega m_s \quad (8)$$

where F_M is the driving force, u_M is the volume velocity at the opening and $S_0 = lb$ is the area of the opening. Hence m_s is the effective oscillatory mass taking into account the mass correction. In other words, the opening is considered to be circular with an equivalent radius S_0/π , so that one can approximately write $m_s \approx \rho_0 S_0 \sqrt{S_0/\pi}$. By adding the impedance given by Eqs. (7) and (8), the combined impedance of the resonator can be obtained. However, by adding the impedances the geometry must be taken into account.

Assuming plane wave propagation, the continuity of pressure yields

$$p_s = p_M \quad (9)$$

while the continuity of mass flux requires

$$S_0 u_M = S u_s \quad (10)$$

Here, S_0 and S are the areas of the opening and of the free cross-section of the duct respectively.

Thus, one can write

$$\frac{p_s}{u_s} = \frac{p_M S}{u_M S_0} = \frac{F_M}{u_M} \frac{S}{S_0^2} \quad (11)$$

or alternatively

$$\frac{F_M}{u_M} = \frac{p_s}{u_s} \frac{S_0^2}{S} \quad (12)$$

By using Eqs. (9) through (12) the total impedance of the resonator can be expressed as

$$Z_t = j\omega m_s + \frac{S_0^2}{S} \left[-j\rho_0 c_0 \frac{K_x \cos K_x(L-l)}{K_0 \sin K_x(L-l)} \right] \quad (13)$$

2.2. Impedance of a panel absorber

The panel absorber under consideration is shown in Fig. 3. It consists of a flexible panel backed by an air cavity of depth h . The bottom of the cavity is lined with a usual

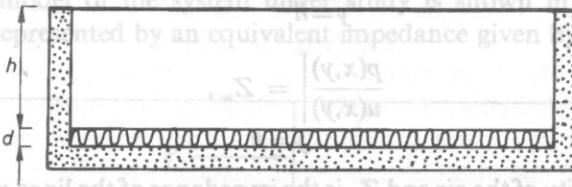


Fig. 3. Geometry of panel absorber.

rock wool layer of thickness d . The impedance of the panel absorber can be considered as the inertance of the vibrating panel and the cavity compliance with damping. In order to take into account the losses in the cavity due to the lining, we have to assume a complex propagation constant K_x in the x -direction. To calculate K_x in a convenient and simple way, we consider the absorber element as infinite, see Fig. 4. By assuming a pressure of the form $p(x, y) = p(y) e^{-jK_x x}$, the two-dimensional acoustic wave equation yields

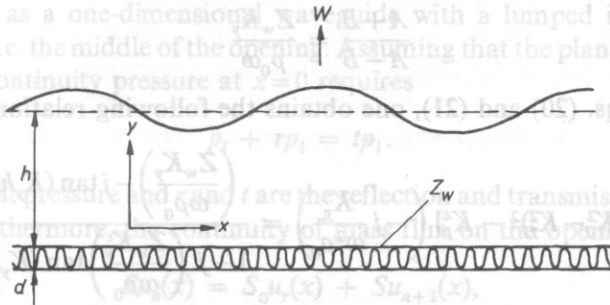


Fig. 4. Idealized model of panel absorber.

$$\frac{\partial^2 p(y)}{\partial y^2} + (K_0^2 - K_x^2) p(y) = 0. \tag{14}$$

The solution for $p(y)$ is

$$p(y) = A e^{-jK_y y} + B e^{+jK_y y}, \tag{15}$$

with

$$K_y^2 = K_0^2 - K_x^2. \tag{16}$$

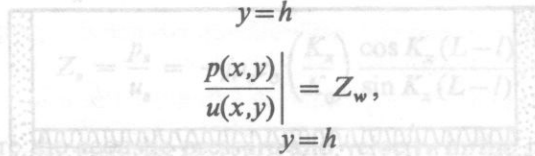
The equation governing the vibratory motion of the plate is

$$(DK_x^4 - \omega m'') w = p(x, y)|_{y=h}, \tag{17}$$

where w is the plate displacement in the y -direction, D is the bending stiffness, and m'' is the mass per unit area of the plate.

The boundary conditions for the acoustic field are

$$\left. \frac{\partial p}{\partial y} \right|_{y=h} = \rho_0 \omega^2 w, \quad (18)$$



$$\left. \frac{p(x,y)}{u(x,y)} \right|_{y=h} = Z_w, \quad (19)$$

where ρ_0 is the density of the air and Z_w is the impedance of the lined wall. By using Eqs. (15) and (18), Eq. (17) becomes

$$D(K_x^4 - K_p^4) \left(-j \frac{K_y}{\rho_0 \omega^2} \right) = \frac{A+B}{A-B} - j \tan K_y h, \quad (20)$$

where K_p is the in vacuo free flexural wavenumber of the plate. Furthermore, by using Eq. (15) the boundary condition of the lining expressed by Eq. (19) can be written as

$$\frac{A+B}{A-B} = \frac{Z_w K_y}{\rho_0 \omega}. \quad (21)$$

By combining Eqs. (20) and (21), one obtains the following relationship for K_y

$$D [(K_0^2 - K_y^2)^2 - K_p^4] \left(-j \frac{K_y}{\omega^2 \rho_0} \right) = \frac{\left(\frac{Z_w K_y}{\omega \rho_0} \right) - j \tan(K_y h)}{1 - j \left(\frac{Z_w K_y}{\omega \rho_0} \right) \tan(K_y h)}. \quad (22)$$

For the sake of simplicity and for the situation examined here (low frequencies and small height) it is reasonable to assume $K_y h \leq 1$ so that $\tan(K_y h) \approx K_y h$. By using the above approximation Eq. (22) becomes

$$\left(\frac{Z_w}{\omega \rho_0} - j h \right) = -j \frac{D}{\omega \rho_0} [(K_0^2 - K_y^2)^2 - K_p^4] \left[1 - j K_y^2 \left(\frac{Z_w h}{\omega \rho_0} \right) \right]. \quad (23)$$

The above equation is of the third order in K_y^2 and thus can lead to three types of free motion. Two of them are closely related to the bending waves on the plate and the third to that of the air waves in the cavity. Equation (23) can be numerically solved for the transverse wave number K_y and by substitution in Eq. (16) the desired wavenumber K_x can be obtained. Finally, the impedance of the panel absorber can be expressed in terms of K_x as

$$Z = j \omega m'' - j \rho_0 c_0 \left(\frac{K_x}{K_0} \right) \frac{\cos(K_x h)}{\sin(K_x h)}. \quad (24)$$

3. Transmission loss

3.1. Helmholtz resonator

The idealized model of the system under study is shown in Fig. 5. Since the resonator can be represented by an equivalent impedance given by Eq. (13) the duct

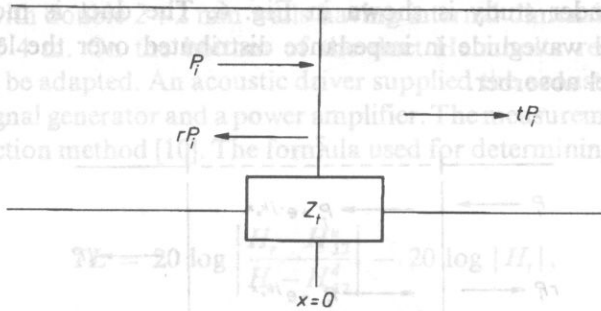


Fig. 5. Idealized model of duct-resonator.

can be modeled as a one-dimensional waveguide with a lumped impedance Z_t at a discrete point, i.e. the middle of the opening. Assuming that the plane wave condition is fulfilled, the continuity pressure at $x=0$ requires

$$p_i + r p_i = t p_i \tag{25}$$

where p_i is incident pressure and r and t are the reflection and transmission coefficients, respectively. Furthermore, the continuity of mass flux on the opening $x=0$ yields

$$S u_n(x) = S_0 u_r(x) + S_{n+1} u(x), \tag{26}$$

where $u_n(x)$, $u_{n+1}(x)$ are the volume velocities before and after the opening, respectively, and $u_r(x)$ is the velocity at the opening. Equation (26) can be written in terms of the incident pressure as

$$S \frac{p_i - r p_i}{\rho_0 c_0} = \frac{t p_i}{Z_t} S_0 + S \frac{t p_i}{\rho_0 c_0}, \tag{27}$$

or alternatively

$$p_i - r p_i = t p_i \frac{\rho_0 c_0 S_0}{Z_t S} + t p_i. \tag{28}$$

Eqs. (25) and (28) can be easily solved for t (assuming $p_i = 1$) yielding

$$t = \frac{1}{1 + \frac{\rho_0 c_0 S_0}{Z_t S}} \tag{29}$$

Finally, the transmission loss can be expressed as

$$TL = 20 \log (1/t). \tag{30}$$

3.2. Panel absorber

The system under study is shown in Fig. 6. The duct is modeled again as a one-dimensional waveguide in impedance distributed over the length L , i.e. the length of the panel absorber.

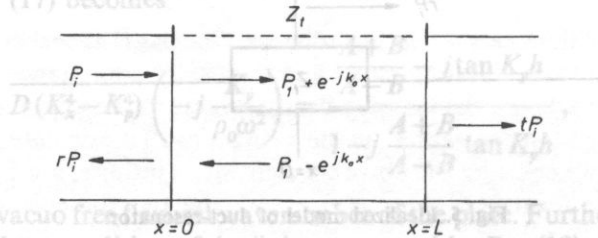


Fig. 6. Idealized model of duct-panel absorber.

By assuming plane wave propagation, the continuity of pressure at $x=0$ requires

$$p_i + r p_i = p_{1+} + p_{1-} e^{-jK_0 L}, \tag{31}$$

while at $x=L$

$$p_{1+} e^{-jK_0 L} + p_{1-} = t p_i, \tag{32}$$

where p_{1+} and p_{1-} are the complex amplitudes of the incident and reflected waves between $x=0$ and $x=L$. On the other hand, the continuity of mass flux at $x=0$ can be expressed as

$$\left(\frac{Z_w}{\omega \rho_0} - jh \right) = \frac{p_i - r p_i}{\rho_0 c_0} = \frac{p_{1+} - p_{1-} e^{-jK_0 L}}{Z_t}, \tag{33}$$

and at $x=L$ similarly

$$\frac{p_{1+} e^{-jK_0 L} - p_{1-}}{Z_t} = \frac{t p_i}{\rho_0 c_0} \tag{34}$$

The system of Eq. (31) through (34) can be easily solved for t and the transmission loss can be expressed as

$$TL = 20 \log (1/t) \tag{35}$$

4. Experimental results

In order to verify the theoretical predictions, a series of transmission loss measurements on Helmholtz resonators and panel absorbers was made. During the measurements the main parameters determining the geometry of the elements were systematically varied.

The experimental arrangement consisted of a square section steel duct (anechoically terminated) with double 2+2 mm walls having internal dimensions 500 × 500 mm and a length of 4 m. On the bottom of the duct Helmholtz resonators or panel absorbers could be adapted. An acoustic driver supplied the acoustic signal fed to the source from a signal generator and a power amplifier. The measurements were made by the transfer function method [10]. The formula used for determining the transmission loss was

$$TL = 20 \log \left| \frac{H_r - H_{12}^u}{H_r - H_{12}^d} \right| - 20 \log |H_t|, \quad (36)$$

where H_{12}^u and H_{12}^d are the transfer functions measured at the upstream and downstream directions respectively, $H_t = \left| \frac{S_{dd}}{S_{uu}} \right|^{1/2}$ with S_{dd} , S_{uu} denoting the autospectra at the downstream and upstream measurement locations. Finally, $H_r = e^{iK_r \lambda}$, where λ is the microphone spacing. To measure the transfer functions, four 1/4 in. condenser microphones, two at either side were used, the outputs of which were fed to a four-channel analyzer. The experimental arrangement is shown in Fig. 7.

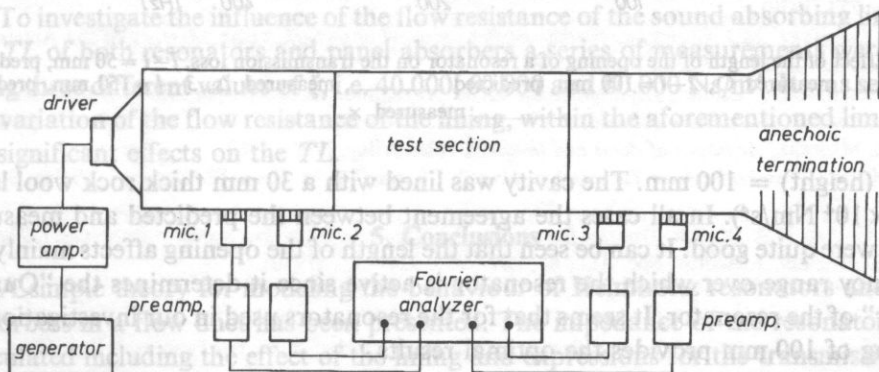


Fig. 7. Experimental arrangement.

The results are presented in form of curves of transmission loss in decibels plotted against frequency in Hz. The theoretical curves were calculated using the procedure described in the previous sections.

To investigate the effect of the main parameters involved on the transmission loss, a series of parametric studies were made, where the length of the opening in case of

system. It seems that for the resonators used in our investigation, an opening of 100 mm provides the optimal results.

2. The variation of the flow resistance of the lining in both cases within the extreme values used ($40.000-80.000 \text{ Ns/m}^4$) has no significant effect on the results.

3. The mounting conditions of the panel in case of a panel absorber affects the TL . Consideration, however, of a finite panel results in a complicated analysis, too difficult to be used for design purposes.

The model developed can be easily extended to describe the sound transmission in ducts lined with an array of Helmholtz resonators or panel absorbers or a combination of both. After the derivation of the impedances for a lined resonator and panel absorber, a duct silencer can be treated as a one-dimensional waveguide with lumped impedances in discrete positions and an expression for the TL of the silencer can be obtained. These aspects will be discussed in a separate publication.

References

- [1] H.V. FUCHS, U. AACKERMAN and W. FROMMHOLD, *Entwicklung von nicht-porösen Absorbern für den technischen Schallschutz*, *Bauphysik*, **11**, 28–36 (1989).
- [2] N. JEHL, *Resonator-Schalldämpfer für schwierige Einsatzfälle*, *VDI-Bericht Nr 437*, 57–60 (1982).
- [3] U. ACKERMANN, H.V. FUCHS and N. RAMBAUSEK, *Neuartiger Schallabsorber aus Metall-Membranen*, *Gesundheits-Ingenieur*, **108**, 67–73, (1987).
- [4] U. INGARD, D.C. PRIDMORE-BROWN, *The effect of partitions in absorptive lining of sound attenuating ducts*, *J. Acoust. Soc. Am.*, **23**, 589–90 (1951).
- [5] J.W. SULLIVAN, *A method for modelling perforated tube muffler components*, *J. Acoust. Soc. Am.*, **66**, 772–777 (1979).
- [6] B.S. SRIDHARA, M.J. CROCKER, *Further studies on panel absorbers*, 114th Meeting of the Acoustical Society of America, Miami, Florida 1987.
- [7] A. CUMMINGS, J. CHANG, *High amplitude sound propagation at low frequencies in a flow duct with resonators: A time domain solution*, *J. Vib. Acoust. Stress and Reliab. Des.*, **110**, 545–551 (1988).
- [8] M.L. MUNJAL, *Acoustics of ducts and mufflers*, John Wiley, N.Y., 1987.
- [9] F. MECHEL, *Taschenbuch der Technischen Akustik*, Chapter VII M. Heckl [Ed] Springer Verlag, Berlin, N.Y. 1975.
- [10] J.Y. CHUNG, D.A. BLASER, *Transfer function method of measuring in duct acoustic properties. I. Theory, II. Experiment*, *J. Acoust. Soc. Am.*, **68**, 907–913, 914–921 (1980).

Received February 2, 1993

ULTRASONIC INVESTIGATIONS OF INCLUSION COMPLEXES OF α -CYCLODEXTRIN WITH AMPHIPHIL SUBSTANCES

A. JUSZKIEWICZ

Department of Chemistry, Jagiellonian University
(30-060 Kraków, ul. Ingardena 3)

A. BALCERZAK

Institute of Fundamental Technological Research of the Polish Academy of Sciences
(00-049 Warszawa, ul. Świętokrzyska 21)

Velocity and attenuation measurements of ultrasonic waves in water solutions of α -cyclodextrin containing different amphiphil substances: sodium octyl sulfate (SOS), sodium decyl sulfate (SDeS), decylpyridinium bromide (DePyB) and sodium caprinate (SCp) were made. The occurrence of an ultrasonic relaxation process connected with the formation of inclusion complexes of α -cyclodextrin with SDeS, DePyB, SCp was established.

1. Introduction

The inclusion complexes are complexes of different substances with macrocyclic ligands. Both ionic and non-ionic substances, which are fitted to the cavity of a macrocyclic organic compound, may be included. Investigations of the inclusion complex give basic information about non-covalence molecular interactions, which are especially important in biological systems. The inclusion complexes with macrocyclic ligands are used among others as models of enzymes and biocatalysts.

The ultrasonic investigations of the inclusion complexes aim at the study of the mechanism of the complexation through the investigations of kinetics and thermodynamics of this process [1]. It enables to determine selective properties of ions and included molecules as well as the ligands forming those complexes.

In literature, one can find only ultrasonic investigations of inclusion complexes of the crown ethers: 15C5 and 18C6 with the cations: Li^+ , Na^+ , K^+ , NH_4^+ , Ag^+ , Sr^{++} , Ba^{++} , Pb^{++} , Hg^{++} in different solvents like water, ethanol, dimethylformamide, methanol, dimethoxyethane and others [2-9].

In this article the first results of ultrasonic investigations of the inclusion complexes of α -cyclodextrin (α -CD) with amphiphil substances: sodium octyl sulfate (SOS), sodium decyl sulfate (SDeS), decylpyridinium bromide (DePyB) and sodium caprylate (SCp) are presented.

2. Experimental part

The ultrasonic velocity and the attenuation coefficient α/f^2 measurements in the water solutions of the α -cyclodextrin with the following detergents: sodium octyl sulfate (SOS), sodium decyl sulfate (SDeS), decylpyridinium bromide (DePyB) and sodium caprylate (SCp) were made in the range of frequency 1–150 MHz at temperature 25°C. The concentration of each component of the solutions was equal to 0.04 M. The measurements for 0.04 M solution of cyclodextrin were also made.

The measurements were made by means of the resonator [10–12] and pulse [1, 13] methods in the frequency range 1–10 MHz and 10–150 MHz, respectively. The measurement errors were about 5% for the former method and below 1% for the latter one. The detailed description of equipment used for the resonator method is presented in [11, 12]. For the pulse method we used a sin wave generator combined with a pulse generator and a modulator as a source of the electrical pulse signal. This signal supplied an ultrasonic wide-band probe emitting ultrasonic waves into a tested liquid. The second probe converted received acoustic waves into the electrical signal that was measured on an oscilloscope. The second probe was joined with an arm of cathetometer for accurate measurements of distance between the probes.

Results of the measurements are presented graphically in Figs. 1–10. Theoretical curves are fitted to the experimental results by means of computer calculation programs. These curves present the known theoretical equations as follows:

$$\frac{\alpha}{f^2} = B + \sum_{i=1}^n \frac{A_i}{1 + (f/fr_i)^2} \quad (1)$$

$$\mu = 2 \sum_{i=1}^n \mu_{\max_i} \frac{f/fr_i}{1 + (f/fr_i)^2} \quad (2)$$

where α is the ultrasonic attenuation, f the measured frequency, fr_i the relaxation frequency, A_i the relaxation amplitude, B the contribution to sound attenuation from any other processes that may be occurring at higher frequencies beyond our frequency range. $\mu = (\alpha - Bf^2) \lambda$ represents the excess attenuation per wavelength λ ($\lambda = c/f$, c is the ultrasonic velocity), μ_{\max_i} the maximum excess attenuation per wavelength. n is the number of relaxation processes.

3. Discussion of results and conclusions

As one can see in Fig. 1 and 2, changes of the attenuation coefficients, α/f^2 and μ , with frequency indicate the occurrence of one relaxation process ($n=1$) with a relaxation frequency of 16.7 MHz in the water solution of α -CD. Especially in Fig. 2,

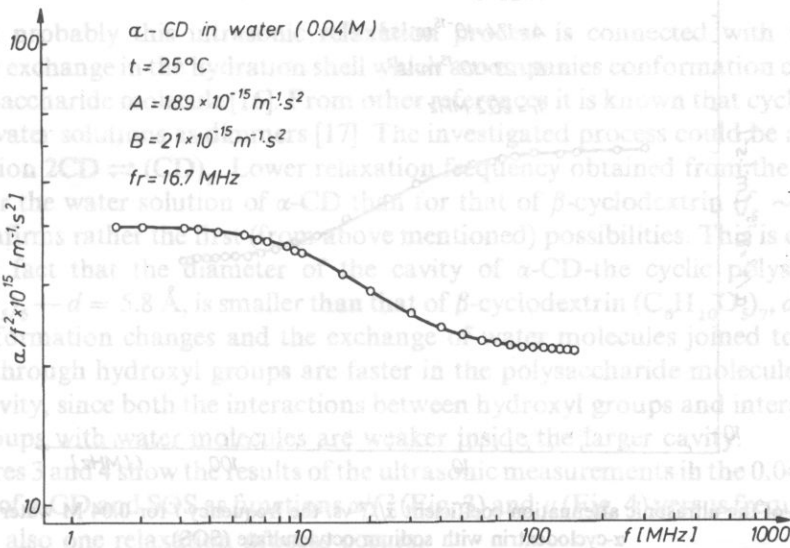


Fig. 1. Plot of the ultrasonic attenuation coefficient α/f^2 vs. the frequency f for 0.04 M water solution of α -cyclodextrin.

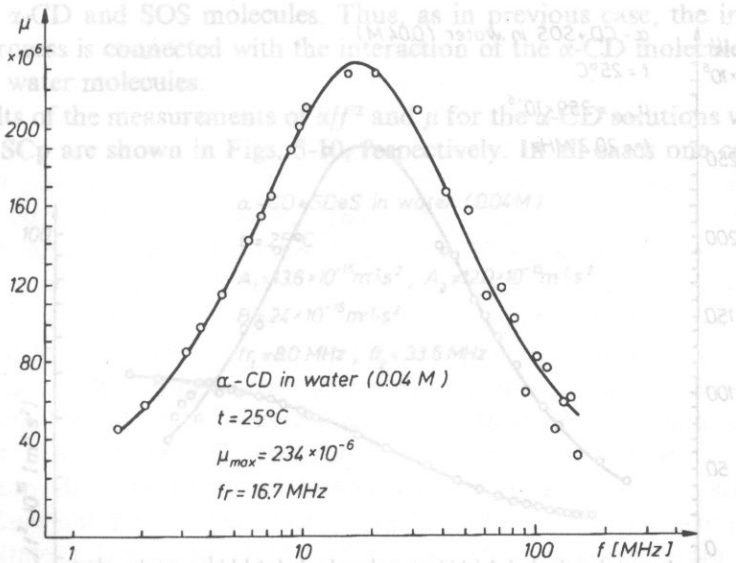


Fig. 2. Plot of the excess ultrasonic attenuation per wavelength μ vs. the frequency f for 0.04 M water solution of α -cyclodextrin.

one can see that because the coefficient μ as a function of frequency f has a regular, gaussian shape typical of single relaxation processes [14, 15]. This result is inconsistent with the data published in ref. [16], in which the occurrence of two relaxation processes was suggested.

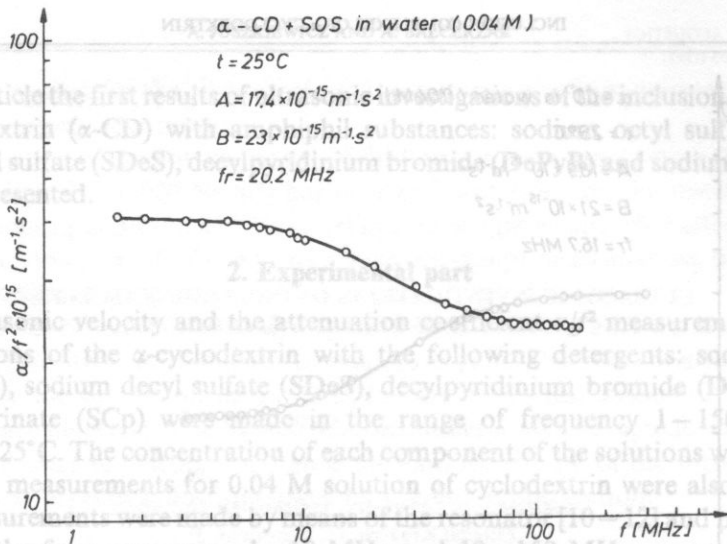


Fig. 3. Plot of the ultrasonic attenuation coefficient α/f^2 vs. the frequency f for 0.04 M water solution of α -cyclodextrin with sodium octyl sulfate (SOS).

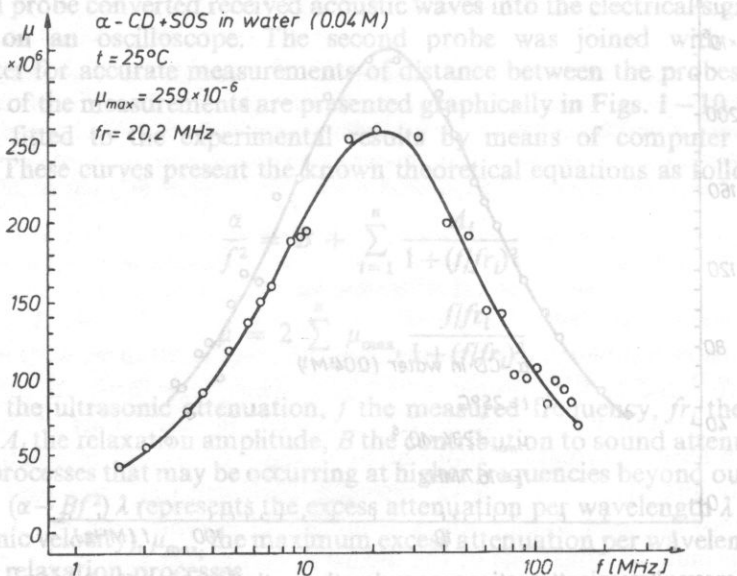


Fig. 4. Plot of the excess ultrasonic attenuation per wavelength μ vs. the frequency f for 0.04 M water solution of α -cyclodextrin with sodium octyl sulfate (SOS).

Most probably this ultrasonic relaxation process is connected with the water molecule exchange in the hydration shell which accompanies conformation changes of the polysaccharide molecule [16]. From other references it is known that cyclodextrins exist in water solutions as dimmers [17]. The investigated process could be a result of the reaction $2\text{CD} \rightleftharpoons (\text{CD})_2$. Lower relaxation frequency obtained from the measurements for the water solution of α -CD than for that of β -cyclodextrin ($f_r \sim 20$ MHz [18]), confirms rather the first (from above mentioned) possibilities. This is connected with the fact that the diameter of the cavity of α -CD—the cyclic polysaccharide ($\text{C}_6\text{H}_{10}\text{O}_5$)₆— $d = 5.8$ Å, is smaller than that of β -cyclodextrin ($\text{C}_6\text{H}_{10}\text{O}_5$)₇, $d = 7.8$ Å. The conformation changes and the exchange of water molecules joined to polysaccharide through hydroxyl groups are faster in the polysaccharide molecule with the greater cavity, since both the interactions between hydroxyl groups and interactions of these groups with water molecules are weaker inside the larger cavity.

Figures 3 and 4 show the results of the ultrasonic measurements in the 0.04 M water solution of α -CD and SOS as functions α/f^2 (Fig. 3) and μ (Fig. 4) versus frequency f . In this case also one relaxation process occurs.

The numerical values of α/f^2 , μ , f_r and A for this solution are approximately equal to those for the α -CD solution. Thus the addition of SOS to the α -CD solution does not cause an essential change in the ultrasonic attenuation and, this suggests no interaction between the α -CD and SOS molecules. Thus, as in previous case, the investigated relaxation process is connected with the interaction of the α -CD molecules with the surrounding water molecules.

The results of the measurements of α/f^2 and μ for the α -CD solutions with SDeS, DePyB and SCp are shown in Figs. 5-10, respectively. In all cases one can observe

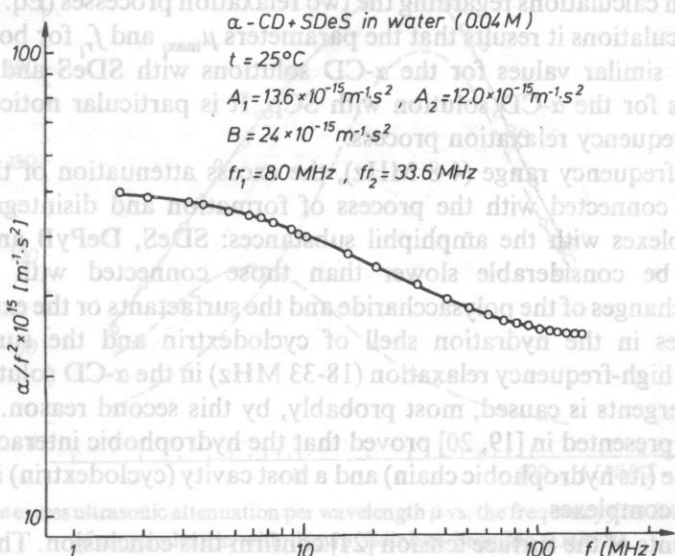


Fig. 5. Plot of the ultrasonic attenuation coefficient α/f^2 vs. the frequency f for 0.04 M water solution of α -cyclodextrin with sodium decyl sulfate (SDeS).

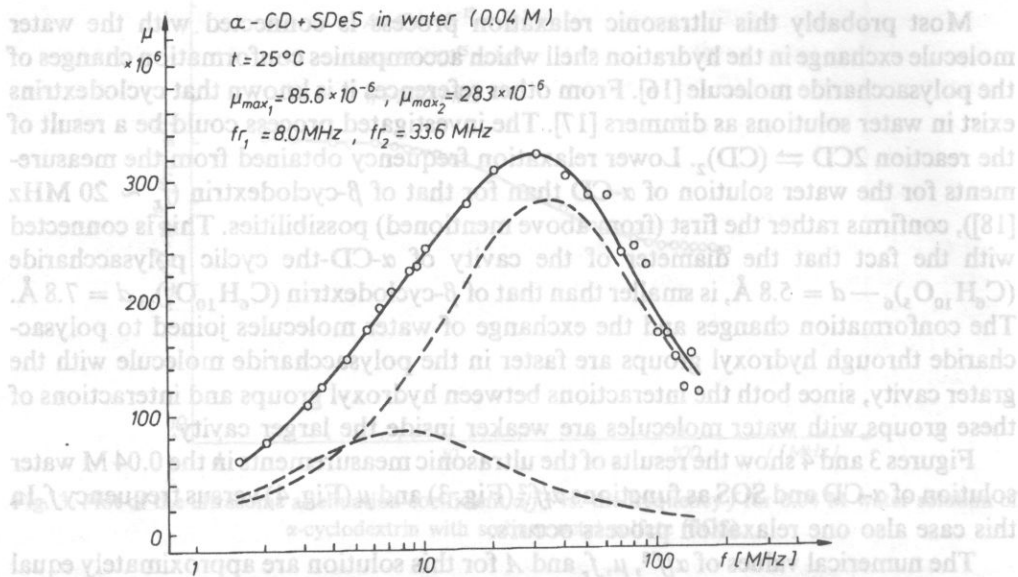


Fig. 6. Plot of the excess ultrasonic attenuation per wavelength μ vs. the frequency f for 0.04 M water solution of α -cyclodextrin with sodium decyl sulfate (SDeS).

a considerable increase of the attenuation coefficients, α/f^2 and μ , and the widened region of the dependence of μ on frequency in comparison to the α -CD and α -CD + SOS solutions. These differences indicate at least two relaxation processes ($n=2$). In Figs. 6, 8 and 10 dashed lines mark the function μ versus frequency obtained from simulation calculations regarding the two relaxation processes (Eq. (2) for $n=2$). From these calculations it results that the parameters μ_{\max_i} and f_{r_i} for both relaxation processes have similar values for the α -CD solutions with SDeS and DePyB and different values for the α -CD solution with SCp. It is particular noticeable for the second, high-frequency relaxation process.

In the low frequency range (4–8 MHz), the excess attenuation of the ultrasonic waves may be connected with the process of formation and disintegration of the inclusion complexes with the amphiphil substances: SDeS, DePyB and SCp. This process must be considerable slower than those connected with the possible conformation changes of the polysaccharide and the surfactants or the exchange of the water molecules in the hydration shell of cyclodextrin and the surfactants. As previously, the high-frequency relaxation (18–33 MHz) in the α -CD solutions with the mentioned detergents is caused, most probably, by this second reason.

The results presented in [19, 20] proved that the hydrophobic interaction between a guest molecule (its hydrophobic chain) and a host cavity (cyclodextrin) are dominant in this kind of complexes.

Measurements of the surface tension [21] confirm this conclusion. The addition of cyclodextrin to the solutions of SDeS, DePyB and SCp causes a significant increase of the surface tension. That must be connected with blocking of the hydrophobic chains

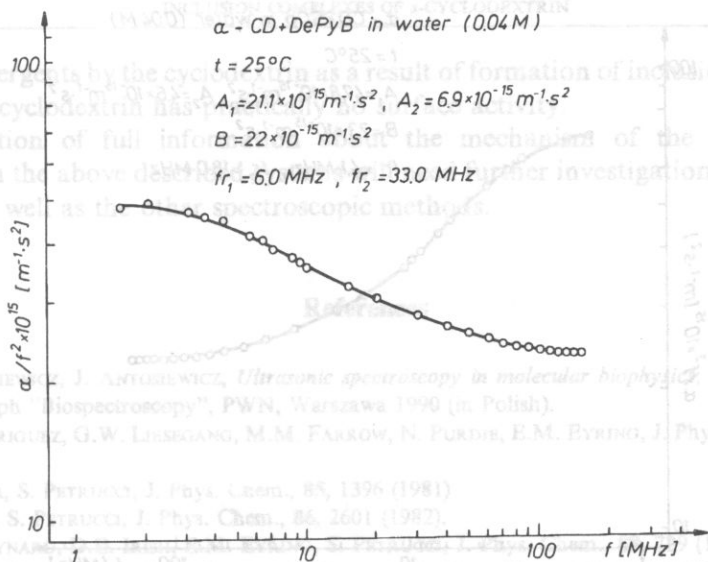


Fig. 7. Plot of the ultrasonic attenuation coefficient α/f^2 vs. the frequency f for 0.04 M water solution of α -cyclodextrin with decylpyridinium bromide (DePyB).

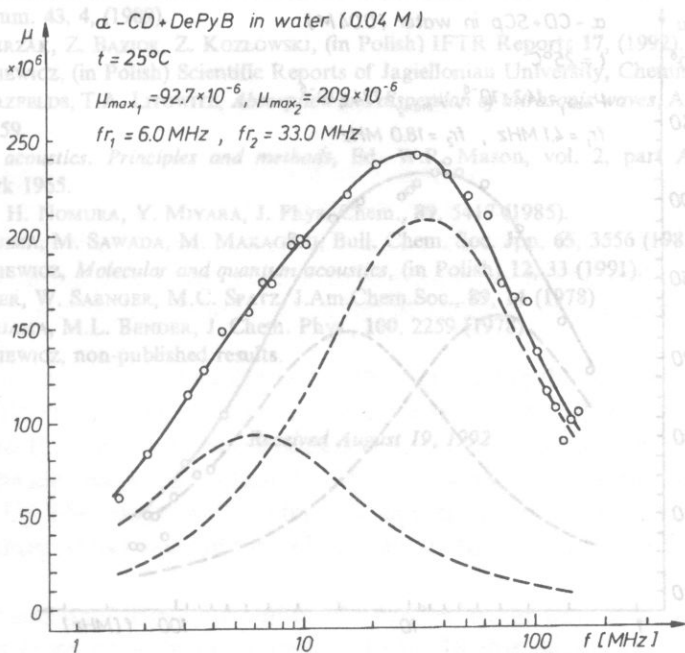


Fig. 8. Plot of the excess ultrasonic attenuation per wavelength μ vs. the frequency f for 0.04 M water solution of α -cyclodextrin with decylpyridinium bromide (DePyB).

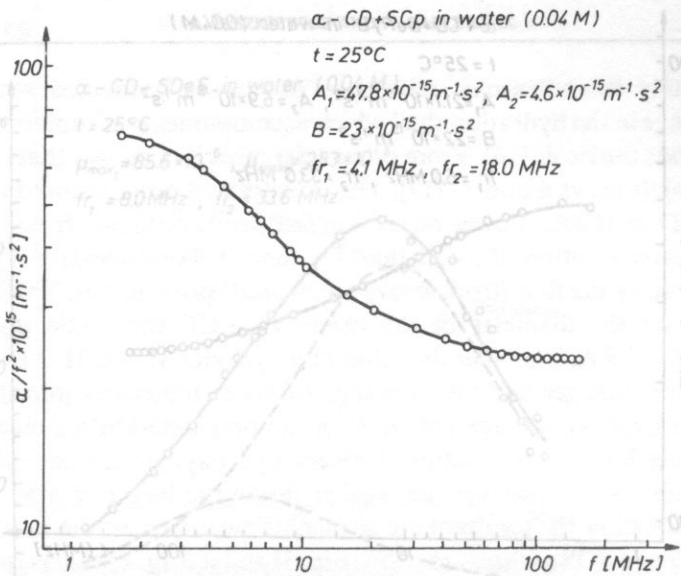


Fig. 9. Plot of the ultrasonic attenuation coefficient α/f^2 vs. the frequency f for 0.04 M water solution of α -cyclodextrin with sodium caprylate (SCp).

Fig. 6. Plot of the excess ultrasonic attenuation per wavelength μ vs. the frequency f for 0.04 M water solution of α -cyclodextrin with sodium decyl sulfate (SDeS).

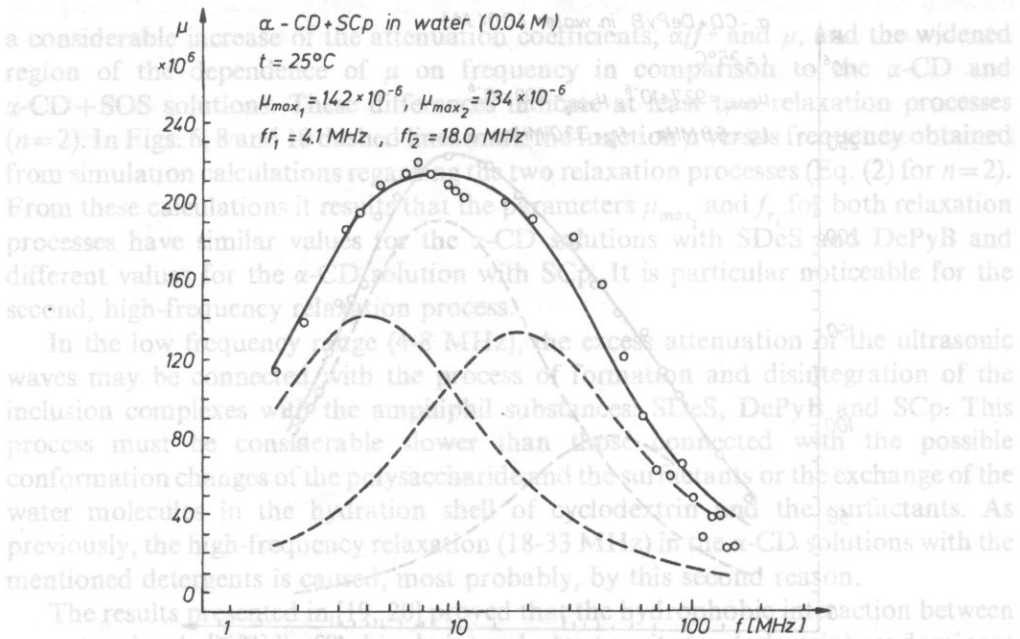


Fig. 10. Plot of the excess ultrasonic attenuation per wavelength μ vs. the frequency f for 0.04 M water solution of α -cyclodextrin with sodium caprylate (SCp).

of these detergents by the cyclodextrin as a result of formation of inclusion complexes, since mere cyclodextrin has practically no surface activity.

Acquisition of full information about the mechanism of the complexation processes in the above described systems will need further investigations by means the acoustic as well as the other spectroscopic methods.

THE APPLICATIONS OF HANKEL TRANSFORM TO THE COMPUTATION
 OF NEARFIELDS OF BAFFLED SOURCES

References

- [1] A. JUSZKIEWICZ, J. ANTOSIEWICZ, *Ultrasonic spectroscopy in molecular biophysics*, part II, vol. 5 in monograph "Biospectroscopy", PWN, Warszawa 1990 (in Polish).
- [2] L.J. RODRIGUEZ, G.W. LIESEBANG, M.M. FARROW, N. PURDIE, E.M. EYRING, *J. Phys. Chem.*, **82**, 647 (1978).
- [3] H. FABER, S. PETRUCCI, *J. Phys. Chem.*, **85**, 1396 (1981)
- [4] C. CHEN, S. PETRUCCI, *J. Phys. Chem.*, **86**, 2601 (1982).
- [5] K.J. MAYNARD, D.E. IRISH, E.M. EYRING, S. PETRUCCI, *J. Phys. Chem.*, **88**, 729 (1984).
- [6] C. CHEN, W. WALLACE, E.M. EYRING, S. PETRUCCI, *J. Phys. Chem.*, **88**, 2541 (1984).
- [7] C. CHEN, W. WALLACE, E.M. EYRING, S. PETRUCCI, *J. Phys. Chem.*, **88**, 5445 (1984).
- [8] W. WALLACE, E.M. EYRING, S. PETRUCCI, *J. Phys. Chem.*, **88**, 6353 (1984).
- [9] H. FARBER, S. PETRUCCI, *J. Phys. Chem.*, **85**, 2987 (1981).
- [10] F. EGGERS, F. FUNCK, K.H. RICHMANN, H. SCHNEIDER, E.M. EYRING, *J. Phys. Chem.*, **91**, 1961 (1987).
- [11] G. GALIŃSKI, Z. KOZŁOWSKI, *Ultrasonic spectroscopy equipment for the 0.5 - 15 MHz frequency range*, *Sci. Instrum.* **43**, 4, (1989).
- [12] A. BALCERZAK, Z. BAZIOR, Z. KOZŁOWSKI, (in Polish) *IFTR Reports* **17**, (1992).
- [13] A. JUSZKIEWICZ, (in Polish) *Scientific Reports of Jagiellonian University, Chemistry*, **19**, 109 (1974).
- [14] K.F. HERZFELDS, T.A. LITOWITZ, *Absorption and dispersion of ultrasonic waves*, Academic Press, New York, 1959.
- [15] *Physical acoustics. Principles and methods*, Ed. W.P. Mason, vol. 2, part A. Academic Press, New York 1965.
- [16] S. KATO, H. NOMURA, Y. MIYARA, *J. Phys. Chem.*, **89**, 5417 (1985).
- [17] K. MIYAJIMA, M. SAWADA, M. MAKAGAKI, *Bull. Chem. Soc. Jpn*, **65**, 3556 (1983).
- [18] A. JUSZKIEWICZ, *Molecular and quantum acoustics*, (in Polish) **12**, 33 (1991).
- [19] F. CRAMER, W. SAENGER, M.C. SPATZ, *J. Am. Chem. Soc.*, **89**, 14 (1978)
- [20] M. KOMIJAMA, M.L. BENDER, *J. Chem. Phys.*, **100**, 2259 (1978).
- [21] A. JUSZKIEWICZ, non-published results.

Received August 19, 1992

In this paper we present a different method of solving the problem of a nearfield of circular baffled sources by means of the integral Hankel transform. Application of this transform to the Helmholtz wave equation in cylindrical coordinates is due to L.U. KING [5]. The idea has been continued by M.C. JUNGER in his monograph [4] and by M. GREENSPAN [3]. The quoted authors limited yet their interest to the far field, computing the proper integral by means of the saddle point method [4], or to the field on the axis of the source.

The method is quite general and can be applied to the case of an arbitrary velocity distribution given on a baffled circular piston. In this paper we have modified the method and obtained the integral representation of the nearfield of a piston with uniform velocity distribution and a membrane, of course with its "natural" Bessel distribution. Both expressions are given in the form of single integral of Bessel functions and are easily calculated numerically.

**THE APPLICATIONS OF HANKEL TRANSFORM TO THE COMPUTATION
OF NEARFIELDS OF CIRCULAR BAFFLED SOURCES**

R. WYRZYKOWSKI AND A. CZYRKA

Department of Acoustics Institute of Physics
(35-310 Rzeszów, ul. Rejtana 16)

In the present paper we give a new method of computation of near sound fields emitted by baffled circular sources. We have applied the Hankel transform and King's integral. Two examples were calculated — namely the piston with uniform velocity distribution and membrane for different values of the rate of the speed of elastic waves in the membrane to the speed in the medium.

1. Introduction

The computation of the near field of a baffled circular piston was given by H. STENZEL [9] and is quoted in every textbook on acoustics [e.g. 11].

Nevertheless the Stenzel's solution has two disadvantages; first — the acoustic pressure is expressed *de facto* in the form of a triple series and is therefore difficult to calculate. Second — the method itself is limited to the special case of uniform velocity distribution.

In this paper we present a different method of solving the problem of a nearfield of circular baffled sources by means of the integral Hankel transform. Application of this transform to the Helmholtz wave equation in cylindrical coordinates is due to L.U. KING [5]. The idea has been continued by M.C. JUNGER in his monograph [4] and by M. GREENSPAN [3]. The quoted authors limited yet their interest to the far field, computing the proper integral by means of the saddle point method [4], or to the field on the axis of the source.

The method is quite general and can be applied to the case of an arbitrary velocity distribution given on a baffled circular piston. In this paper we have modified the method and obtained the integral representation of the nearfield of a piston with uniform velocity distribution and a membrane, of course with its "natural" Bessel distribution. Both expressions are given in the form of single integral of Bessel functions and are easily calculated numerically.

2. The general problem of an arbitrary velocity distribution on a circular baffled piston

We will consider the problem of computing the acoustical potential Φ , which in the case of harmonic vibrations is proportional to the acoustic pressure p :

$$p = i\rho_0\omega\Phi = i\rho_0c_0k\Phi, \quad (1)$$

where ρ_0 is the density of the medium at rest, ω is the angular frequency of vibrations, k is the wave number and c_0 adiabatic velocity of sound.

The velocity of vibrations u , called also the acoustic velocity, is by definition the gradient of the acoustic potential:

$$\vec{u} = -\text{grad } \Phi, \quad (2)$$

Introducing the cylindrical coordinates system, that is natural in our problem, we can write down the Helmholtz equation for the acoustic potential in the form:

$$\frac{\partial^2\Phi}{\partial r^2} + \frac{1}{r} \frac{\partial\Phi}{\partial r} + \frac{\partial^2\Phi}{\partial z^2} + k^2\Phi = 0, \quad (3)$$

Here the field is considered to be independent of the angular coordinate φ . For a given function $u(r)$ representing the velocity distribution on the source, equation (3) has to obey the following boundary conditions:

$$\left. \frac{\partial\Phi}{\partial z} \right|_{z=0} = \begin{cases} u(r) & 0 < r \leq a, \\ 0 & r > a, \end{cases} \quad (4)$$

where a denotes the radius of the piston. We apply the zero order Hankel transform to both sides of the equation (3). There are several definitions of Hankel transform used in literature. In the present paper we use the form accepted in the monograph [6]. The transform of the acoustic potential $\Phi(r, z)$, denoted as $U(\rho, z)$ we write therefore in the form:

$$U(\rho, z) = \int_0^\infty r \Phi(r, z) J_0(\rho r) dr, \quad (5)$$

where $J_0(\cdot)$ is the Bessel function of zero order. The sum of the two first terms in equation (3) is transformed, according to the basic property of Hankel transform [6] into:

$$\frac{\partial^2\Phi}{\partial r^2} + \frac{1}{r} \frac{\partial\Phi}{\partial r} = -\rho^2 U \quad (6)$$

The transformed equation (3) takes now the form:

$$\frac{d^2U}{dz^2} - (\rho^2 - k^2) U = 0, \quad (7)$$

It is, of course, the differential equation for the transformed potential i.e. $U(\rho, z)$. The Hankel transform can also be applied to the boundary condition (4). For that purpose we must transform the velocity distribution $u(r)$. That transform, denoted as $H_0(\rho)$ is equal (5):

$$H_0(\rho) = \int_0^a r u(r) J_0(\rho, r) dr, \quad (8)$$

We change the upper limit of the integral defining the transform from ∞ to a because $u(r) \neq 0$ only for $r \leq a$. Since differentiation with respect to z is independent of the integration variable in the Hankel transform, the transformed boundary conditions takes the form:

$$\left. \frac{dU}{dz} \right|_{z=0} = H_0(\rho) \quad (9)$$

The general solution of equation (7) has the form:

$$U(\rho, z) = A(\rho) e^{-\sqrt{\rho^2 - k^2} z} + B(\rho) e^{\sqrt{\rho^2 - k^2} z}, \quad (10)$$

The second term of the r.h.s. (10) tends to infinity when z increases and $\rho > k$. Therefore we have to put:

$$B(\rho) = 0, \quad (11)$$

and finally get:

$$U(\rho, z) = A(\rho) e^{-\sqrt{\rho^2 - k^2} z}, \quad (12)$$

now we can calculate easily the l.h.s. of the boundary condition (9). We have namely from (12):

$$\left. \frac{dU}{dz} \right|_{z=0} = -A(\rho) \sqrt{\rho^2 - k^2}. \quad (13)$$

Thus the unknown in (12) $A(\rho)$ is equal:

$$A(\rho) = -\frac{1}{\sqrt{\rho^2 - k^2}} \left. \frac{dU}{dz} \right|_{z=0}, \quad (14)$$

Substituting in r.h.s. (14) $\left. \frac{dU}{dz} \right|_{z=0}$ from (9) we obtain:

$$A(\rho) = -\frac{1}{\sqrt{\rho^2 - k^2}} H_0(\rho), \quad (15)$$

While examining specific cases (examples) we know the accepted distribution $u(r)$ and therefore we can find its transform $H_0(\rho)$ (9) which allows us to compute $A(\rho)$ (15) and the transform $U(\rho)$ of the acoustic potential by means of the formula (12). Then:

$$U(\rho, z) = -\frac{1}{\sqrt{\rho^2 - k^2}} H_0(\rho) e^{-\sqrt{\rho^2 - k^2} z}. \quad (16)$$

The potential can be computed as the inverse Hankel transform of order 0:

$$\Phi(r, z) = \int_0^{\infty} U(\rho, z) J_0(\rho r) \rho \, d\rho, \quad (17)$$

and, after substituting in (17) the value $U(\rho, z)$ (16) we have finally:

$$\Phi(r, z) = -\int_0^{\infty} \frac{J_0(\rho r)}{\sqrt{\rho^2 - k^2}} H_0(\rho) e^{-\sqrt{\rho^2 - k^2} z} \rho \, d\rho \quad (18)$$

The above integral can be obtained also by means of another methods, e.g. by integrating the adequate Green function [4]. It is called the King' integral. However the method presented in this paper seems to be clearer and simpler.

In practical applications we must integrate (18) from 0 to k and from k to ∞ , to obtain real and imaginary part of $\Phi(r, z)$.

3. Acoustic potential in the nearfield of a baffled rigid piston with uniform velocity distribution

The velocity distribution $u(r)$ has in our case the form:

$$u(r) = \begin{cases} u_0 & 0 < r \leq a \\ 0 & r > a \end{cases} \quad (19)$$

According to the formula (8) the Hankel transform of that distribution is:

$$H_0(\rho) = u_0 \int_0^a r J_0(\rho r) \, dr. \quad (20)$$

The r.h.s. of (20) represents an elementary integral [2] [9] and we write:

$$H_0(\rho) = u_0 a \frac{J_1(\rho a)}{\rho}, \quad (21)$$

where $J_1(\)$ is a first order Bessel function. According to the formula (18) the acoustic potential takes now the form:

$$\Phi(r, z) = -u_0 a \int_0^{\infty} \frac{e^{-\sqrt{\rho^2 - k^2} z}}{\sqrt{\rho^2 - k^2}} J_1(\rho a) J_0(\rho r) \, d\rho. \quad (22)$$

The formula (22) can be written in a simpler form introducing a new variable:

$$x = \rho a \quad (23)$$

Then:

$$\Phi\left(\frac{r}{a}, \frac{z}{a}\right) = -u_0 a \int_0^\infty \frac{e^{-\sqrt{x^2 - (ka)^2} \frac{z}{a}}}{\sqrt{x^2 - (ka)^2}} J_1(x) J_0\left(\frac{r}{a} x\right) dx \quad (24)$$

In the formula (24) we have only the relative values $\frac{r}{a}, \frac{z}{a}$ and the so called diffraction parameter ka . We divide the integral into two parts namely from 0 to k and from k to ∞ . We separate the real and imaginary part and obtain:

$$\begin{aligned} \Phi\left(\frac{r}{a}, \frac{z}{a}\right) &= u_0 a \int_0^k \frac{\sin\left(\sqrt{(ka)^2 - x^2} \frac{z}{a}\right)}{\sqrt{(ka)^2 - x^2}} J_1(x) J_0\left(\frac{r}{a} x\right) dx + \\ &- u_0 a \int_k^\infty \frac{e^{-\sqrt{x^2 - (ka)^2} \frac{z}{a}}}{\sqrt{x^2 - (ka)^2}} J_1(x) J_0\left(\frac{r}{a} x\right) dx + \\ &+ i u_0 a \int_0^k \frac{\cos\left(\sqrt{(ka)^2 - x^2} \frac{z}{a}\right)}{\sqrt{(ka)^2 - x^2}} J_1(x) J_0\left(\frac{r}{a} x\right) dx. \end{aligned} \quad (25)$$

In the formula (1) expressing the acoustical pressure p by means the potential Φ we have in our case the following coefficient before the integral namely $\omega \rho u_0 a$, which has the dimensions of a pressure. For that reason we will compute and show in figures the relative pressure equal:

$$p_{\text{rel}} = \frac{p}{\omega \rho u_0 a} \quad (26)$$

4. Circular membrane

We have a circular membrane fastened on its edge. The displacement distribution, independent of the angular variable φ has the form:

$$\xi(r, t) = A J_0(k_n^{(r)} r) e^{i\omega t} = \xi_0(r) e^{i\omega t}. \quad (27)$$

In the above formula $k_n^{(r)}$ denotes the wave number of standing waves in the membrane, depending on the variable r . The set of admissible wave numbers is a discrete one and for that reason we have the index n . On the edge i.e. for the value $r = a$ the displacement must fulfil the condition:

$$\xi_0(a) = 0, \quad (28)$$

or:

$$J_0(k_n^{(r)} a) = 0. \quad (29)$$

That condition gives us the set of admissible wave numbers $k_n^{(r)}$. Denoting by α_{0n} the value of n -th zero of zero order Bessel function we have:

$$k_n^{(r)} = \frac{\alpha_{0n}}{a} \rho \quad (30)$$

The velocity of vibration on the membrane equals therefore (27):

$$u(r, t) = \frac{\partial \xi}{\partial t} = i\omega A J_0(k_n^{(r)} r) e^{i\omega t} = i\omega A J_0\left(\alpha_{0n} \frac{r}{a}\right) e^{i\omega t} \quad (31)$$

and can be written as:

$$u(r) = \begin{cases} u_0 J_0\left(\alpha_{0n} \frac{r}{a}\right) & 0 \leq r \leq a \\ 0 & r > a \end{cases} \quad (32)$$

where:

$$u_0 = i\omega A \quad (33)$$

The presence of i in (33) is of course meaningless — we can, for instance, accept an imaginary value of A — it is only the problem of the phase shift.

According to the formula (8) the Hankel transform of the velocity distribution (32) has now the form:

$$H_0(\rho) = u_0 \int_0^a r J_0\left(\alpha_{0n} \frac{r}{a}\right) J_0(\rho r) dr \quad (34)$$

The integral in the r.h.s. (34) is given in the tables [2], [7] and we obtain:

$$H_0(\rho) = u_0 \frac{\alpha_{0n} J_1(\alpha_{0n}) J_0(\rho a) - \rho a J_0(\alpha_{0n}) J_1(\rho a)}{\left(\frac{\alpha_{0n}}{a}\right)^2 - \rho^2} \quad (35)$$

Of course $J_0(\alpha_{0n}) = 0$ and we get:

$$H_0(\rho) = u_0 \frac{\alpha_{0n} J_1(\alpha_{0n}) J_0(\rho a)}{\left(\frac{\alpha_{0n}}{a}\right)^2 - \rho^2} \quad (36)$$

The wave number k in the formula (18) is the wave number of waves propagating in the medium (e.g. air). The angular frequency of these waves is:

$$\omega_n = k_n^{(r)} \cdot c_m \quad (37)$$

where c_m denotes the velocity of elastic waves on the membrane. To this frequency corresponds the wave number in the medium equal:

$$k_n = \frac{\omega_n}{c} = \frac{\alpha_{0n}}{a} \cdot \frac{c_m}{c} \quad (38)$$

where c denotes the velocity of sound in the considered medium.

Substituting $H_0(\rho)$ (34) into the formula (18) we get the acoustical potential in the nearfield of the membrane in the form:

$$\Phi(r, z) = -\alpha_{0n} u_0 J_1(\alpha_{0n}) \int_0^{\infty} \frac{e^{-\sqrt{\rho^2 - k_n^2} z} J_0(\rho a) J_0(\rho r)}{\left[\left(\frac{\alpha_{0n}}{a} \right)^2 - \rho^2 \right] \sqrt{\rho^2 - k_n^2}} \rho d\rho \quad (39)$$

We introduce in the formula (39) the variable x (23) and we get:

$$\Phi\left(\frac{r}{a}, \frac{z}{a}\right) = -\alpha_{0n} u_0 J_1(\alpha_{0n}) \int_0^{\infty} \frac{e^{-\sqrt{x^2 - k_n^2} \frac{z}{a}} J_0(x) J_0\left(\frac{r}{a} x\right)}{(\alpha_{0n}^2 - x^2) \sqrt{x^2 - k_n^2}} x dx \quad (40)$$

According to the formula (38) we have:

$$k_n a = \alpha_{0n} \frac{c_m}{c} \quad (41)$$

Therefore we can write (40) in the form:

$$\Phi\left(\frac{r}{a}, \frac{z}{a}\right) = -\alpha_{0n} u_0 a J_1(\alpha_{0n}) \int_0^{\frac{c_m}{c}} \frac{e^{-\sqrt{x^2 - \left(\alpha_{0n} \frac{c_m}{c}\right)^2} \frac{z}{a}} J_0(x) J_0\left(\frac{r}{a} x\right)}{(\alpha_{0n}^2 - x^2) \sqrt{x^2 - \left(\alpha_{0n} \frac{c_m}{c}\right)^2}} x dx \quad (42)$$

We separate in (42) the real and imaginary parts and get finally:

$$\begin{aligned} \Phi\left(\frac{r}{a}, \frac{z}{a}\right) = & \alpha_{0n} u_0 a J_1(\alpha_{0n}) \int_0^{\frac{c_m}{c}} \frac{\sin\left(\sqrt{\left(\alpha_{0n} \frac{c_m}{c}\right)^2 - x^2} \frac{z}{a}\right) J_0(x) J_0\left(\frac{r}{a} x\right)}{(\alpha_{0n}^2 - x^2) \sqrt{\left(\alpha_{0n} \frac{c_m}{c}\right)^2 - x^2}} x dx + \\ & - \alpha_{0n} u_0 a J_1(\alpha_{0n}) \int_0^{\frac{c_m}{c}} \frac{e^{-\sqrt{x^2 - \left(\alpha_{0n} \frac{c_m}{c}\right)^2} \frac{z}{a}} J_0(x) J_0\left(\frac{r}{a} x\right)}{(\alpha_{0n}^2 - x^2) \sqrt{x^2 - \left(\alpha_{0n} \frac{c_m}{c}\right)^2}} x dx + \\ & + i \alpha_{0n} u_0 a J_1(\alpha_{0n}) \int_0^{\frac{c_m}{c}} \frac{\cos\left(\sqrt{\left(\alpha_{0n} \frac{c_m}{c}\right)^2 - x^2} \frac{z}{a}\right) J_0(x) J_0\left(\frac{r}{a} x\right)}{(\alpha_{0n}^2 - x^2) \sqrt{\left(\alpha_{0n} \frac{c_m}{c}\right)^2 - x^2}} x dx. \end{aligned} \quad (43)$$

To compare the results obtained for the piston and the membrane we must normalize the formulae for the membrane in a way assuming the same output for both sources. We denote by u_{om} the velocity amplitude for the membrane — now we must distinguish between that value for the piston and of the membrane. According to (32) the output of the membrane equals:

$$Q_m = \int_0^a \int_0^{2\pi} u_{om} J_0\left(\frac{\alpha_{om}}{a} r\right) r dr d\varphi = 2\pi u_{om} \int_0^a J_0\left(\frac{\alpha_{om}}{a} r\right) r dr. \quad (44)$$

The integral in the r.h.s. (44) is an elementary one [2] and:

$$Q_m = 2\pi u_{om} \frac{a^2}{\alpha_{om}} J_1(\alpha_{om}). \quad (45)$$

The output of the piston with the constant velocity distribution u_0 equals:

$$Q_p = \pi a^2 u_0. \quad (46)$$

Equating (46) to (45) we get:

$$u_{om} = \frac{\alpha_{om}}{2 J_1(\alpha_{om})} u_0 \quad (47)$$

In the figures we represent of course the amplitude of the relative pressure (26). The numbers ka for the piston were chosen the same as for the membrane e.i. corresponding to the successive zeros of $J_0(\)$.

5. Conclusions

We have computed numerically the normalized pressure modulus versus the relative distance from the axis (r/a) and the relative value z/a for a piston and a membrane.

The computations were performed for the values of ka corresponding to successive zeros of the Bessel function $J_0(\)$. Besides, for the membrane, the computations were performed for the C_m/C equal 0.5; 1.0 and 1.5.

Of course the modulus of the pressure depends on the value of ka for both the piston and the membrane and with the increase of ka the sound field becomes more complicated — if one may use that word in the nearfield — more "directional". For the membrane the increase of the ratio C_m/C deteriorates the "directivity". (Fig. 1...3)

The figures 3 and 4 represent the normalized pressure modulus of the z axis, namely for $r/a = 0$.

The numbers of figures were represented in a very clear way, namely denoted for P by the piston, $M(a)$, $M(b)$, $M(c)$ for the membrane ($C_m/C = 0.5; 1.0; 1.5$).

Fig. 1P. The normalized pressure modulus (P) as a function of normalized distance along z -axis z/a and normalized radial coordinate r/a for rigid pistone. The normalized wavenumber (diffraction parameter) $ka=2.404\dots$ is equal to the value of the first zero of the Bessel function $J_0()$.

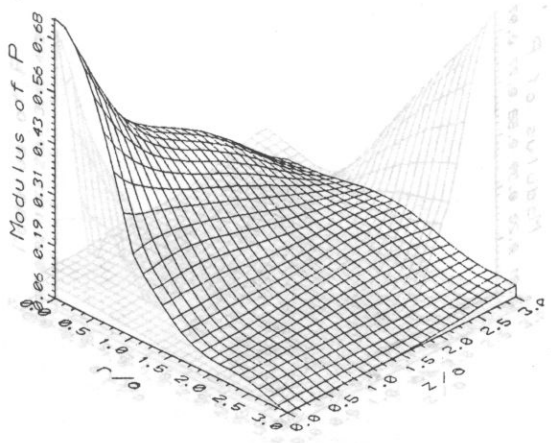


Fig. 1M(a) The normalized pressure modulus (P) as a function of normalized distance along z -axis z/a and normalized radial coordinate r/a for membrane. The normalized wavenumber (diffraction parameter) $ka=2.404\dots$ is equal to the value of the first zero of the Bessel function $J_0()$. Coefficient $C_m/C=0.5$

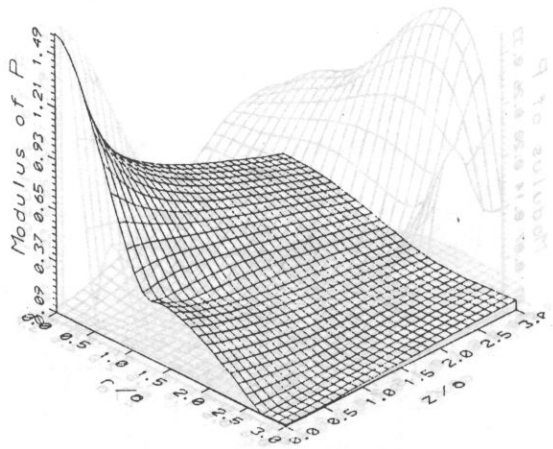
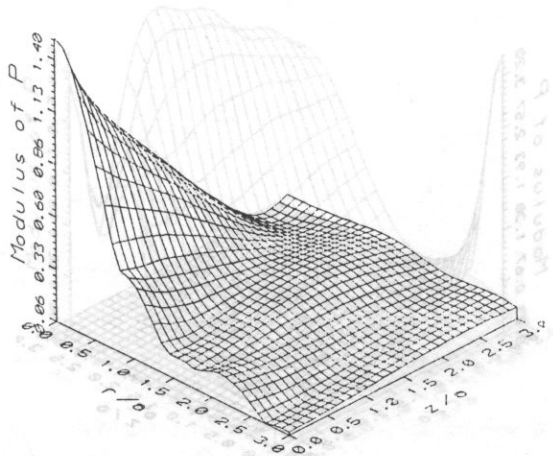


Fig. 1M(b) Same as Fig. 1M(a) but coefficient $C_m/C=1$.



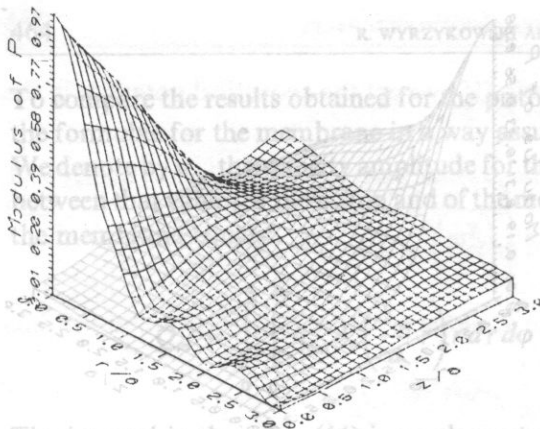


Fig. 1M(c) Same as Fig. 1M(a) but coefficient $C_m C = 1.5$.

The integral in the r.h.s. (44) is an elementary one [2] and:

$$Q_m = 2\pi u_0 \int_0^a \frac{a^2}{r} J_1(x_{0m}) r dr. \quad (45)$$

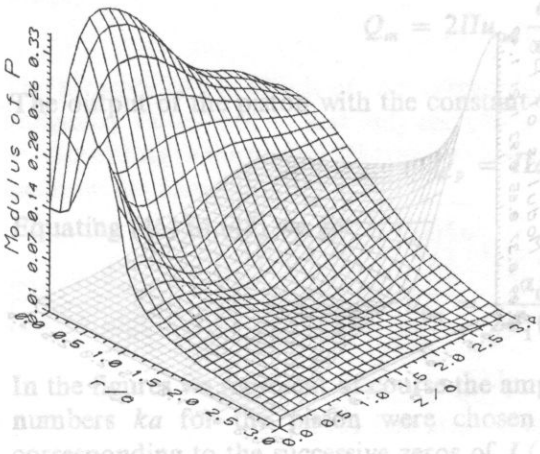


Fig. 2P The normalized pressure modulus (P) as a function of normalized distance along z -axis z/a and normalized radial coordinate r/a for rigid pistone. The normalized wavenumber (diffraction parameter) $ka = 5.520\dots$ is equal to the value of the second zero of the Bessel function $J_0(0)$.

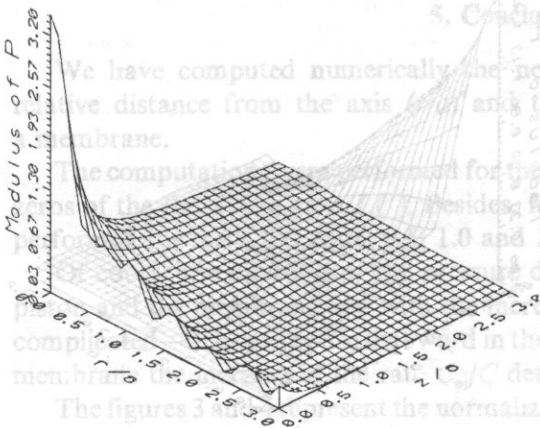


Fig. 2M(a) The normalized pressure modulus (P) as a function of normalized distance along z -axis z/a and normalized radial coordinate r/a for membrane. The normalized wavenumber (diffraction parameter) $ka = 5.520\dots$ is equal to the value of the first zero of the Bessel function $J_0(0)$. Coefficient $C_m C = 0.5$

5. Conclusions

We have computed numerically the normalized pressure modulus versus the distance from the axis z/a and the relative value r/a for a piston and membrane.

The computations were done for the values of ka corresponding to successive zeros of the Bessel function $J_0(x)$. Besides, for the membrane, the computations were done for the values of ka corresponding to successive zeros of the Bessel function $J_1(x)$. The figures 3 and 4 present the normalized pressure modulus P for $r/a = 0$.

The numbers of figures were represented in a very clear way, namely denoted for P by the piston, $M(a)$, $M(b)$, $M(c)$ for membrane ($C_m C = 0.5; 1.0; 1.5$).

Fig. 2M(b) Same as Fig. 2M(a) but coefficient $C_m C = 1$.

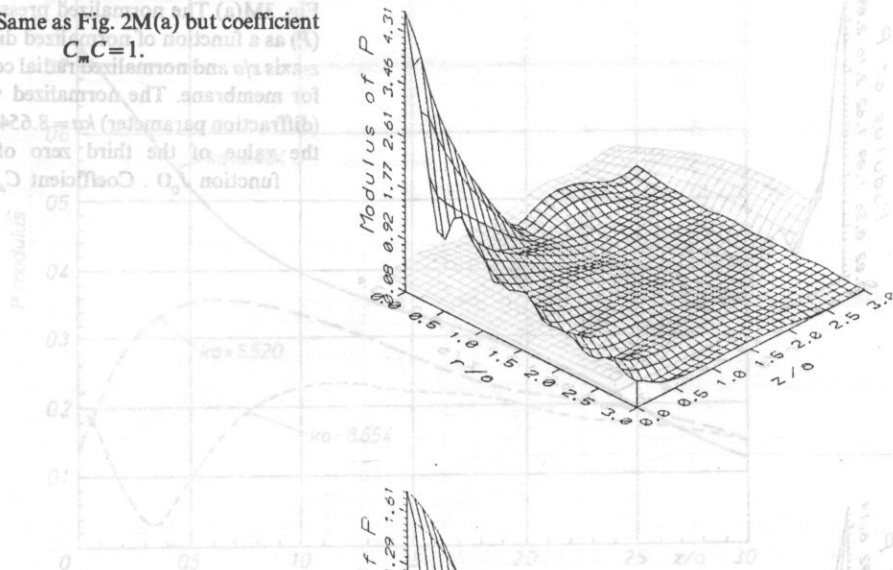


Fig. 4P The normalized pressure modulus (P) on z -axis of rigid pistone versus normalized coordinate z/a ($r/a=0$) for $ka=2.404$.

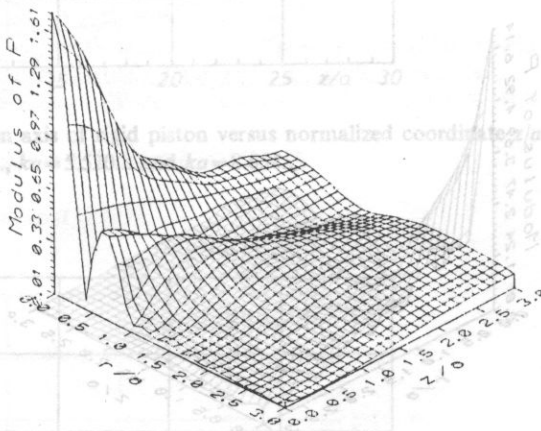


Fig. 2M(c) Same as Fig. 2M(a) but coefficient $C_m C = 1.5$.

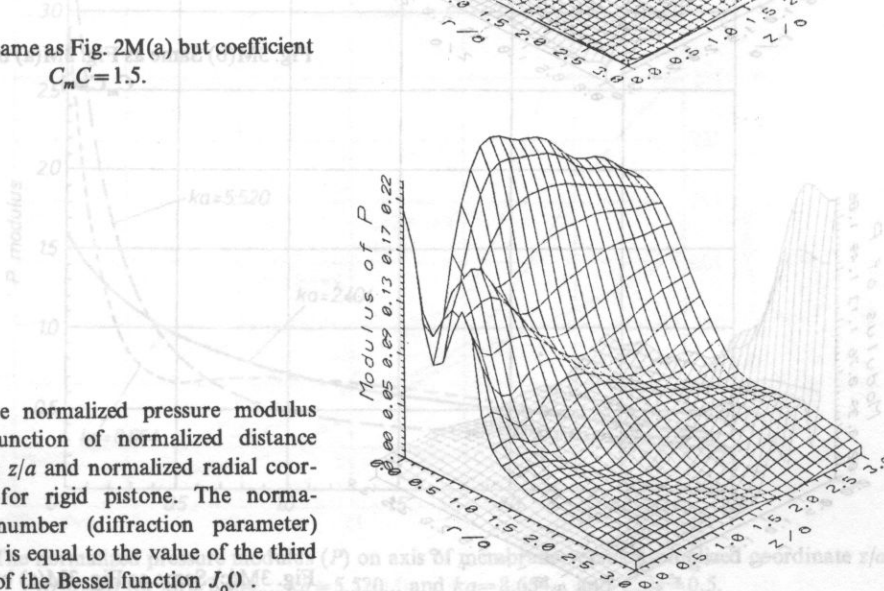


Fig. 3P The normalized pressure modulus (P) as a function of normalized distance along z -axis z/a and normalized radial coordinate r/a for rigid pistone. The normalized wavenumber (diffraction parameter) $ka=8.654$... is equal to the value of the third zero of the Bessel function $J_0()$.

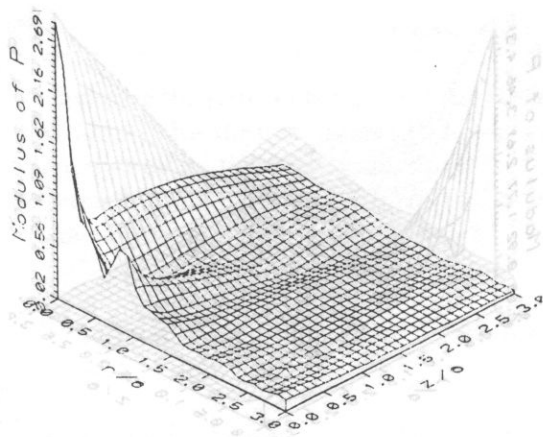


Fig. 3M(a) The normalized pressure modulus (P) as a function of normalized distance along z -axis z/a and normalized radial coordinate r/a for membrane. The normalized wavenumber (diffraction parameter) $ka = 8.654\dots$ is equal to the value of the third zero of the Bessel function $J_0()$. Coefficient $C_m/C = 0.5$

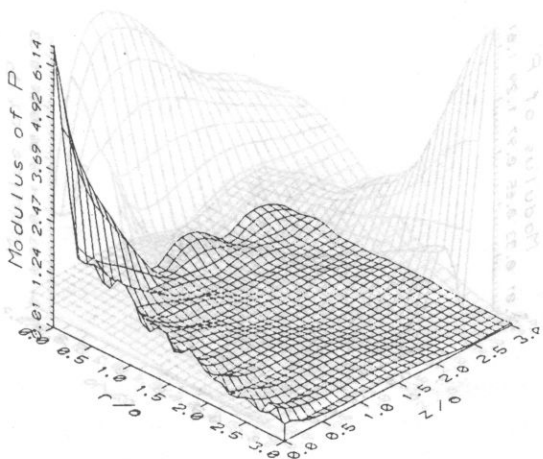


Fig. 2P The normalized pressure modulus (P) as a function of normalized distance along z -axis z/a and normalized radial coordinate r/a for rigid pistons. The normalized wavenumber (diffraction parameter)

Fig. 3M(b) Same as Fig. 3M(a) but coefficient $C_m/C = 1$.

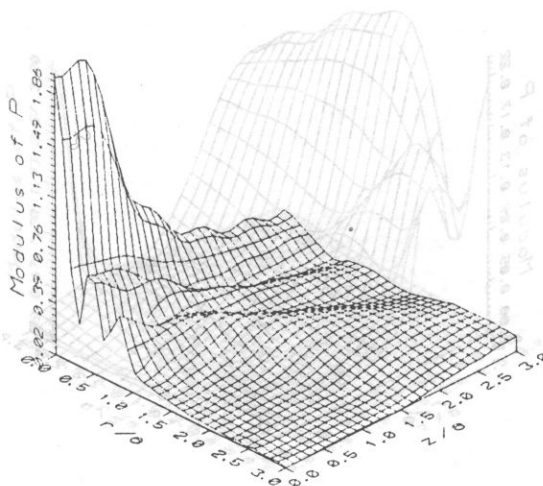


Fig. 3M(c) Same as Fig. 3M(a) but coefficient $C_m/C = 1.5$.

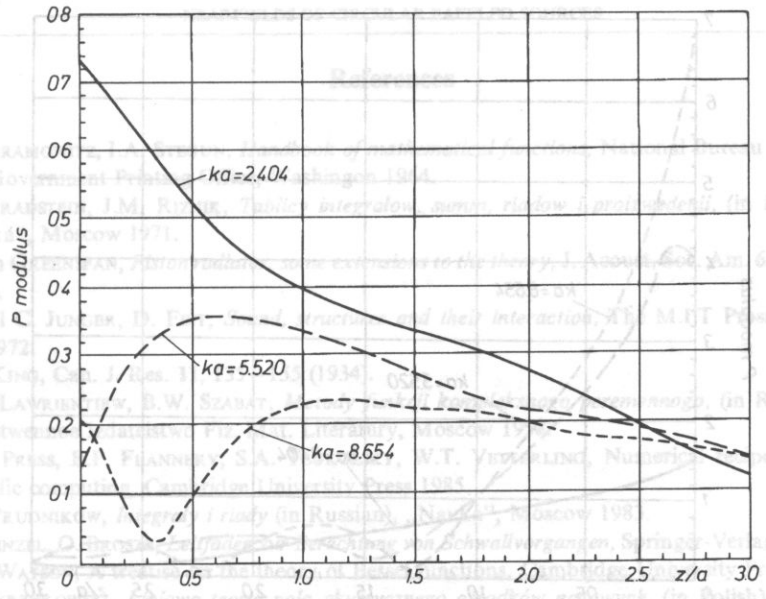


Fig. 4P The normalized pressure modulus (P) on axis of rigid piston versus normalized coordinate z/a ($r/a=0$) for $ka=2.404\dots$, $ka=5.520\dots$ and $ka=8.654\dots$

Received April 6, 1992

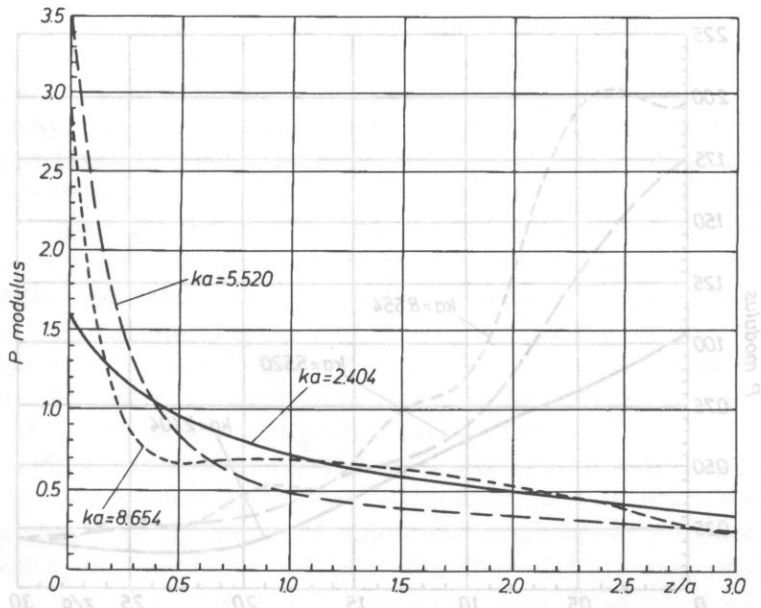


Fig. 4M(a) The normalized pressure modulus (P) on axis of membrane versus normalized coordinate z/a ($r/a=0$) for $ka=2.404\dots$, $ka=5.520\dots$ and $ka=8.654\dots$ and $C_m/c=0.5$.

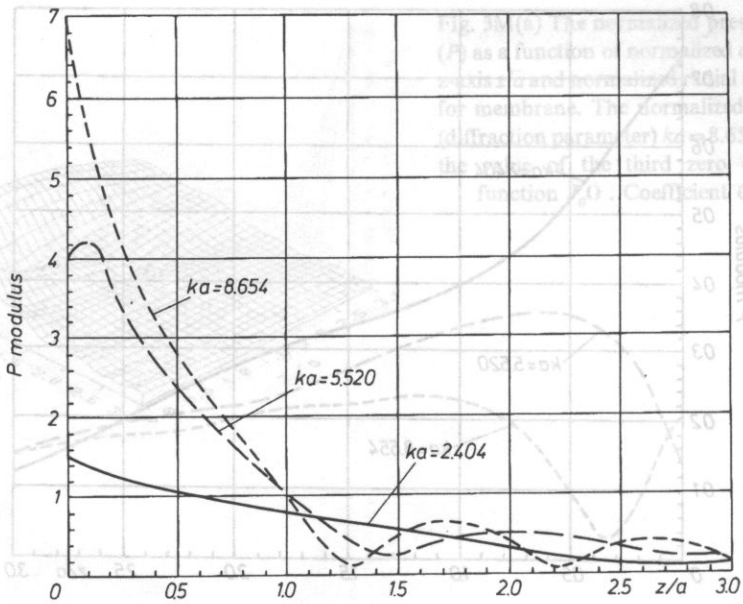


Fig. 4M(b) Same as Fig. 4M(a) but coefficient $C_m/c=1$.

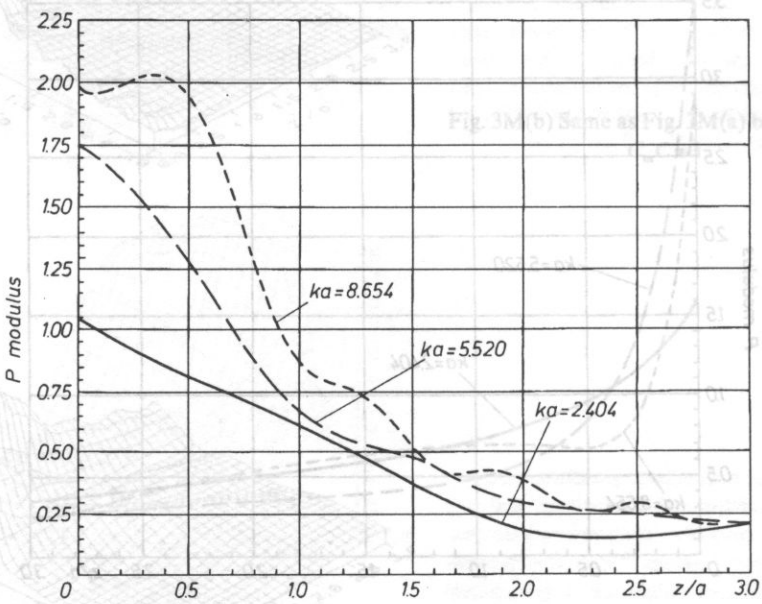


Fig. 4M(c) Same as Fig. 4M(a) but coefficient $C_m/c=1.5$.

References

- [1] M. ABRAMOWITZ, I.A. STEGUN, *Handbook of mathematical functions*, National Bureau of Standards, U.S. Government Printing Office, Washington 1964.
- [2] J.S. GRADSTEIN, J.M. RIZHIK, *Tablicy integralow, summ, riadow i proizwedenii*, (in Russian), Izd. „Nauka”, Moscow 1971.
- [3] Martin GREENSPAN, *Piston radiator: some extensions to the theory*, J. Acoust. Soc. Am. **65**, 3, 608—621 (1979).
- [4] Miguel C. JUNGER, D. FEIT, *Sound, structures and their interaction*, The M.I.T Press, Cambridge, MA 1972.
- [5] L.V. KING, Can. J. Res. **11**, 135—155 (1934).
- [6] M.A. LAWRIENTIEW, B.W. SZABAT, *Metody funkcji kompleksnego peremennogo*, (in Russian), Gosudarstvennoe Izdatelstwo Fiz.-Mat. Literatury, Moscow 1958.
- [7] W.H. PRESS, B.P. FLANNERY, S.A. TEUKOLSKY, W.T. VETTERLING, *Numerical recipes: The art of scientific computing*, Cambridge University Press 1985.
- [8] A.P. PRUDNIKOW, *Integraly i riady* (in Russian), „Nauka”, Moscow 1983.
- [9] H. STENZEL, O. BROSZE, *Leitfaden zur Berechtung von Schwallvorgangen*, Springer-Verlag, Berlin 1958.
- [10] G.N. WATSON, *A treatise on the theory of Bessel functions*, Cambridge University Press, 1944.
- [11] R. WYRZYKOWSKI, *Liniowa teoria pola akustycznego ośrodków gazowych*, (in Polish), RTPN-WSP Rzeszów 1972.

(00-049 Warszawa, ul. Świętokrzyska 21)

Received April 6, 1992

The technique of acoustic emission (AE) is still currently applied to the investigations of the plastic deformation of metals and alloys (e.g. [1, 2]). One of the controversial problems is the explanation of the influence of grain size on the acoustic emission (AE) activity [3, 4]. Some of the experimental results indicate that AE increases with diminishing grain size; however, there are cases where an increase of AE has been observed with increasing grain size. WADLEY et al. [3] suggested that a reduction in grain size and, consequently, diminishing of the area of the individual dislocations slips should lead to a reduction in AE activity. The controversy lies in the fact that on the other hand, Gillis [4] suggested that if two polycrystals differing only in grain size d , become deformed to the same value of strain, ϵ ($\epsilon = b\rho_m L = \text{const}$, b — the Burgers vector, ρ_m — mobile dislocation density, $L \cong d$ — mean free path of dislocation), then more dislocation segments must be activated in a smaller grain, hence the AE activity in a greater grain should be smaller.

Recently [5], it has been suggested that the problem may be considered on the basis of the concept of AE where the origins of AE sources during plastic deformation are considered mainly as the results of dislocation annihilation processes which are accompanied by the operation of the dislocation sources (e.g. Frank — Read type). In this paper we present, qualitatively, that the experimentally observed AE activity in technically pure polycrystalline copper is greater in the material of a smaller grain size than in that of greater one, and that this result may be quite well explained on the basis of the dislocation annihilation concept of AE sources. Moreover, using the same concept of AE, some suggestions about the possibility of the inverse dependence of AE on the grain size has also been briefly discussed.

ACOUSTIC EMISSION DEPENDENCE ON GRAIN SIZE IN COPPER

A. PAWEŁEK, Z. JASIEŃSKI, S. PILECKI AND W. BOCHNIAK

Aleksander Krupkowski Institute of Metal Research
Polish Academy of Sciences
(30-059 Kraków, ul. Reymonta 25)

Institute of Fundamental Technological Research
Polish Academy of Sciences
(00-049 Warszawa, ul. Świętokrzyska 21)

1. Introduction

The technique of acoustic emission (AE) is still currently applied to the investigations of the plastic deformation of metals and alloys (e.g. [1, 2]). One of the controversial problems is the explanation of the influence of grain size on the acoustic emission (AE) activity [3, 4]. Some of the experimental results indicate that AE increases with diminishing grain size; however, there are cases where an increase of AE has been observed with increasing grain size. WADLEY et al. [3] suggested that a reduction in grain size and, consequently, diminishing of the area of the individual dislocations slips should lead to a reduction in AE activity. The controversy lies in the fact that on the other hand, Gillis [4] suggested that if two polycrystals differing only in grain size d , become deformed to the same value of strain, ε , ($\varepsilon = b\rho_m L = \text{const}$, b — the Burgers vector, ρ_m — mobile dislocation density, $L \cong d$ — mean free path of dislocation), then more dislocation segments must be activated in a smaller grain, hence the AE activity in a greater grain should be smaller.

Recently [5], it has been suggested that the problem may be considered on the basis of the concept of AE where the origins of AE sources during plastic deformation are considered mainly as the results of dislocation annihilation processes which are accompanied by the operation of the dislocation sources (e.g. Frank — Read type). In this paper we present, qualitatively, that the experimentally observed AE activity in technically pure polycrystalline copper is greater in the material of a smaller grain size than in that of greater one, and that this result may be quite well explained on the basis of the dislocation annihilation concept of AE sources. Moreover, using the same concept of AE, some suggestions about the possibility of the inverse dependence of AE on the grain size has also been briefly discussed.

2. Experiments and results

Three kinds of plane specimens of standard sizes (100 mm × 10 mm × 1 mm) were performed. Each of them was annealed for 45 min in air: the first at 400°C, the second at 600°C and the third one at 850°C. This way we obtained the samples of three different grain size, arbitrarily referred hereafter to as small, average and large grained material, respectively. The specimens were deformed at room temperature using the standard testing machine of INSTRON type. Tensile tests were carried out at constant strain rate $\dot{\epsilon} = 1.5 \times 10^{-4} \text{ s}^{-1}$ and the AE parameter $\Delta N/\Delta t$, i.e., the number ΔN of AE events detected in a time interval Δt , was measured simultaneously. The AE impulses

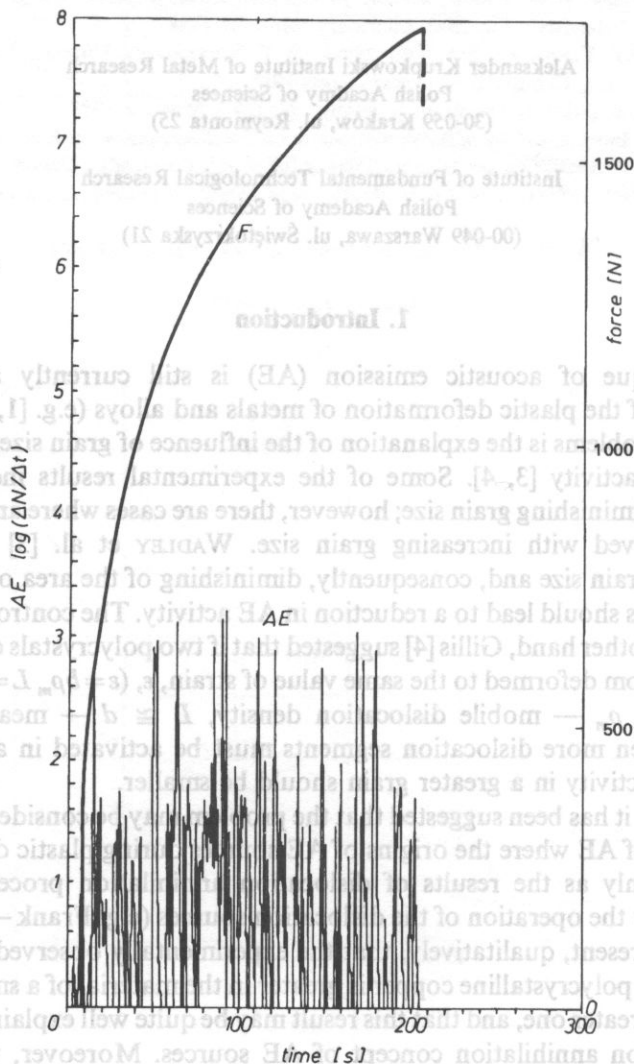


Fig. 1. AE and force characteristics for a small grained polycrystalline copper.

were detected by using the broad-band (from 50 kHz to 600 kHz) piezoelectric sensor in $\Delta t = 1$ s time intervals. The threshold voltage of the discriminator was 0.73 V and the total amplification including the preamplifier was 94 dB; for more details about the AE apparatus see [6].

Figures 1 to 3 show the behaviour of both AE activity and tensile force during the deformation of the samples of small, average and large grain size, respectively. Comparing these figures we can state that the AE activity is greater in the sample of smaller grain and that this fact seems to be correlated with the plasticity feature, i.e., the total elongation of the sample of greater grain is also smaller than of the sample of smaller grain. However, on the other hand, we realize that this correlation may be of

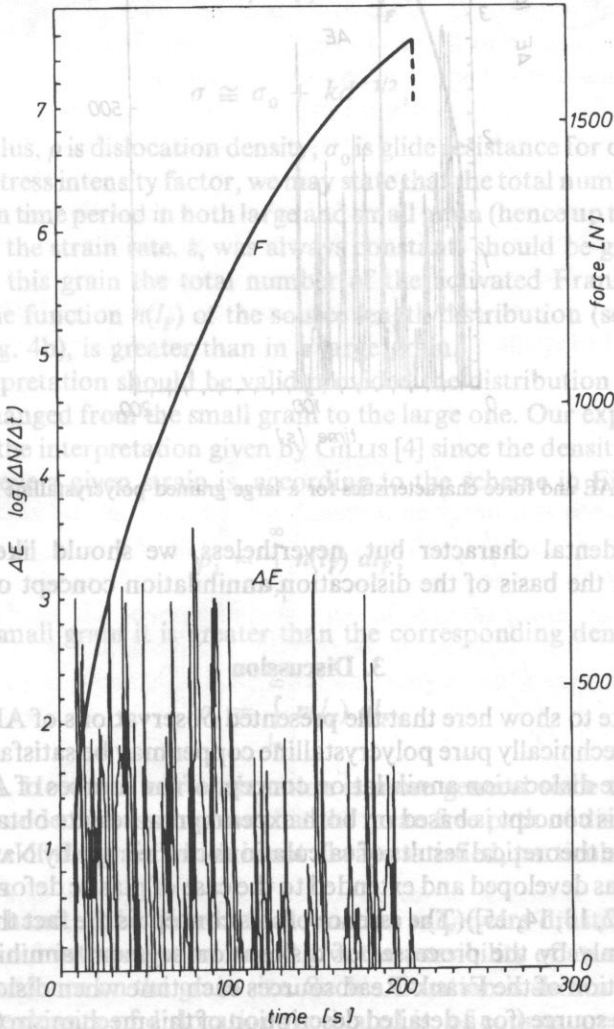


Fig. 2. AE and force characteristics for a polycrystalline copper of intermediate grain size.

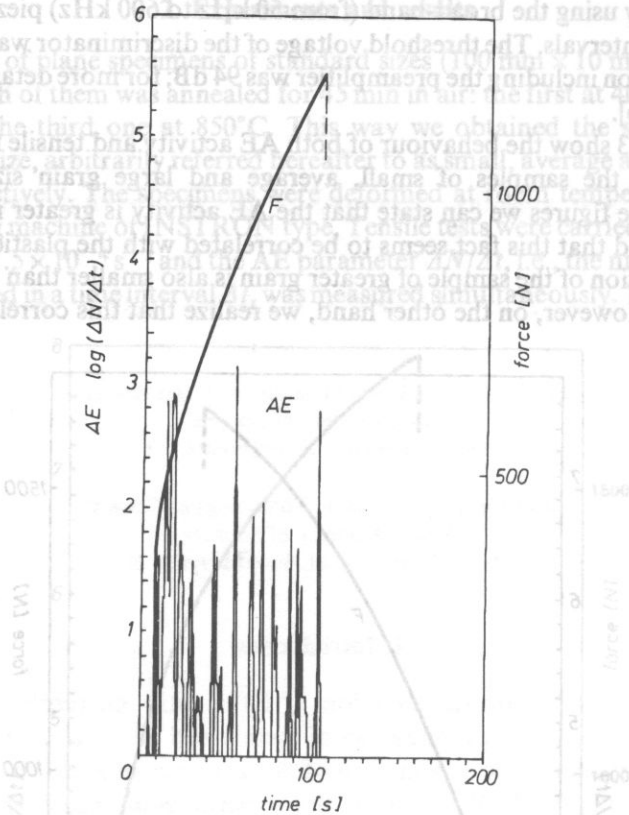


Fig. 3. AE and force characteristics for a large grained polycrystalline copper.

virtual and incidental character but, nevertheless, we should like to discuss this problem also on the basis of the dislocation annihilation concept of AE source.

3. Discussion

We would like to show here that the presented observations of AE dependence on the grain size in technically pure polycrystalline copper may be satisfactorily explained on the basis of the dislocation annihilation concept of the sources of AE during plastic deformation. This concept is based on both experimental results obtained by BOIKO et al. [7, 8, 9] and the theoretical results of calculations carried out by NATSIK et al. [10, 11] and this way it was developed and extended to the case of plastic deformation of metals (see for details [12, 13, 14, 15]). The essence of this concept is the fact that the AE events are induced mainly by the processes of dislocation segment annihilation occurring during the operation of the Frank-Read sources each time when dislocation loops are released from the source (for a detailed description of this mechanism (see [16, 17]) [The concept includes also the possibility of the annihilation processes occurring during the

escape of dislocation from the specimen to its free surface we do not exclude either that some contribution to the detected AE pulses may originate by other dislocation processes related, for example to the non-stationary movement of dislocations].

In order to explain the AE dependence on the grain size, it is very reasonable to assume that the length, l_{AE} of the dislocation segments, the annihilation of which induces the AE events, and which is required for the closing of the dislocation loop (see Fig. 4a), is proportional to the length, l_F , of the dislocation segment being potentially the Frank-Read source, i.e., $l_{AE} = \alpha l_F$, where α is a factor independent of the grain size.

Using well-known relations for plastic flow stress [20]

$$\sigma \cong \mu b \sqrt{\rho} \cong \frac{\mu b}{l_F}, \quad (1)$$

and [21]

$$\sigma \cong \sigma_0 + kd^{-1/2}, \quad (2)$$

μ is a shear modulus, ρ is dislocation density, σ_0 is glide resistance for dislocations, and k is microscopic stress intensity factor, we may state that the total number of AE events detected in a given time period in both large and small grain (hence up to the same value of strain, ϵ , since the strain rate, $\dot{\epsilon}$, was always constant) should be greater in a small grain because in this grain the total number of the activated Frank-Read sources, determined by the function $n(l_F)$ of the source length distribution (see the schematic illustration in Fig. 4b), is greater than in a large grain.

Such an interpretation should be valid provided the distribution function $n(l_F)$ is not drastically changed from the small grain to the large one. Our explanation is then convergent with the interpretation given by GILLIS [4] since the density of dislocations activated to achieve a given strain is, according to the scheme in Fig. 4b, equal to

$$\rho_1 = \int_{l_{r_1}}^{\infty} n(l_F) dl_F, \quad (3)$$

and thus in the small grain it is greater than the corresponding density

$$\rho_2 = \int_{l_{r_2}}^{\infty} n(l_F) dl_F, \quad (4)$$

in the large grain. However, our explanation is more general since the one given by GILLIS [4] is valid under the assumption that the mean free path of dislocation is equal to the average size of the grain which is not always satisfied, particularly in very large grained materials.

On the other hand, if the distribution function $n(l_F)$ were drastically different in both grains, then our interpretation would give the possibility of an occurrence of the inversed AE dependence on the grain size. Such a situation is shown schematically in Fig. 4c, where the density of dislocations activated is, of course, greater in a smaller grain but it is possible that the number $n(l_F)$ of dislocation segments activated as

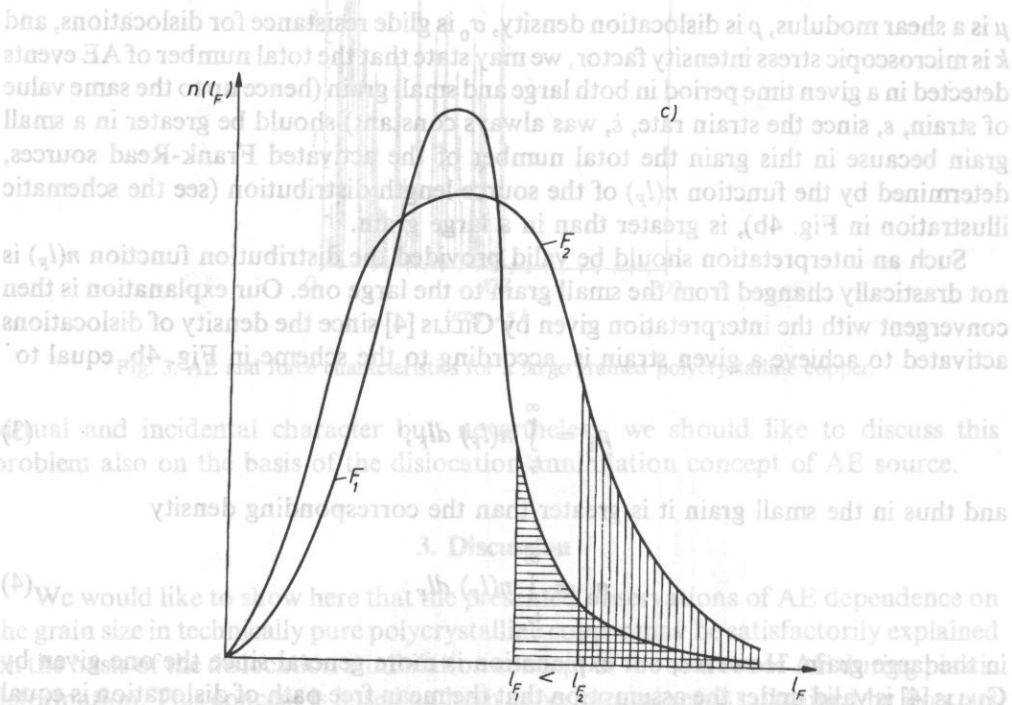
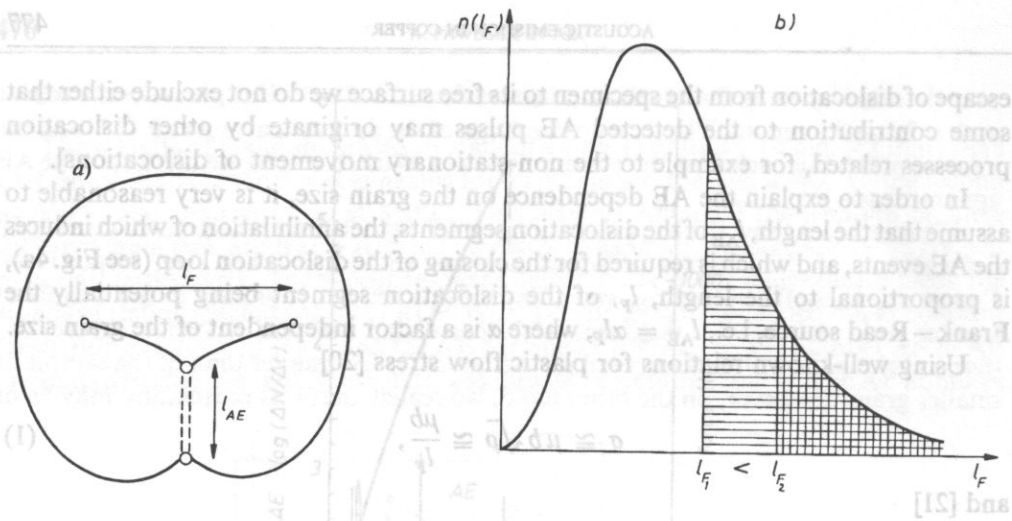


Fig. 4. A schematic illustration of the dislocation annihilation process during the operation of a Frank-Read source (a); (b) — the case when the function of source length distribution is the same for different grain sizes, and (c) — the case when this function is drastically changed from the one grain (F_1) to another (F_2).

Frank — Read sources — and so the total number $n(l_{AE})$ of AE events — is greater in a large grain than in a smaller one.

Now we discuss briefly the possible correlation of AE to the plasticity feature, i.e., to the total elongation of the sample up to the fracture. The fact that the strain localization, leading to the fracture, occurs faster in a large grain in pure polycrystalline metals than in a small one (e.g. [18]) has been experimentally stated. There are two reasons for this. First, the size of the local "geometric defect" formed at a free surface of a large grained specimen (e.g. due to the operation of two slip systems at least) is deeper than the size of such a "geometric effect" formed at the same time in a small grained specimen; hence in the former case the tendency to necking and fracture is faster. Second, the number of adjacent grains belonging to a given grain in a large grained sample is smaller than the number of grains surrounding a given grain in a small grained sample, and thus the changes in grain orientations caused by their rotation as well as the possibility for slip transfer from one grain to another are easier in the large grained material. Then also a „transcrystallographic" slip, if required for macroscopic strain localization, may occur in an easy way. One can see that the dislocation processes responsible for AE and for total elongation are, in fact different in nature, and the correlation between AE behaviour and this plasticity feature seems to be rather virtual and incidental, though we do not exclude that the inverse dependence of AE on the grain size (reported, e.g. in [4]) may be related to the inverse dependence of total elongation on the grain size i.e. the faster tendency to strain localization in a small grained material, evidenced in some alloys of low stacking fault energy, e.g. in [19].

4. Conclusions

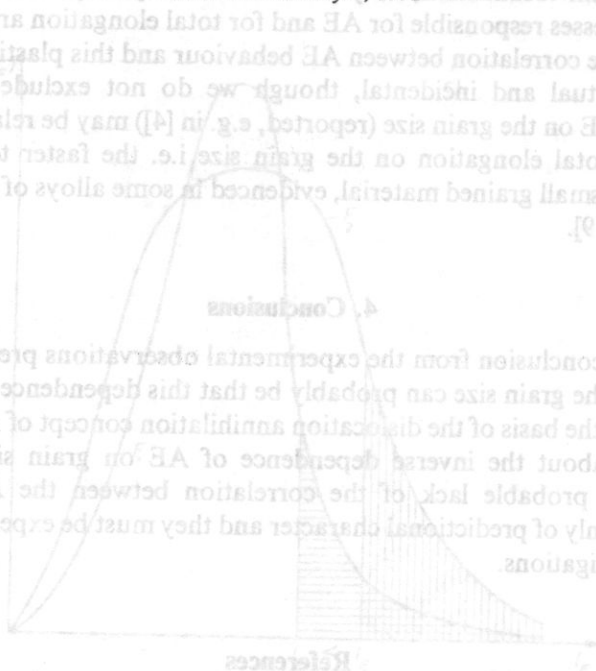
The general conclusion from the experimental observations presented here of AE dependence on the grain size can probably be that this dependence may be explained qualitatively on the basis of the dislocation annihilation concept of AE sources. Other considerations about the inverse dependence of AE on grain size as well as the statement on a probable lack of the correlation between the AE and the total elongation are only of predictional character and they must be experimentally verified in further investigations.

References

- [1] S. PILECKI, *Archiwum Akustyki*, **21**, 109 (1986).
- [2] A. POLAKOVIČ, P. MINOR, H. HYROSS, Z. JASIEŃSKI, A. LITWORA and A. PIĄTKOWSKI, *Kovové Materialy*, **24**, 114 (1986).
- [3] H.N.G. WADLEY, G.B. SCRUBY and J.H. SPEAKE, *Int. Metals Review*, **249**, 41 (1980).
- [4] P.P. GILLIS, *Acoustic Emission. ASTM Spec. Tech. Publ.*, **505**, 20 (1972).
- [5] A. PAWELEK, W. BOCHNIAK, H. DYBIEC, and W. STRYJEWSKI, *Archives of Metallurgy*, **33**, 645 (1988).
- [6] W. STRYJEWSKI, G. ZAPALSKI and A. PAWELEK, *Archives of Metallurgy*, **33**, 485 (1988).

- [7] V.S. BOIKO, R.I. GARBER, L.F. KRIVENKO and S.S. KRIVULYA, *Fiz. Tverd. Tela*, **15**, 321 (1973).
 [8] V.S. BOIKO, R.I. GARBER, and L.F. KRIVENKO, *Fiz. Tverd. Tela*, **16**, 1233 (1974).
 [9] V.S. BOIKO, R.I. GARBER, V.F. KIVSHIK and L.F. KRIVENKO, *ZhETF*, **71**, 708 (1976).
 [10] V.D. NATSIK and K.A. CHISHKO, *Fiz. Tverd. Tela*, **14**, 3126 (1972).
 [11] V.D. NATSIK and A.N. BURKHANOV, *Fiz. Tverd. Tela*, **14**, 12896 (1972).
 [12] A. PAWELEK, W. STRYJEWSKI, W. BOCHNIAK, H. DYBIEC, *Phys. Stat. Sol. (a)*, **90**, 531 (1985).
 [13] A. PAWELEK, H. DYBIEC, W. BOCHNIAK and W. STRYJEWSKI, *Archives of Metallurgy*, **34**, 239 (1989).
 [14] A. PAWELEK, W. STRYJEWSKI, H. DYBIEC and W. BOCHNIAK, *Archives of Acoustics* **15**, 211 (1990).
 [15] A. PAWELEK and S. PILECKI, *Archives of Metallurgy* in press.
 [16] A. PAWELEK, *Archives of Acoustics*, **18**, 166 (1993).
 [17] A. PAWELEK, *J. Appl. Phys.* **63**, 5320 (1989).
 [18] Z. JASIENSKI, A. PIATKOWSKI, A. LITWORA and H. PAUL, *Spr. IPM PAN, CPBP 02.07, temat 5.1, zadanie 5.1.13*, 1990.
 [19] Z. JASIENSKI and A. LITWORA, *Spr. wew. IPM PAN* 1988.
 [20] A.H. COTTRELL, *The Mechanical properties of matter*, Wiley, New York, 1964.
 [21] N.J. PETCH, *Phil. Mag.*, **1**, 866 (1956).

Received February 4, 1992



The general conclusion from the experimental observations presented here of AE dependence on the grain size can probably be that this dependence may be explained qualitatively on the basis of the dislocation annihilation concept of AE sources. Other considerations about the inverse dependence of AE on grain size as well as the statement on a probable lack of the correlation between the AE and the total elongation are only of a predictive character and they must be experimentally verified in further investigations.

- [1] S. PILECKI, *Archives of Metallurgy*, **37**, 109 (1986).
 [2] A. PAWELEK, W. BOCHNIAK, H. DYBIEC, A. LITWORA and A. PIATKOWSKI, *Archives of Metallurgy*, **37**, 114 (1986).
 [3] H.N.G. WAHLEY, D.B. KROBY and J.H. SEELER, *Int. Metals Review*, **29**, 41 (1980).
 [4] F.P. GILLIS, *Acoustic Emission, ASTM Spec. Tech. Publ.*, **502**, 20 (1973).
 [5] A. PAWELEK, W. BOCHNIAK, H. DYBIEC, and W. STRYJEWSKI, *Archives of Metallurgy*, **33**, 642 (1988).
 [6] W. STRYJEWSKI, G. ZABALSKI and A. PAWELEK, *Archives of Metallurgy*, **33**, 482 (1988).